PhD Program in Neuroscience

Instituto de Neurociencias (CSIC-UMH)

Intron detention as a mechanism to tightly control the timing of neural differentiation

---

Doctoral Thesis presented by

Ainara González-Iglesias

Thesis Director

Professor M. Angela Nieto Toledano

Thesis Co-director

Professor Isabel Fariñas Gómez

Universidad Miguel Hernández

- 2021 -

San Joan d'Alacant, 15th March, 2021

To whom it may concern,

The doctoral thesis entitled "Intron detention as a mechanism to tightly control the timing of neural differentiation" has been developed by myself, Ainara González-Iglesias. This thesis is presented in a conventional format and is based on experimental studies undertaken at the Neuroscience Institute of Alicante during the PhD program in Neuroscience of the Miguel Hernández University.

Yours sincerely,

AINARA| GONZALEZ| IGLESIAS

Firmado digitalmente por AINARA| GONZALEZ| IGLESIAS
Fecha: 2021.03.15 19:04:48 +01'00'

Ainara González-Iglesias

San Joan d'Alacant, 15th March, 2021

To whom it may concern,

The doctoral thesis entitled "Intron detention as a mechanism to tightly control the timing of neural differentiation" has been developed by myself, Ainara González-Iglesias. This thesis includes the following congress communications, of which I am the first author. I declare that the congress communications have not been used and will not be used in any other thesis in agreement with my thesis director Prof. M. Angela Nieto and co-director Prof. Isabel Fariñas:

- González-Iglesias, A., Domingo-Muelas, A., Fariñas, I., Nieto, M.A.. (2016). *Scratch factors in the neural stem cell niche*. 11th Meeting of the Spanish Society for Developmental Biology, Girona, Spain.
- González-Iglesias, A., Domingo-Muelas, A., Fariñas, I., Nieto, M.A.. (2017). *Scratch1 in the neural stem cell niche*. 17th National Congress of the Spanish Society of Neuroscience, Alicante, Spain.
- González-Iglesias, A., Domingo-Muelas, A., Fariñas, I., Nieto, M.A.. (2018). *Scratch1 in the adult neural stem cell niche*. Symposium "Cell plasticity in development and disease", San Juan de Alicante, Spain.

- González-Iglesias, A., Domingo-Muelas, A., Arcas, A., Mancini, E., Valcárcel, J., Fariñas, I., Nieto, M.A.. (2018). *Intron retention regulates Scratch1 expression during adult neurogenesis*. 4th Meeting of the Portuguese Society for Developmental Biology, Porto, Portugal.
- González-Iglesias, A., Domingo-Muelas, A., Arcas, A., Mancini, E., Valcárcel, J., Fariñas, I., Nieto, M.A.. (2019). *Intron retention as a mechanism to tightly control the timing of neuronal differentiation*. European Developmental Biology Congress, Alicante, Spain.

Yours sincerely,

AINARA| GONZALEZ| IGLESIAS
Firmado digitalmente por AINARA| GONZALEZ| IGLESIAS
Fecha: 2021.03.15 15:46:46 +01'00'

NIETO TOLEDANO M.ANGELA - DNI 50694461T
2021.03.15 16:25:11 +01'00'

MARIA ISABEL FARIÑA GOMEZ - NIF:36562901P
Firmado digitalmente por MARIA ISABEL FARIÑA GOMEZ - NIF:36562901P
Fecha: 2021.03.15 18:29:14 +01'00'

Ainara González- Iglesias

Prof. M. Angela Nieto
Thesis director

Prof. Isabel Fariñas
Thesis co-director

INSTITUTO DE NEUROCIENCIAS

UNIVERSITAS Miguel Hernández

San Joan d'Alacant, 15 de marzo de 2021

Dª. M. Angela Nieto Toledano, Profesora de Investigación del Consejo Superior de Investigaciones Científicas; y Dª Isabel Fariñas Gómez, Catedrática del Departamento de Biología Celular, Biología Funcional y Antropología Física de la Universidad de Valencia,

AUTORIZAMOS la presentación de la Tesis Doctoral titulada "Intron detention as a mechanism to tightly control the timing of neural differentiation", realizada por Dª Ainara González-Iglesias, bajo nuestra inmediata dirección y supervisión como directora y co-directora de su Tesis Doctoral en el Instituto de Neurociencias (CISC-UMH) y que presenta para la obtención del grado de Doctor por la Universidad Miguel Hernández.

Y para que conste, a los efectos oportunos, firmamos el presente certificado.

NIETO TOLEDANO M.ANGELA - DNI 50694461T 2021.03.15 16:26:15 +01'00'

Prof. M. Angela Nieto Toledano

Directora de Tesis

MARIA ISABEL FARIÑA GOMEZ - NIF:36562901P

Firmado digitalmente por MARIA ISABEL FARIÑA GOMEZ - NIF:36562901P Fecha: 2021.03.15 18:29:31 +01'00'

Prof. Isabel Fariñas Gómez

Co-directora de Tesis

INSTITUTO DE NEUROCIENCIAS

UNIVERSITAS Miguel Hernández

San Joan d'Alacant, 15 de marzo de 2021

Dª. Elvira de la Peña García, Profesora titular y Coordinadora del programa de doctorado en Neurociencias del Instituto de Neurociencias de Alicante, centro mixto de la Universidad Miguel Hernández (UMH) y de la Agencia Estatal Consejo Superior de Investigaciones Científicas (CSIC),

CERTIFICO:

Que la Tesis Doctoral titulada "Intron detention as a mechanism to tightly control the timing of neural differentiation" ha sido realizada por Dª. Ainara González-Iglesias, bajo la dirección de Dª. M. Angela Nieto Toledano como directora y de Dª Isabel Fariñas Gómez como co-directora, y doy mi conformidad para que sea presentada a la Comisión de Doctorado de la Universidad Miguel Hernández.

Y para que conste, a los efectos oportunos, firmo el presente certificado.

ELVIRA MARIA DE LA PEÑA GARCIA - NIF:21488194F

Firmado digitalmente por ELVIRA MARIA DE LA PEÑA GARCIA - NIF:21488194F
Fecha: 2021.03.15 16:12:22 +01'00'

Dra. Elvira de la Peña García

Este trabajo de Tesis Doctoral ha sido posible gracias a una beca predoctoral del Programa de Formación de Profesorado Universitario (FPU), financiada por el Ministerio de Educación, Cultura y Deporte (MECD); y a un contrato como titulado superior en actividades técnicas y profesionales financiado por el Ministerio de Ciencia, Innovación y Universidades (MICIU). La investigacuón ha sido financiada por los siguientes proyectos de investigación:

- "STEMT" ISIC 2012/20, Generalitat Valenciana (2012-2015).

- "La familia génica Snail en Biomedicina", PROMETEOII/2013/002, Generalitat Valenciana (2013-2016).

- "La plasticidad celular en biomedicina", PROMETEO2017/150 (2017-actualidad)

Acknowledgements

Me gustaría aprovechar este momento para dar las gracias a todas las personas que han estado a mi lado durante estos años, apoyándome y haciendo posible que haya llegado hasta aquí y esté finalmente escribiendo esta tesis.

En primer lugar, me gustaría darle las gracias a mi directora de tesis, Angela Nieto, por haber confiado en mí y haberme dado la oportunidad de formar parte de su laboratorio. He aprendido mucho de ti en este tiempo y me gustaría agradecerte tu guía y tu ayuda en todo momento. También me gustaría agradecerle su apoyo a mi co-directora, Isabel Fariñas. Aún recuerdo un seminario tuyo al que asistí, el primero nada más empezar la carrera, y que me inspiró para adentrarme en el mundo de la Neurociencia.

No puedo olvidarme tampoco de mis compañeros de laboratorio. Quiero daros las gracias a todos y cada uno de vosotros, tanto a los que ya os habéis ido como a los que seguís ahí, haciendo que el laboratorio sea lo que es. Con vosotros he compartido infinidad de momentos, los éxitos y las frustraciones típicos del día a día en investigación. Gracias de verdad por haber estado ahí, ofreciéndome siempre vuestra ayuda y vuestro apoyo. Sin vosotros nada de esto habría sido posible. Recordando a los que ya se fueron, quiero dar las gracias especialmente a Diana. Tú estuviste a mi lado en mis primeros pasos en el laboratorio. Tu alegría y tu sonrisa incondicional hacían que el día a día fuera, simplemente, mejor. Con tu marcha el laboratorio perdió un poquito de luz, pero estoy segura que tú vas a seguir iluminando el mundo allá por donde pases.

También quiero agradecer de forma especial su apoyo a Andrea, Fran García, Cabello, Quiles, Javi, Marilyn, Marta y Noemi; con los que más de cerca he compartido los buenos y los malos momentos, los llantos y las risas. Echo (y echaré) mucho de menos nuestras comidas al sol. Gracias por alegrarme los días, por animarme cuando yo lo daba todo por perdido y por haberme ayudado a llegar hasta aquí. Y después de este último año tan complicado, no puedo dejar de darles las gracias a mis compañeros del “afternoon shift” por hacer las largas tardes en el laboratorio mucho más amenas. Con vosotros al lado da gusto ir a trabajar cada día.

Además, este tiempo en el Instituto me ha permitido conocer a muchas otras personas maravillosas. Nada más llegar, el máster me dio la oportunidad de conocer a mi querida Lucy, que junto con Fran me ha acompañado a lo largo de todo este viaje. Muchos

años, muchos buenos momentos, aunque creo que ni una sola foto “buena” juntos para recordarlo. Pero no desistamos; algún día lo conseguiremos. Mucho más recientemente llegó Aysha, siempre dispuesta a animar a todos los que le rodean. Aunque desde que llegaste nos han tenido confinados la mitad del tiempo, es como si llevaras aquí toda la vida. Y no me puedo olvidar de ti, Irene. Gracias por estar siempre ahí, escuchándome y haciendo todo lo posible para ayudarme y apoyarme. No sé qué habría sido de mi salud mental sin nuestros terapéuticos paseos de los domingos por la tarde. Por haberos conocido a vosotros, todo esto ha merecido la pena.

No puedo dejar de dar las gracias tampoco a Álvaro, Camila, Laura, Miguel, Sonia, Sara y Toni. Gracias por haber estado a mi lado desde nuestros inicios en BCB hasta ahora (y lo que nos queda). Y sobre todo tengo que darle las gracias a mi Sasaiz. Gracias por haber estado siempre ahí, en los buenos y en los malos momentos, por animarme, por aguantarme y por apoyarme incondicionalmente.

También quiero aprovechar este momento para darte las gracias a ti, Andrea. Aunque últimamente hemos podido vernos aún menos de lo normal, contigo es como si no hubiera pasado ni un solo día desde que dejamos el colegio. Gracias por ser siempre tan positiva, por ver siempre el lado bueno de las cosas y estar ahí transmitiéndome ese optimismo.

Por último, quiero dar las gracias a mi familia. A mis padres, Luis y Pilar, gracias por vuestro apoyo incondicional y por haberme ayudado a convertirme en la persona que soy. No os lo digo nunca, pero sabéis que os quiero muchísimo. También quiero darte las gracias a ti, Iker. Por haber estado siempre a mi lado, por ser mi pequeño saltamontes y por las veces que has hecho de hermano mayor conmigo, aunque ese no fuera el papel que te correspondía. Tampoco quiero olvidarme de mis abuelos, de las que están y de los que se han ido. Esta tesis os la dedico a vosotros.

A todos vosotros, sinceramente, ¡mil gracias!

Table of contents

Abbreviations list

3'SS	3' splice site
3'UTR	3' unstranslated region
5'SS	5' splice site
A	A cell or neuroblast
ac^{4}C	N^4-acetylcytidine
ALKBH5	alkB homolog 5
AP	alkaline phosphatase
AS	alternative splicing
ASE	alternative splicing event
B_1	B_1 cell or neural stem cell
BBB	blood-brain barrier
bFGF	basic fibroblast growth factor
bHLH	basic helix-loop-helix
BLBP	brain lipid-binding protein
BMP	bone morphogenetic protein
BP	branch point
BSA	bovine serum albumin
BV	blood vessel
C	C cell or transit amplifying progenitor
cc	corpus callosum
CDK	cyclin-dependent kinase
CES-1	cell death specification 1
CES-2	cell death specification 2
CSF	cerebrospinal fluid
DAA	3-deazaadenosine
DCX	doublecortin
DEG	differentially expressed genes
DEPC	diethyl pyrocarbonate
DG	dentate gyrus
DI	detained intron
DIG	digoxigenin
DIV	days in vitro
DMEM	Dulbecco's modified Eagle medium
DMSO	dimethyl sulfoxide
DNJ-11	DnaJ domain-11
DTT	dithiothreitol
E	E cell or ependymal cell
EBSS	Earle's balanced salts solution
ECM	extracellular matrix
EGF	epidermal growth factor
EGFR	epidermal growth factor receptor
egl-1	egg-laying abnormal-1
eIF3	eukaryotic translation initiation factor 3
EJC	exon-junction complex
ELAVL1	ELAV-like protein 1
EpiSC	epiblast stem cell
ESC	embryonic stem cell
ESE	exonic splicing enhancer
ESS	exonic splicing silencer
F12	Ham's F-12 nutrient mixture
FBS	fetal bovine serum
FGF	fibroblast growth factor
FISH	fluorescent *in situ* hybridization
FMRP	fragile X mental retardation protein
FTO	fat mass and obesity-associated protein
GCL	granule cell layer
GL	glomerular layer
GMEM	Glasgow minimum essential medium
GFP	green fluorescent protein
GFAP	glial fibrillary acid protein
GLAST	glutamate aspartate transporter
GO	gene ontology
GSC	germ line stem cell
hESC	human embryonic stem cell
HBS	Hepes Buffered Saline
HEPES	4-(2-hydroxyethyl)-1-piperazineethanesulfonic acid
hm^{5}C	5-hydroxymethylcytidine
hnRNP	heterogeneous nuclear ribonucleoprotein
HEK	human embryonic kidney cells

HSC	hematopoietic stem cell
IFF	immunofluorescence
ICM	inner cell mass
ID	intron detention
IGF2BP	insulin-like growth factor 2 mRNA-binding protein
IPC	intermediate progenitor cell
iPSC	induced pluripotent stem cell
IR	intron retention
ISE	intronic splicing enhancer
ISH	*in situ* hybridization
ISMARA	integrated system for motif activity response analysis
ISS	intronic splicing silencer
LIF	leukemia inhibitory factor
lncRNA	long non-coding RNA
LV	lateral ventricle
LV	lentivirus
m^{1}A	N^1-methyladenosine
m^{5}C	5-methylcytidine
m^{6}A	N^6-methyadenosine
m^{6}Am	N^6,2'-O-dimethyadenosine
m^{7}G	N^7-methylguanosine
METTL3	methyltransferase-like 3
METTL14	methyltransferase-like 14
mESC	mouse embryonic stem cell
miR	microRNA
mRNP	messenger ribonucleoprotein particle
MTC	methyltransferase complex
NB	neuroblast
nBAF	neuron-specific chromatin remodelling complex
NEAA	non-essential amino acids
NeuN	neuronal nuclei
NPC	nuclear pore complex
npBAF	neural progenitor-specific chromatin remodelling complex
nPTB	neural PTB
NSC	neural stem cell
NSD	non-sense mediated decay
NSM	neurosecretory motor neuron
nt	nucleotide
Nup	nucleoporin
OB	olfactory bulb
oIPC	oligodendrocytic progenitor cell
o/n	overnight
OPC	oligodendrocyte progenitor cell
PFA	paraformaldehyde
PBS	phosphate-buffered saline
PGZ	pallial germinal zone
POD	peroxidase
PPT	polypyrimidine tract
Prrc2a	proline rich coiled-coli 2A
PSC	pluripotent stem cell
PTB	polypyrimidine tract binding protein
qPCR	quantitative PCR
RGC	radial glial cell
RIP	RNA immunoprecipitation
RMS	rostral migratory stream
RT	room temperature
SC	stem cell
Scrt1	*Scratch1*
Scrt2	*Scratch2*
SEM	standard error of the mean
SEZ	subependymal zone
SGZ	subgranular zone
Shh	sonic hedgehog
SNAG	Snail/Gfi
sncRNA	small non-coding RNA
snRNA	small nuclear RNA
SR	serine/arginine
SSC	somatic stem cell
st	striatum
TAP	transit amplifying progenitor
tGFP	turbo GFP
TST	Tris-Saline-Tween buffer
TU	transforming units
v	ventricle
V-SVZ	ventricular-subventricular zone
VZ	ventricular zone
WTAP	Wilms tumor 1 associated protein
ψ	pseudouridine

Abstract

Abstract

The life-long persistence of adult neural stem cells (NSCs) requires the accurate balance between their self-renewal, proliferation and differentiation. Recent studies analyzing the transcriptomic dynamics that take place during adult neurogenesis have reveal that post-transcriptional regulation may have a more relevant role than anticipated in the control of NSC biology and function. In this thesis, we have uncovered a novel regulatory mechanism that refines the control of *Scratch1* expression during adult neurogenesis. We have shown that this gene is expressed in the adult subependymal zone (SEZ), both in NSCs, transient amplifying progenitors (TAPs) and neuroblasts, exhibiting increasing levels as NSCs progress into the lineage; and fulfilling several functions during the process of differentiation. On the one hand, this transcription factor acts downstream of p53, repressing the transcription of it targets *Bbc3* (Puma) and *Cdkn1a* (p21), which in turn protects the differentiating cells form undergoing apoptosis and, at the same time, stimulates their proliferation. On the other hand, Scratch1 promotes neuronal differentiation, favoring neurogenesis at the expense of gliogenesis. Additionally, we have also determined that *Scracth1* starts to be expressed when stem cells acquire the neural identity, but its transcripts are retained in the nucleus of NSCs due to intron detention. This event of regulated splicing is possible thanks to the progressive enlargement of the polypyrimidine tract of its only intron during the evolution of vertebrates, leading to the generation of a suboptimal splice site in mammals. By contrast, in response to the neural differentiation signal, *Scratch1* mRNA is m^6A modified and consequently spliced and exported to the cytoplasm, where it can be translated. Finally, we have shown that intron detention in this context is not specific for *Scratch1* mRNA, but rather it also controls the translational availability of multiple transcripts associated with adult NSC differentiation. Interestingly, a complementary regulation of intron detention occurs in mRNAs from genes involved in the maintenance of stemness. Thus, intron detention is a novel mechanism to fine-tune neurogenesis in the adult NSC niche.

Resumen

El mantenimiento de la población de células madres neurales (NSCs) durante toda la vida del individuo requiere un balance preciso entre su auto-renovación, proliferación y diferenciación. Estudios recientes en los que se han analizado los cambios transcripcionales que tienen lugar durante la neurogénesis adulta han revelado que la regulación post-transcripcional podría tener un peso mayor en el control de la biología y la función de las NSCs de lo que se pensaba previamente. En esta tesis, hemos identificado un nuevo mecanismo de regulación de la expresión del factor de transcripción *Scratch1* durante la neurogénesis adulta. Hemos mostrado que este gen se expresa en la zona subependimaria (SEZ) adulta, tanto en NSCs como en progenitores (TAPs) y neuroblastos, presentando niveles crecientes de expresión a medida que las NSCs progresan en el linaje. Además, Scratch1 lleva a cabo diversas funciones durante el proceso de diferenciación. Por una parte, actúa por debajo de p53, reprimiendo la transcripción de sus dianas *Bbc3* (Puma) y *Cdkn1a* (p21), y protegiendo a las células en diferenciación de sufrir apoptosis a la vez que estimula su proliferación. Por otra parte, Scratch1 promueve la diferenciación neuronal, favoreciendo la neurogénesis a expensas de la gliogénesis. Además, hemos determinado que *Scratch1* empieza expresarse cuando las células madre adquieren la identidad neural, aunque sus tránscritos permanecen dentro del núcleo de las NSCs debido a un procesamiento deficiente del único intrón en su mRNA. Este evento de splicing regulado es posible gracias a la expansión progresiva de la serie de polipirimidinas (PPT) durante la evolución de los vertebrados, dando lugar a la generación de un sitio de splicing subóptimo en mamíferos. En respuesta a la señal de diferenciación, se induce la metilación (m^6A) del mRNA y los tránscritos son procesados y exportados al citoplasma, donde pueden ser traducidos. Por último, hemos encontrado que la detención de intrones no solo regula la expresión de *Scratch1*, sino que también controla la localización subcelular y la disponibilidad para ser traducidos de múltiples tránscritos relacionados con la diferenciación de las NSCs. Más aun, el control de la retención de intrones se realiza de forma contraria en los transcritos correspondientes a genes relacionados con las células madre. Por lo tanto, aquí definimos un nuevo mecanismo que controla de forma precisa la neurogénesis adulta.

Introduction

1. Stem cells: a spectrum of potentialities

At the very firsts stages of embryonic development, stem cells (SCs) are, during a very limited period of time, totipotent, meaning that they have the potential to generate the whole embryo and extraembryonic tissues, including the placenta, the umbilical cord and the embryonic membranes (Weissman, 2000). With the first divisions of the zygote, embryonic stem cells (ESCs) lose this property and become pluripotent, still retaining the ability to differentiate into cells derived from the three embryonic germ layers, namely the ectoderm, the mesoderm and the endoderm. As development proceeds, cells become progressively more restricted in their capacity to generate different cell lineages and are then considered multipotent, only capable of giving rise to a limited subset of cell types (Wagers and Weissman, 2004, **Figure 1**).

1.1. Pluripotent stem cells

Pluripotent stem cells (PSCs) are characterized by two properties: their ability to generate all the cell types present in the adult body (pluripotency); and their capacity for indefinite self-renewal (immortality). Although pluripotency is a very transitory state *in vivo*, only found during a narrow window of embryonic development, PSCs can be derived from embryos and maintained infinitely in an undifferentiated state in culture (Pera and Tam, 2010). ESCs were isolated for the first time from the inner cell mass (ICM) of a mouse blastocyst in 1981 (Evans and Kaufman, 1981); and from human embryos several years later, in 1998 (Thomson et al., 1998). ESCs derived from these two species differ in some features, including colony morphology and cytokine requirements, being human ESCs (hESCs) more similar to mouse epiblast stem cells (EpiSCs), another population of PSCs that is generated later on during development and can be isolated from the epiblast of post-implantation embryos (Pera and Tam, 2010; Rowe and Daley, 2019; Takahashi and Yamanaka, 2015).

The maintenance of these populations of PSCs *in vitro* requires specific culture conditions in order to ensure the preservation of their properties. Regarding mouse ESCs (mESCs), their self-renewal and pluripotency rely on the presence of leukemia inhibitory factor (LIF) and either serum or bone morphogenetic proteins (BMPs) in the medium. Conversely, both hESCs and EpiSCs require FGF2, especially in the case of hESCs, and

the activation of Nodal or Activin signaling to maintain the undifferentiated state; and do not respond to LIF (Chambers and Smith, 2004; Pera and Tam, 2010).

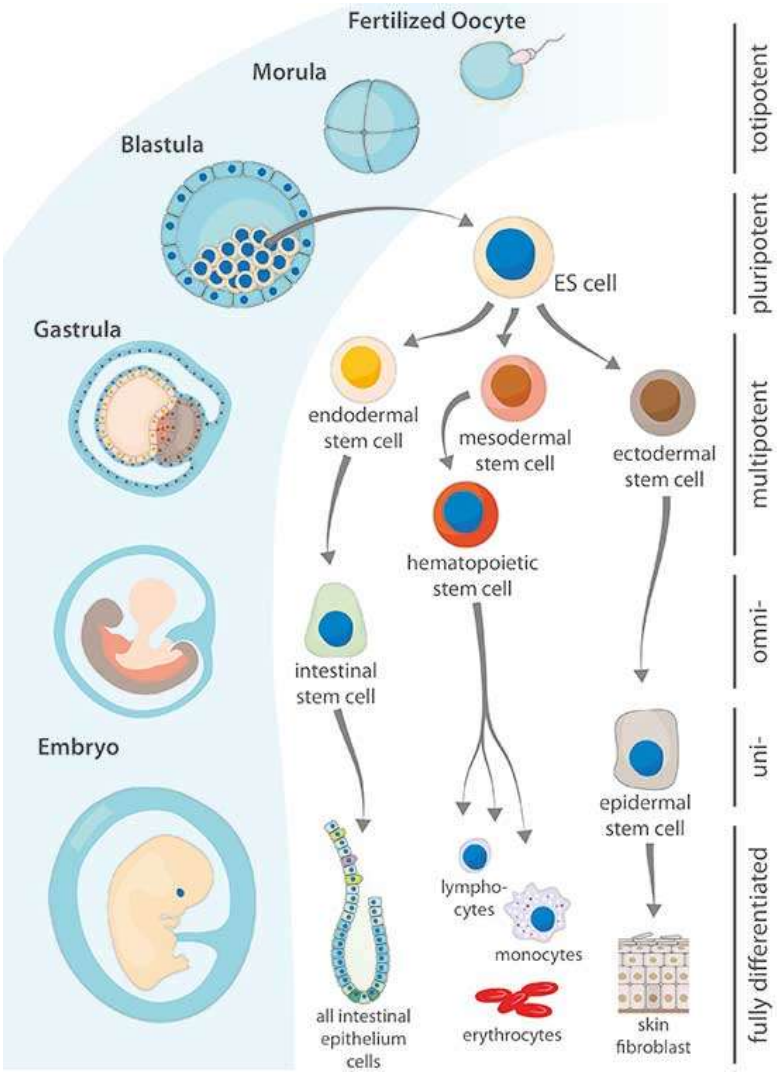

Figure 1| Differentiation potential of stem cells during development. The earliest stem cells in ontogeny (the zygote and the first stages of the morula) are totipotent. As development proceeds, these stem cells give rise to the blastocyst, in which pluripotent embryonic stem cells (ESCs) can be derived from the inner cell mass (ICM). From then on, stem cells gradually increase their commitment, losing their pluripotency and generating more restricted tissue-specific stem cells, including germ-line stem cells (GSCs), required for reproduction, and somatic stem cells (SSCs), responsible for organogenesis. The potential of both GSCs and SSCs is progressively restricted, leading to the emergence of discrete populations of multipotent stem cells, which give rise to all the variety of tissue-specific differentiated cell types present in the adult body. Remarkably, some of these multipotent stem cells remain all throughout the postnatal and adult stages, ensuring tissue renewal and enabling certain degree of tissue repair and regeneration. Adapted from Enzo Life Science, TechNotes.

Additionally, PSCs can be artificially obtained by the reprogramming of somatic cells, case in which they are referred as induced pluripotent stem cells (iPSCs). In 2006, Takahashi and Yamanaka identified for the first time the combination of factors (Oct4, Klf4, Sox2 and c-myc), now known as Yamanaka factors, required for the reprogramming of human fibroblasts into iPSCs (Takahashi and Yamanaka, 2006). From then on, iPSCs have being obtained by reprogramming of multiple somatic tissues from mouse and human *in vitro* (Rowe and Daley, 2019) and also in living mice (Abad et al., 2013). The development of this technology was a major breakthrough in the field of biomedical research and a significant step forward for regenerative medicine, since the use of iPSCs allows to bypass the ethical concerns associated to ESC. In addition, it also opened new possibilities for disease modelling, enabling the generation of patient-specific SCs, which can be subsequently expanded and differentiated into any specific cell type. Nevertheless, the use of iPSCs still presents some technical limitations, such as the need of using oncogenes for reprogramming or the low efficiency of the process (Kim and Koo, 2020).

1.2. Tissue-resident adult stem cells

A small proportion of the multipotent stem cells that originate during embryonic development persist during the postnatal and adult life of the organism, constituting life-long reservoirs of somatic stem cells (SSCs), which endow tissues and organs with the ability to maintain their integrity and function by replenishing the cells that are lost during the organism's lifespan, either due to wear (homeostatic replacement) or as a consequence of an injury (Fuchs et al., 2004; Orford and Scadden, 2008).

Adult SCs are defined by their ability to produce new tissue-specific differentiated cells (multipotency) while maintaining the SC population itself (self-renewal). Nevertheless, the properties and the potential of different population of SCs is determined by the combination of their intrinsic characteristics and the specific microenvironment in which they reside, the niche, which play a crucial role in the regulation of their function, especially regarding cell-fate decisions such as self-renewal and commitment (Fuchs et al., 2004; Graf and Stadtfeld, 2008; Orford and Scadden, 2008).

Among the different SC populations that exist in adult mammals, bone marrow-resident hematopoietic stem cells (HSCs) were the first ones to be identified (Till and McCulloch, 1961). From then on, they have been discovered in many other tissues, such as the skin, the hair follicles, the intestinal epithelium, the peripheral and central nervous system or the

muscles (Biteau et al., 2011; Graf and Stadtfeld, 2008). This wide variety of adult SC populations exhibit remarkable differences in their proliferative behavior, reflecting the diversity in the regenerative requirements of each tissue (Biteau et al., 2011). On the one hand, there are high-turnover tissues, such as the blood, the skin or the intestine, that require continuously cycling SCs. However, in adult mammals, the majority of the tissues display very low turnover and, accordingly, their resident adult SCs are mostly quiescent under normal circumstances (Biteau et al., 2011; Orford and Scadden, 2008; Wagers and Weissman, 2004). Furthermore, SCs not only differ in their proliferation dynamics in homeostasis, but also in their proliferative plasticity, meaning their capacity to respond to damage. While some of these SCs, such as cardiac stem cells, respond poorly to regenerative pressure; others respond quite well, as is the case of satellite cells, whose proliferative activity can be strongly induced by injury (Biteau et al., 2011; Wagers and Weissman, 2004).

In homeostatic conditions, adult SCs divide to produce new SCs and non-renewing, rapidly-cycling cells, also known as transit amplifying progenitors (TAPs), which eventually generate tissue-specific differentiated cells after a given number of cycles. This hierarchical organization ensures the life-long maintenance of adult SC populations, preserving their genomic integrity and preventing their premature differentiation. In any case, tissue homeostasis relies on the accurate control of SC activity, which requires a finely regulated balance between self-renewal and differentiation, in order to respond appropriately to tissue requirements and ensure the efficient replacement of the cells, while avoiding overproliferation, which may lead to pathological situations such as cancer (Biteau et al., 2011).

During aging, the functionality of adult SCs declines, both by cell-intrinsic damage and by alterations in the niche microenvironment and in the circulating blood, resulting eventually in tissue or organ malfunction (Ermolaeva et al., 2018). Moreover, similar to the age-related decline in SC activity, the loss of SC self-renewal underlies the development of certain degenerative diseases. At the same time, if this self-renewal capacity is not properly controlled, it entails a risk to the organism, as aforementioned, since SCs have the potential to generate a large amount of descendant cells, which would disrupt the architecture of the tissue. Furthermore, the existence of these highly undifferentiated SCs makes them a potential substrate for malignant conversion, which is of especial concern in the case of long-living organisms (Avgustinova and Benitah, 2016; Orford and Scadden, 2008)

On the opposite side, their ability to self-renew together with their capacity to generate tissue-specific differentiated cells has brought adult SCs forward, together with ESCs and iPSCs, as a prominent cell source for clinical applications, such as regenerative medicine and tissue repair. However, to open up the possibility of achieving a significant clinical benefit, it is crucial to understand the biology and regulation of these SCs, which will allow the design of better strategies for cell therapy that can improve clinical outcomes (Tewary et al., 2018; Trounson and DeWitt, 2016).

1.3. Neural stem cells and adult neurogenesis

It has been well established that discrete populations of neural stem cells (NSCs) remain in the adult rodent brain, maintaining the ability for long-term self-renewal and enabling the generation of new neurons and glia throughout life (Bond et al., 2015). Adult NSCs reside within specialized niches, being mainly found in two germinal regions: the subgranular zone (SGZ) of the dentate gyrus (DG) in the hippocampus, where the newly-generated neurons play a role in learning, memory and pattern separation (Ming and Song, 2011); and the subependymal zone (SEZ; also known as ventricular-subventricular zone (V-SVZ)) on the walls of the lateral ventricles (LVs). The newly-formed neurons generated in this latter region migrate towards the olfactory bulb (OB), contributing to the plasticity of olfactory information processing (Obernier and Alvarez-Buylla, 2019).

1.3.1. The SEZ neurogenic niche

The SEZ is a very active neurogenic region and constitutes the largest germinal region in mammalian adult brain. It has been estimated that in young adult mice, SEZ-resident NSCs (also called B1 cells) generate around 10,000 new neurons every day. This is achieved through the generation of transient amplifying progenitors (TAPs or C cells), which divide three or four times before generating neuroblasts (also known as A cells). These neuroblasts, which also divide a couple of times to further amplify the number of neurons generated, migrate collectively towards the OB following the rostral migratory stream (RMS), a tangential path formed by a chain of migrating neuroblasts that are surrounded by a layer of astrocytes. Once they arrive to the OB, the newly-formed neurons start to migrate radially towards the glomerular layer (GL) and the granule cell layer (GCL), where they differentiate into several subtypes of inhibitory interneurons and integrate in the local circuits (Chaker et al., 2016; Obernier and Alvarez-Buylla, 2019; Ponti et al., 2013; **Figure 2**).

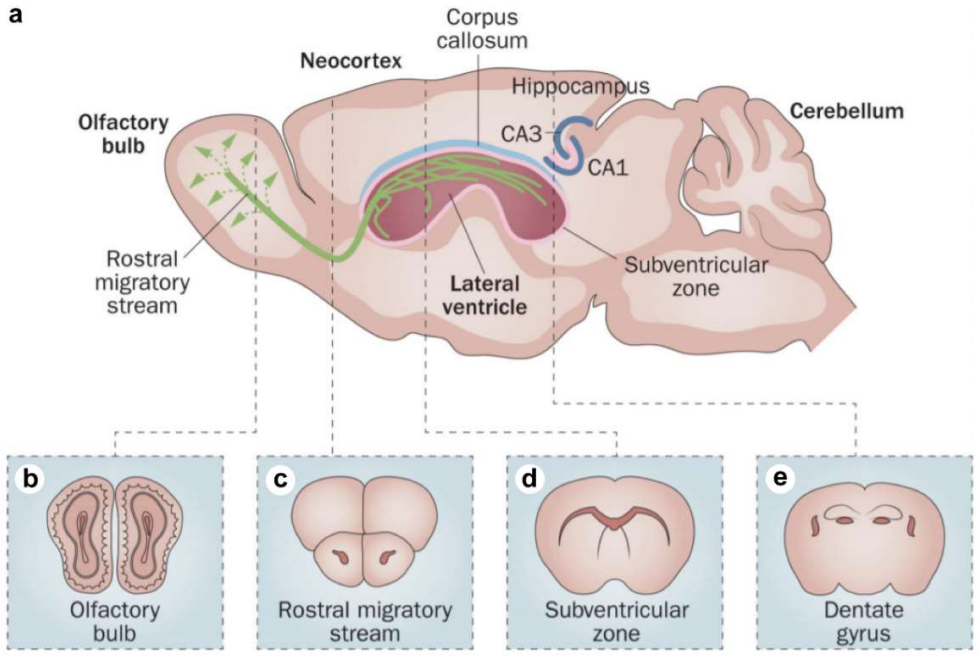

Figure 2| Neurogenic regions in the adult mouse brain. (a) Sagittal view of the main adult neurogenic areas in mammals (highlighted in pink): the subependymal or subventricular zone (SEZ/SVZ) of the lateral ventricles and the subgranular zone (SGZ) in the dentate gyrus of the hippocampus. Neuroblasts generated in the SEZ (green) migrate tangentially following the rostral migratory stream (RMS) towards the olfactory bulb. **(b-e)** Coronal sections of the olfactory bulb **(b)**, the RMS **(c)**, the SEZ **(d)** and the dentate gyrus **(e)**. Adapted from Ziegler et al., 2015.

Remarkably, apart from the OB neurogenesis, the SEZ-resident NSC also contribute to the generation of glia, although to a lesser extent. NSCs are able to generate both oligodendrocytes, which mainly contribute to the re-myelination of the corpus callosum (CC; Menn et al., 2006); and astrocytes, which migrate either to the RMS or the CC (Sohn et al., 2015). The multipotency of these cells has been demonstrated by *in vitro* analysis of NSCs derived from the adult brain, which can be maintained and expanded in cultured in the presence of epidermal growth factor (EGF) and basic fibroblast growth factor (bFGF) for extended periods of time, giving rise to floating aggregates known as neurospheres. When the cells that compose those neurospheres are induced to differentiate by culturing them onto an adhesive substrate in the presence of serum, they give rise to neurons, astrocytes and oligodendrocytes, evidencing their multipotent nature (Belenguer et al., 2016; Reynolds and Weiss, 1992). However, it remains to be determined whether individual NSCs are also multipotent *in vivo*, being able to generate both neurons and glia; or whether, on the

contrary, several subpopulations of fate-restricted NSCs co-exist within the SEZ (Obernier and Alvarez-Buylla, 2019).

1.3.2. Adult NSCs: Embryonic origin and glial identity

During embryonic development, cortical neurogenesis begins approximately around E9-E10, when neuroepithelial cells start to acquire distinctive features of glial cells, becoming radial glial cells (RGCs). These cells maintain the apico-basal polarity exhibited by neuroepithelial cells, contacting both the pial and the ventricular surfaces; and divide mainly asymmetrically to simultaneously self-renew and produce either intermediate progenitor cells (IPCs) or neurons, which migrate along the radial processes of RGCs towards the cortical plate. RGCs can also give rise to oligodendrocytes through the generation of specific intermediate progenitor cells (oIPCs). At the end of cortical development, most RGCs release their ventricular attachment and migrate towards the cortical plate, where most of them transform into astrocytes. After birth, the remaining RGCs differentiate either into ependymal cells, which cover the surface of the ventricular walls, or into glial cells, including adult NSCs, which will populate the adult neurogenic niches (Kriegstein and Alvarez-Buylla, 2009; **Figure 3**). Moreover, during mid-embryonic development (E13.5-E15.5), a subpopulation of RGCs produce pre-NSCs that remain largely quiescent until the adulthood, when they can be reactivated and contribute to the generation of OB interneurons (Fuentealba et al., 2015; Furutachi et al., 2015; Yuzwa et al., 2017).

Due to their embryonic origin, adult NSCs maintain many reminiscent features of RGCs, including their glial nature, which is reflected in the expression of astrocytic markers, such as glial fibrillary protein (GFAP), glutamate aspartate transporter (GLAST) and brain lipid-binding protein (BLBP). Additionally, similar to RGCs, SEZ-resident NSCs exhibit a clear apico-basal polarity, presenting apical processes that contact the ventricle, ending in a single primary cilium; and basal end-feet on blood vessels. In the adult brain, the NSC cell bodies are displaced from the ventricular surface by the ependymal cells (E cells), but they remain in contact with the cerebrospinal fluid (CSF) through their thin apical processes, which are encircled by the large apical surfaces of E cells, forming characteristic pinwheel-like structures. Considering the elongated structure of NSCs, which bridge all the compartments of the SEZ, it has been proposed that this germinal region can be subdivided into different domains that may be relevant in the regulation of NSCs biology and function,

providing them with different extrinsic signals along their apicobasal axis (Lim and Alvarez-Buylla, 2016; Obernier and Alvarez-Buylla, 2019; **Figure 4**).

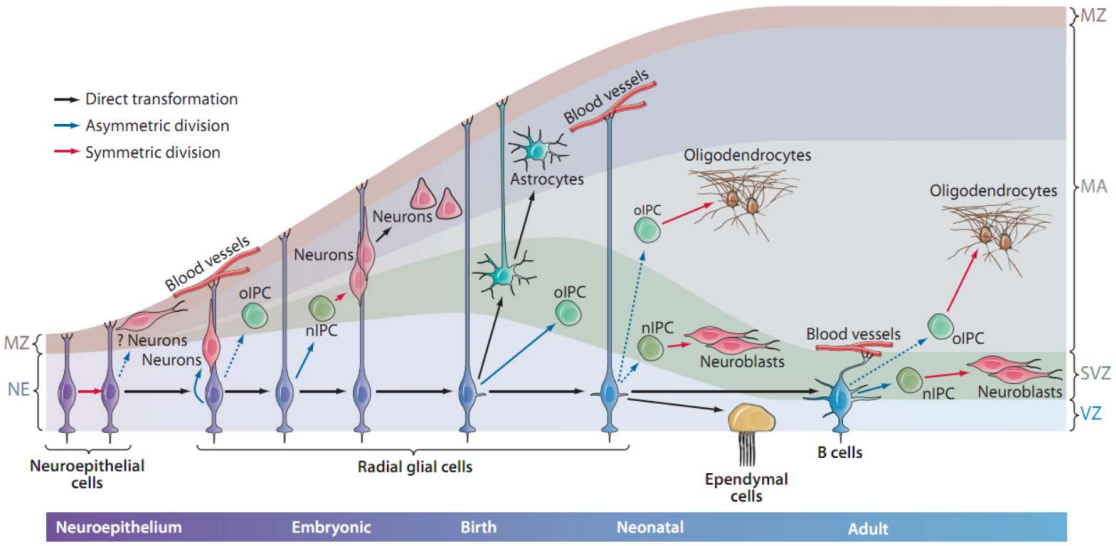

Figure 3| Embryonic origin of adult NSCs. During embryonic development, radial glial cells (RGCs) located in the ventricular zone (VZ) generate neurons, astrocytes, oligodendrocytes and ependymal cells either directly or through intermediate progenitor cells (IPCs). At late stages of development, some of these RGCs are converted into NSCs (B cells) that remain through the postnatal and adult life. Adapted from Kriegstein and Alvarez-Buylla, 2009.

1.3.3. The regulation of SEZ-resident NSCs

The SEZ constitutes a complex microenvironment in which quiescence, self-renewal and differentiation of NSCs are tightly regulated, both by extrinsic and intrinsic factors. Although the characterization of adult NSCs has progressed significantly since their identification more than fifty years ago (Altman and Das, 1965), the mechanisms that underlie the life-long maintenance of the NSC pool while ensuring neurogenesis are still not fully understood (Obernier and Alvarez-Buylla, 2019).

1.3.3.1. Niche-dependent regulation: extrinsic factors

Within the niche, NSCs are in close contact with the other cellular components (other NSCs, ependymal cells, TAPs and neuroblasts). Moreover, the cytoarchitecture of the SEZ allows their simultaneous interaction with the local extracellular matrix (ECM), which can retain cytokines and growth factors, and with soluble factors produced either locally or systemically (Obernier and Alvarez-Buylla, 2019).

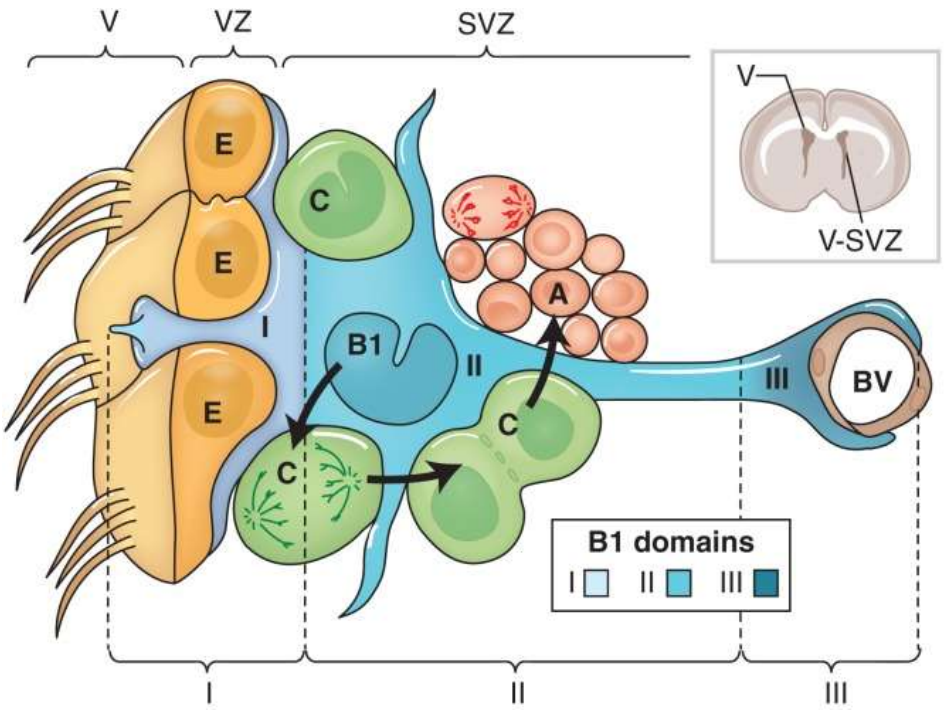

Figure 4| Cytoarchitecture and cellular composition of the SEZ. The SEZ can be subdivided into three domains according to the structure and organization of NSC (blue): the apical domain (I), which contains the apical processes of NSCs and the body of ependymal cells (yellow); the intermediate domain (II), containing the soma of most NSCs, in contact with TAPs (green) and newly-formed neuroblasts (light red); and the basal domain, which contains the basal processes of NSCs, with end-feet on blood vessels (brown). E, ependymal cells; B1, NSC; C, TAPs; A, neuroblasts; BV, blood vessel. Adapted from Lim and Alvarez-Buylla, 2016.

On their apical portion, NSCs are in contact with the cerebrospinal fluid (CSF) that fills the ventricular system through their primary cilium, which is likely involved in signal transduction. The CSF is continuously propelled by the motile cilia bundles of ependymal cells and contains multiple signaling molecules, such as Shh, FGFs or LIF, which are fundamental for the regulation of NSCs and their progeny (Mirzadeh et al., 2008; Obernier and Alvarez-Buylla, 2019). On the other hand, on their basal part, NSCs interact with blood vessels at specialized sites where the blood-brain barrier (BBB) is more permeable due to the absence of astrocyte end-feet, establishing highly dynamic interactions. There, NSCs are in contact with factors secreted by endothelial cells and also receive signals from the blood stream, including cytokines, hormones and metabolites that can pass through the BBB (Chaker et al., 2016; Obernier et al., 2018). Additionally, NSCs respond to multiple neurotransmitters and receive multiple neuronal inputs, either from SEZ-resident cells, as

for instance neuroblasts, or from distant sources, such as serotonergic neurons from the dorsal raphe nucleus or dopaminergic neurons from the *substantia nigra* and the ventral tegmental area (Obernier and Alvarez-Buylla, 2019).

1.3.3.2. Intrinsic regulators of adult NSCs

On the one hand, cell-cycle progression needs to be tightly regulated in the case of NSC to ensure both their self-renewal and the generation of new neurons and glia throughout adult life. In order to safeguard NSC maintenance and to avoid the exhaustion of the pool, CDK (cycling-dependent kinases) inhibitors such as p21, p27 or p57 are essential (Ming and Song, 2011). For instance, p21 acts simultaneously favoring NSC self-renewal, which is at least in part mediated by the repression of *Sox2*; and preventing the premature differentiation of these cells by the negative regulation of *Bmp2* expression (Kippin et al., 2005; Marqués-torrejón et al., 2013; Porlan et al., 2013).

On the other hand, NSC behavior is highly regulated both at the transcriptional and post-transcriptional levels. As in the case of other systems, transcription factors play a crucial role. Nevertheless, many other components contribute to the regulation of NSC gene expression, as non-coding RNAs or chromatin-modifying proteins, involving both DNA methylation and histone modifications (Bond et al., 2015; Lim and Alvarez-Buylla, 2016). Recently, thanks to the availability of single-cell RNA-seq (scRNA-seq) datasets from the adult SEZ (Dulken et al., 2017; Llorens-Bobadilla et al., 2015; Mizrak et al., 2019) it has been possible to better understand the complex gene regulatory networks that regulate NSC biology and function at the whole-genome level (Bond et al., 2015). Additionally, these analyses have reveal that mRNAs typically associated with differentiated cells can be already detected in NSCs (Beckervordersandforth et al., 2010; Dulken et al., 2017; Llorens-Bobadilla et al., 2015). Moreover, it has been recently shown that in this context some transcripts are translated less efficiently than would be expected considering their mRNA levels (Baser et al., 2019). Altogether, these observations point to an important influence of post-transcriptional regulation in the control of adult neurogenesis; and suggest the existence of additional regulatory mechanisms that remain to be identified.

2. *Scratch* genes

Scratch and Snail families originated by duplication of an ancestral *snail* gene in the metazoan ancestor and together compose the Snail superfamily (Barrallo-Gimeno and Nieto, 2009; Manzanares et al., 2001). Snail superfamily members encode for C_2H_2 zinc-finger transcription factors, which play essential roles both during embryonic development and in some pathological situations (Barrallo-Gimeno and Nieto, 2005; Nieto, 2002). Both Snail and Scratch transcription factors are widely expressed during embryonic development, although they occupy complementary territories, being Snail family members expressed in mesenchymal and mesodermal cells, whereas Scratch genes are neural-specific (Marín and Nieto, 2006; Nakakura et al., 2001a; Nieto, 2002).

2.1. Evolutionary history of the Snail superfamily

Although related, Snail and Scratch families are two independent entities. The phylogenetic analysis of the member genes in different species revealed that both families share a common origin in evolution, constituting an independent subgroup within the C_2H_2 zinc-finger transcription factors (Barrallo-Gimeno & Nieto, 2009; Manzanares et al., 2001; **Figure 5**).

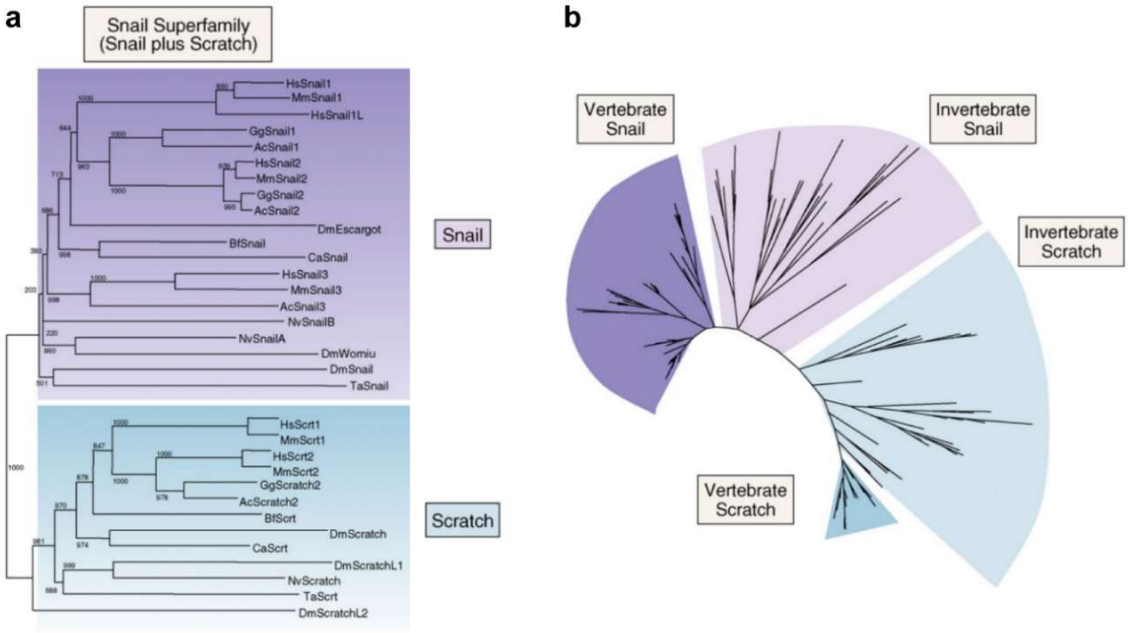

Figure 5| Phylogenetic trees of the Snail superfamily. (a) Neighbor-joining phylogenetic tree of

the Snail superfamily, including both vertebrate and invertebrate members. **(b)** Phylogenetic tree of the Snail superfamily generated using the Bayesian Interference method and considering >150 sequences from 52 different species. Modified from Barrallo-Gimeno & Nieto, 2009.

The divergence of the Snail and Scratch families was the result of the duplication of a single proto-*snail* gene at the base of metazoans, giving rise to *snail* and *scratch* (**Figure 6a;** Barrallo-Gimeno and Nieto, 2009). Subsequently, in Protostomes additional tandem duplications gave rise to the three members of the Scratch family in insects (*scratch*, *scratchL1* and *scratchL2*) and also to the triplication of Snail genes (*snail*, *escargot* and *worniu*) in the *Drosophilidae* lineage. In vertebrates, the current paralogs of the superfamily arose from independent whole-genome duplications. The first duplication in the vertebrate lineage led to the generation of *Snail1*/*Snail2* ancestor, as well as *Snail3*. This duplication event also generated *Scratch1* and *Scratch2*. Afterwards, a second genome duplication in teleosts increased the number of members of the superfamily in this lineage (Barrallo-Gimeno & Nieto, 2009; **Figure 6b**).

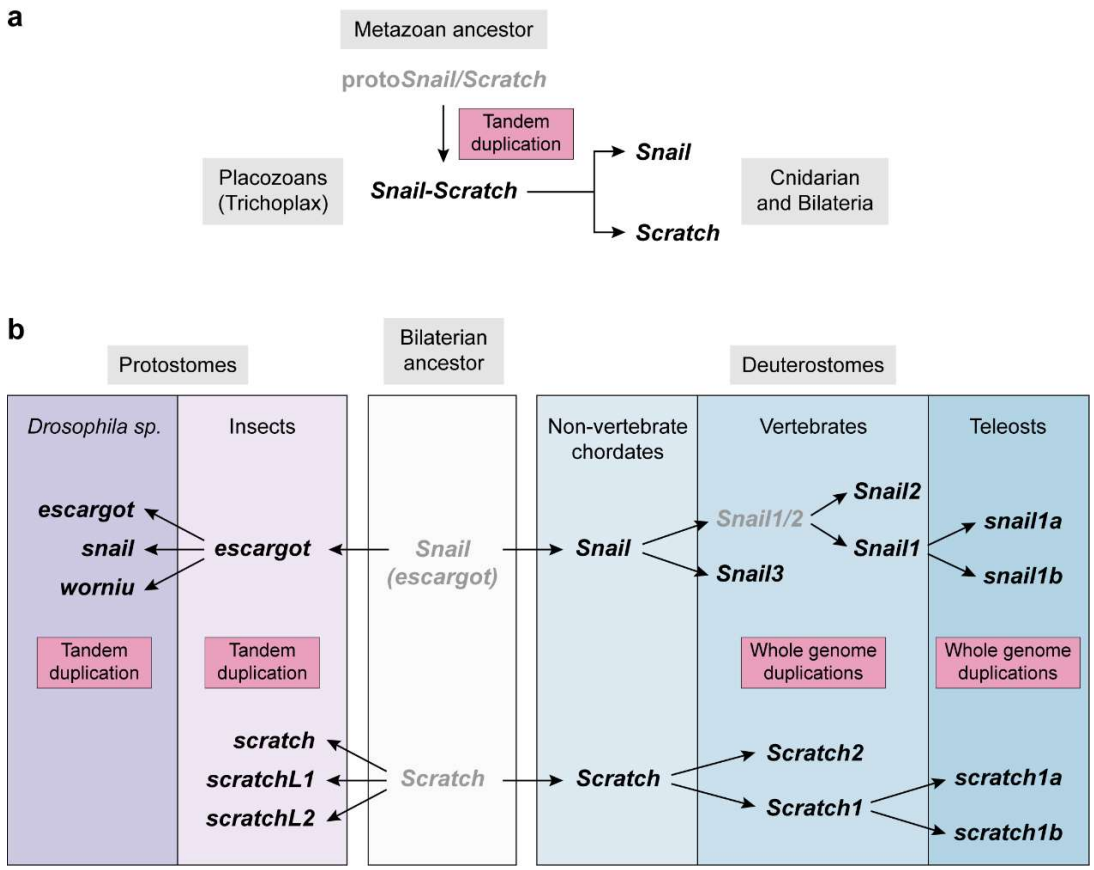

Figure 6| Putative evolutionary history of the Snail/Scratch superfamily. (a) The superfamily

had its origin at the base of metazoans, when the duplication of an ancestral gene gave rise to *Snail* and *Scratch*. **(b)** Subsequently, independent duplications in Protostomes and Deuterostomes increased the number of members in Bilaterians, resulting in the current composition of the Snail/Scratch superfamily. Ancestral genes are shown in grey. Modified from Barrallo-Gimeno & Nieto, 2009.

2.2. Structure and signature domains of Scratch proteins

All the transcription factors of the Snail superfamily share a similar organization (**Figure 7**). Their C-terminal portion contains from four to six C_2H_2 zinc-fingers, which act as a sequence-specific DNA-binding motifs, and is highly conserved among the members of the two families (Barrallo-Gimeno and Nieto, 2009; Manzanares et al., 2001). These zinc-fingers specifically recognize the consensus binding sequence for Snail superfamily transcription factors, which is identical to the E box (CAGGTG), the core of the consensus binding site of basic helix-loop-helix (bHLH) transcription factors, suggesting that these two families of proteins might compete for the same biding sites (Nieto, 2002; Reece-Hoyes et al., 2009).

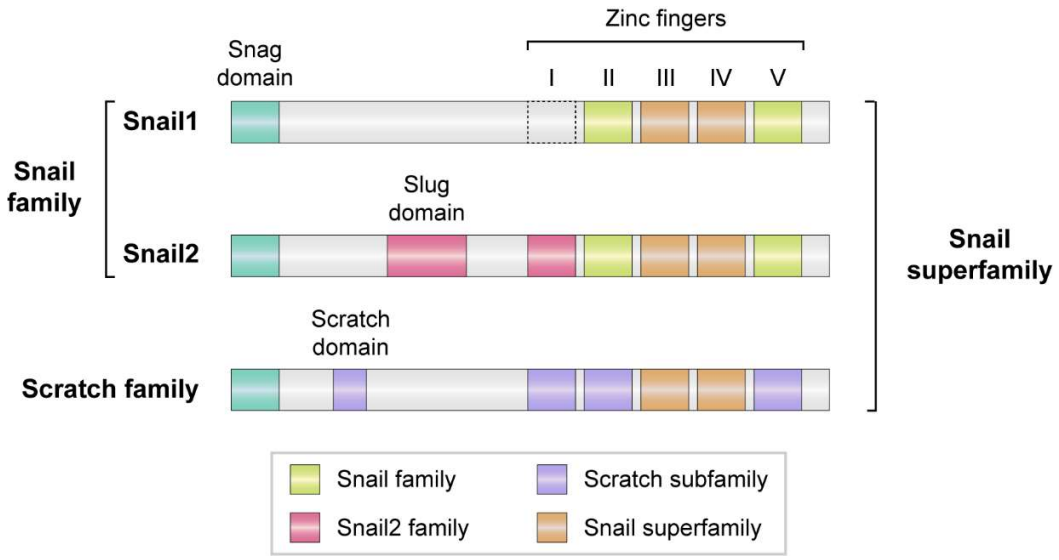

Figure 7| Structure of Snail superfamily members in vertebrates. The SNAG domain, located in the N-terminal end of the protein, and the zinc-fingers are conserved in all the members. In mammals and teleosts Snail1 has lost the first finger, which seems to be dispensable, as it does not contact the DNA. Scratch family proteins are characterized by the presence of the Scratch domain, whereas the Slug domain is exclusive of the Snail2 subfamily. Domains that define the different groups of proteins are depicted according with the following color code: Snail superfamily: orange; Snail family: yellow; Scratch family: purple; and Snail2 subfamily: pink. Modified from Manzanares et al., 2001.

On the other hand, the N-terminal half of the protein exhibits more variability among the members, but also contains a conserved motif located at the very N-terminal end of the protein, the SNAG (Snail/Gfi) domain, which is involved in transcriptional repression, since it is required for the interaction with co-repressors (Langer et al., 2008; Peinado et al., 2004, 2005). This domain, although present in all Snail superfamily proteins, can be detected in other C_2H_2 zinc-finger transcription factors as well and, therefore, is not a distinctive feature of this superfamily (Barrallo-Gimeno and Nieto, 2009; Dam et al., 2011; Manzanares et al., 2001).

In addition, both Snail2 and Scratch present specific domains in this N-terminal portion of the protein. Regarding Snail2, all the members described so far in different species present the Slug domain. Scratch proteins contain the Scratch domain, conserved in vertebrates, or an equivalent domain, as is the case for *Drosophila* scratch (Manzanares et al., 2001).

2.3. The function of Scratch transcription factors

The first member of the Scratch family to be described was *Drosophila scratch* (Roark et al., 1995). This gene, as all the other members of the family, is exclusively expressed in the nervous system (Barrallo-Gimeno and Nieto, 2009; Dam et al., 2011; Roark et al., 1995; Vieceli et al., 2013). In particular, *Drosophila scratch* is expressed in the vast majority of neuronal precursors, where it promotes the acquisition of neuronal fates by repressing the transcription of genes that favor non-neuronal cell fates (Roark et al., 1995). Additionally, it was shown later that, in the cell lineages that give rise to the *Drosophila* sensory organs, Scratch contributes to the neuronal specification by repressing the expression of Notch pathway target genes, reducing the activity of this signaling pathway and contributing to maintain neural commitment (Ramat et al., 2016).

Accordingly, Scratch proteins promote neuronal differentiation in other species, as is the case of *Caenorhabditis elegans* Scratch homolog CES-1 (cell death specification 1; Metzstein & Horvitz, 1999). Moreover, in nematodes, CES-1 plays a crucial role in the neurosecretory motorneuron (NSM) lineage, where it simultaneously regulates cell cycle progression, cell polarity and apoptosis. This lineage originates from a NSM neuroblast, which asymmetrically divides to give rise to two different daughter cells: the NSM, which survives and differentiates in a serotonergic motorneuron; and the NSM sister cell, which undergoes apoptosis (Hatzold and Conradt, 2008; Sulston et al., 1983). In this system, a

gain of function mutation in *ces-1* confers to the NSM sister cell resistance to cell death by displacing bHLH transcription factors HLH-2 and HLH-3 from E boxes, which in turn prevents the expression of the cell death activator *egl-1* (egg-laying abnormal-1; Ellis and Horvitz, 1991; Metzstein and Horvitz, 1999; Thellmann et al., 2003). Remarkably, the *ces-1* gain of function mutation also alters the cell polarity of the NSM neuroblast, which in this context divides symmetrically instead of asymmetrically, as happens in wild-type animals (Hatzold and Conradt, 2008). This is at least in part mediated by the CES-1-dependent repression of *pig-1*, which promotes NSM neuroblast asymmetric division (Wei et al., 2017). Furthermore, CES-1 also regulates NSM neuroblast cell cycle progression by repressing the expression of *cdc-25.2* gene, which encodes a phosphatase required to counteract the inhibition of Cyclin-dependent kinases (CDKs) by phosphorylation and, therefore, to activate them (Yan et al., 2013). In this lineage, the expression of *ces-1* is negatively regulated by CES-2 (cell specification-2) and DNJ-11 (DnaJ domain-11), which cooperate to reduce CES-1 levels in the NSM sister cell, promoting apoptosis (Ellis and Horvitz, 1991). The repression of *ces-1* expression by these two factors is also important for the establishment of NSM neuroblast polarity required for the asymmetric division of this cell. After this asymmetric division, CES-1 protein is restricted to the NSM, where it promotes survival by repressing the expression of *egl-1* (Hatzold and Conradt, 2008). According to this, in *ces-2*, *dnj-11* or *ces-1* mutants the levels of CES-1 protein are altered in the NSM neuroblast, which as a consequence divides symmetrically, giving rise to two daughter cells, both containing CES-1 protein, which survive (Hatzold and Conradt, 2008). Therefore, CES-1 plays a prominent role in the NSM lineage, where it regulates key processes that are fundamental for the normal development of these neurons.

On the other hand, moving on to vertebrates, three *scratch* paralogs (*scratch1a*, *scratch1b* and *scratch2*) have been identified in zebrafish (Dam et al., 2011). The expression of these genes is restricted to the central nervous system, being the three of them detectable in several regions of the developing brain. In addition, *scratch2* is also expressed in the spinal cord of zebrafish, where it is essential to ensure that the appropriate number of neurons is generated during development (Rodríguez-Aznar and Nieto, 2011; Rodríguez-Aznar et al., 2013). This is achieved in part thanks to the repression of *puma* expression by scratch2, which protects the newly formed neurons from undergoing apoptosis during normal embryonic development. Moreover, this regulatory network also controls programed cell death in response to DNA damage, situation in which *scratch2* expression is activated directly by p53 to antagonize damage-induced apoptosis (Rodríguez-Aznar and Nieto,

2011). On the other hand, scratch2 also prevents the re-entry of spinal cord postmitotic neurons into the cell cycle by repressing the expression of miR-25, which in turn contributes to maintain high levels of the cell cycle inhibitor p57 (Rodríguez-Aznar et al., 2013). Therefore, in the zebrafish spinal cord, scratch2 simultaneously controls the survival and the proliferation of the newly generated neurons, contributing to safeguard their homeostasis.

Furthermore, two Scratch family members have been identified in mammals: *Scratch1* and *Scratch2* (Manzanares et al., 2001; Nakakura et al., 2001a), which are widely expressed in several regions of the developing and adult brain, as well as in the spinal cord and in the inner nuclear layer of the retina (Marín and Nieto, 2006; Nakakura et al., 2001a). During cortical development, these two transcription factors, whose expression is activated by some proneural bHLH proteins, such as Neurog1, Neurog2 or Ascl1, play determinant roles (Itoh et al., 2013; Paul et al., 2014). On the one hand, both Scratch1 and Scratch2 favor neuronal migration during the development of mouse neocortex, at least in part through the repression of bHLH target genes after binding to their E-boxes (Itoh et al., 2013; Nakakura et al., 2001a; Paul et al., 2014). On the other hand, as described in other species such as *Drosophila* or *C. elegans* (Metzstein and Horvitz, 1999; Roark et al., 1995), they are also involved in promoting neuronal differentiation (Nakakura et al., 2001b; Paul et al., 2014). In the context of mammalian cortical development, Scratch2 favors the direct mode of neurogenesis, promoting the production of neurons at the expense of the generation of intermediate progenitors. By this means, Scratch2 stimulates neuronal differentiation without impacting on the proliferation or the cell cycle exit of the intermediate progenitors (Paul et al., 2014). In addition, it has been recently shown that *Scratch1* is one of the first genes that are expressed in response to the artificial induction of microglia-neuron reprogramming, pointing to a role for this transcription factor driving the acquisition of the neuronal fate during the early stages of this process (Matsuda et al., 2019).

3. RNA metabolism and post-transcriptional regulation of gene expression

3.1. RNA processing and nuclear export

In eukaryotes, transcription and translation take place in two different compartments of the cell, physically separated by the nuclear envelop. This compartmentalization enables an extensive processing of the transcripts before they are available for translation, including capping, splicing and polyadenylation. These processing reactions are conducted by a complex machinery of ribonuclear proteins, which coordinate the different steps in the gene expression pathway and couple them to nuclear export, ensuring that only mature mRNAs arrive to the cytoplasm to be translated (Stewart, 2019).

3.1.1 Splicing

Most metazoans genes contain introns, which need to be removed to obtain mature mRNAs before the translation of an uninterrupted protein coding sequence takes place (Stewart, 2019).

Splicing is based on the recognition of introns and exons by the splicing machinery. Intron boundaries are defined by the 5' (5'SS) and 3' splice sites (3'SS), which typically comprise the dinucleotides GU and AG respectively. These two sites, together with the branch point (BP), are the substrates for splicing catalysis. The BP is located about 18-40 nucleotides upstream from the 3'SS, separated from each other by a sequence enriched in pyrimidines, known as the polypyrimidine tract (PPT), which facilitates the recognition of the 3'SS during spliceosome assembly (Herzel et al., 2017; Keren et al., 2010; **Figure 8a**).

Pre-mRNA splicing involves two sequential transesterification reactions. In the first step (branching), the hydroxyl group of the conserved BP adenosine exerts a nucleophilic attack on a phosphate present in the 5'SS, producing a free 5' exon and a branched intron lariat attached to the 3' exon. In the second step (ligation), the free 3' hydroxyl group of the 5' exon attacks a phosphate in the 3'SS, generating a ligated exon and a residual lariat intron (Herzel et al., 2017; Ren et al., 2019; **Figure 8b**). These two transesterification reactions are chemically simple, but their catalysis involves a large ribonucleoprotein complex, known as the spliceosome, integrated by five small nuclear RNAs (snRNAs) and over 175 proteins in human (Fica and Nagai, 2017; Herzel et al., 2017). Spliceosome assembly, which takes

place *de novo* for each intron of a given pre-mRNA, depends rigorously on the detection of the 5'SS, the BP and the 3'SS, which at the first stages of the process induced the recruitment of the different components of this complex (Shi, 2017).

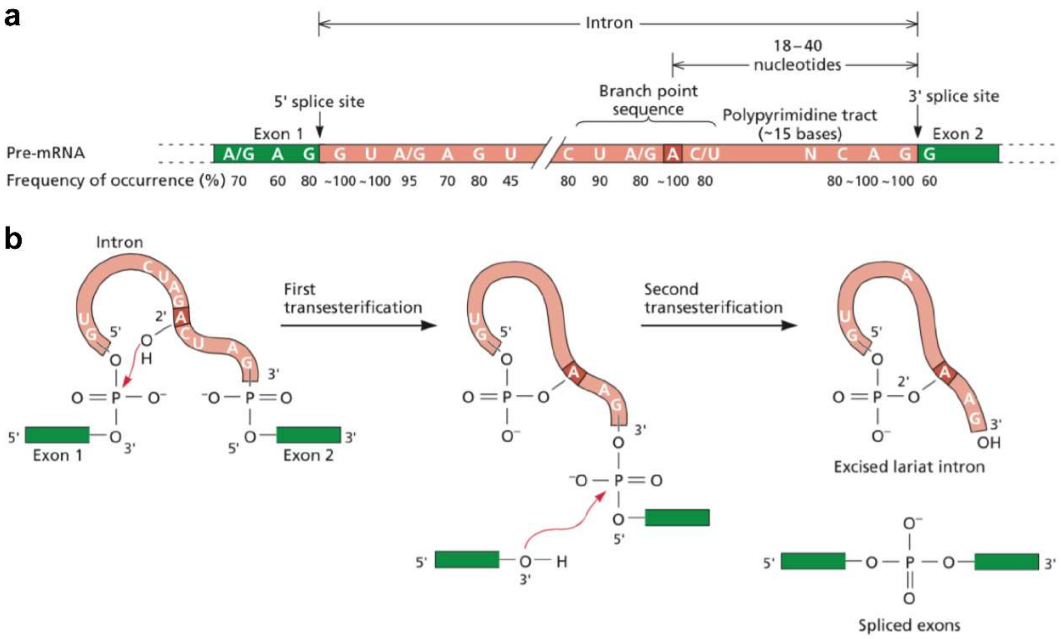

Figure 8| Intron architecture and mRNA splicing catalysis. (a) The main four conserved motifs that enable the recognition of introns by the spliceosome are the 5' and 3' splice sites (5'SS and 3'SS, respectively), the branch point (BP) and the polypyrimidine tract (PPT). **(b)** A two-step transesterification reaction that take place during pre-mRNA splicing. First, the BP attacks the 3'SS and after the 5'SS attacks the 3'SS, yielding a ligated 5' exon–3' exon and releasing the intron lariat. Adapted from Principles of Virology (2009), American Society for Microbiology.

Splicing is regulated at several levels, most of the times in a tissue- or developmental stage-specific manner. Splicing sites can be classified as strong or weak depending on the divergence between their sequence and the consensus sequence, which determines their affinity for the different components of the spliceosome. Strong splice sites usually lead to constitutive splicing, whereas the usage of weak splice sites depends on the cellular context and is regulated by both cis-regulatory sequences, including intronic splicing enhancers (ISEs), intronic splicing silencers (ISSs), exonic splicing enhancers (ESEs) and exonic splicing silencers (ESSs); and trans-acting factors, such as serine/arginine (SR) proteins, heterogeneous nuclear ribonucleoproteins (hnRNPs) or tissue-specific factors as PTP and nPTB (Kornblihtt et al., 2013).

3.1.2 mRNA nuclear export

Nuclear export of mature mRNAs to the cytoplasm is a conserved mechanism in eukaryotes, from yeast to humans, although it presents its own peculiarities in each species. Although some endogenous mRNAs and viral RNAs are exported following a pathway dependent on CRM1 (also known as exportin 1), most mRNAs associate with the complex formed by NXF1 and its cofactor p15 for their export through nuclear pore complexes (NPCs). In addition to transport factors, which binds RNA in a non-specific manner, export adaptors are needed to mediate the interaction between the mRNA molecule and the export receptors (Köhler and Hurt, 2007; Stewart, 2019).

Nuclear export is a key step for gene expression in eukaryotes and only takes place when mature mRNAs have been generated, which requires a precise coordination between this process and the nuclear processing of the transcripts in terms of polyadenylation, capping and splicing (Stewart, 2019). The integration of the nuclear steps of gene expression and the nuclear export of the mature mRNAs is achieved thanks to the TREX complex, which is primarily recruited by the splicing machinery through its binding to the exon-junction complex (EJC), contributing to the generation of export-competent messenger ribonucleoprotein particles (mRNPs). Then, these particles move to the nuclear periphery and the mRNA is transferred from the TREX complex to the NXF1/p15 complex to transit to the NPCs towards the cytoplasm, where transcripts can be translated. Once there, mRNPs disassemble, ensuring that the mRNA do not re-enter into the nucleus ((Köhler and Hurt, 2007; Stewart, 2019; Wickramasinghe and Laskey, 2015); **Figure 9**).

Although splicing and nuclear export were initially thought to be of the few constitutive steps in gene expression, there is accumulating evidence indicating that in some cases they can be highly selective, preventing the translation of some transcripts or, on the contrary, giving priority to some in specific contexts. This specificity can modulate multiple biological processes, including the maintenance of pluripotency, cell proliferation, cell survival or hematopoiesis, among others (Sibley et al., 2016; Wickramasinghe and Laskey, 2015).

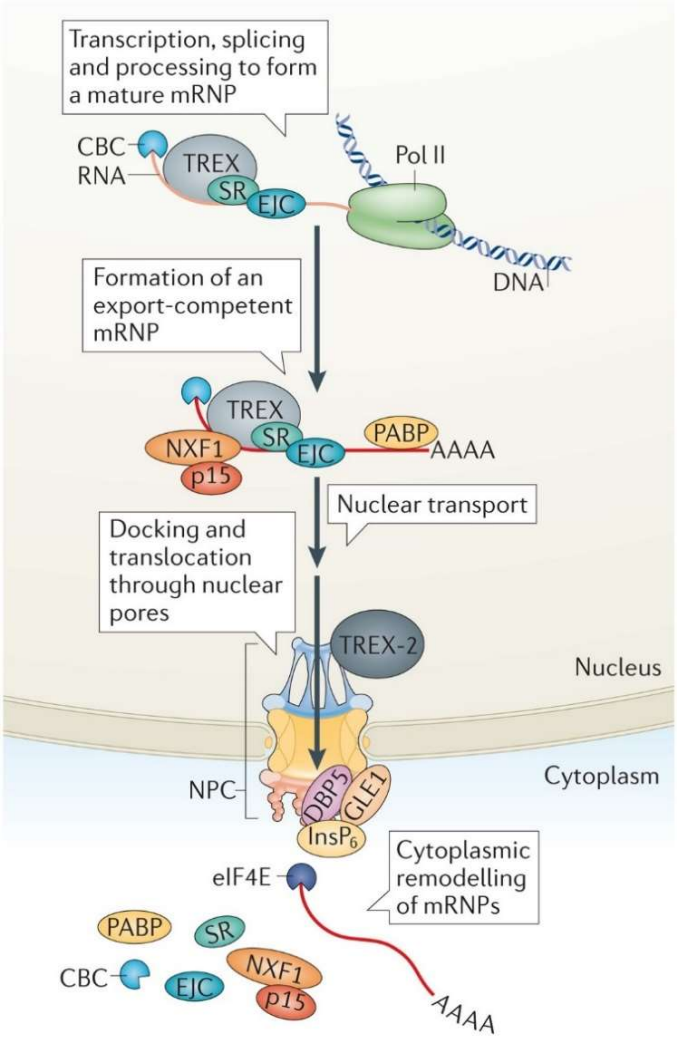

Figure 9| Splicing-coupled mRNA export. Nuclear export is coupled to capping, splicing and polyadenylation of the nascent transcripts. During this process, the splicing machinery is responsible for the recruitment of the TREX complex once transcripts have been spliced. Then, cargo mRNAs are transferred from this complex to the NXF1/p15 complex for their transit through nuclear pore complexes (NPCs). Once in the cytoplasm, the export receptors are removed from the cargo mRNAs, preventing their re-entry into the nucleus. Adapted from Wickramasinghe and Laskey, 2015.

3.2. Intron retention

Nuclear export has been shown to be the default pathway for mature mRNAs, unless they contain elements that actively promote their nuclear retention (Akef et al., 2015). This raises the question of what happens with transcripts that, due to alternative splicing events (ASEs), suffer intron retention (IR). Although this type of alternative splicing has been classically considered to be the result of the malfunctioning of splicing machinery and to lead only to reduced expression, mRNAs containing retained introns may have different fates, including nuclear degradation and elimination once in the cytoplasm via non-sense mediated decay (NMD), but also the generation of alternative protein isoforms when they are translated (Jacob and Smith, 2017).

Recently, it has become evident the existence of introns that remain unspliced in polyadenylated transcripts in which other introns have been removed. These introns, which can be later spliced in response to specific signals, are known as detained introns (DI; Boutz et al., 2015). This type of retained introns is much more prevalent than anticipated, affecting most of the protein-coding genes in mammals and occurring in all the tissues analyzed so far, although most of the events are tissue or cell type-specific (Braunschweig et al., 2014; Middleton et al., 2017).

Intron retention is associated with particular cis-acting features, including the presence of weaker splice sites compared to those present in constitutively spliced introns, a higher GC content and a shorter length on average (Braunschweig et al., 2014). Furthermore, intron detention (ID) events tend to affect only one intron in each gene and tend to occur in long pre-mRNAs. Consistent with the latter, it has been proposed that ID facilitates the response to external stimuli within a shorter timeframe, allowing the rapid production of protein without requiring *de novo* transcription (Monteuuis et al., 2019). Additionally, ID-mRNAs enables the generation of reservoirs of pre-mRNAs that can be posteriorly spliced and translated, allowing changes in gene expression even in cell types that are not transcriptionally active, as is the case of platelets (Denis et al., 2005; Schwertz et al., 2006; Shashkin et al., 2008).

Intron detention is involved in the regulation of multiple biological processes, such as spermatogenesis (Naro et al., 2017) or hematopoiesis (Cho et al., 2014; Edwards et al., 2015; Ni et al., 2016; Pimentel et al., 2016; Wong et al., 2013), affecting in many cases the expression of proteins that have cell type-specific functions (Jacob and Smith, 2017). Moreover, detained introns can be spliced in response to a variety of stimuli, including neuronal activation (Mauger et al., 2016) or cellular stress (Ninomiya et al., 2011; Shalgi et al., 2014). These observations highlight the relevance of intron detention in the fine-tuning of gene expression, standing as an additional layer of regulation at the post-transcriptional level.

4. The epitranscriptome: Dynamic RNA modifications

It has become increasingly evident that post-transcriptional mRNA modifications play an important role in the regulation of gene expression. Although some of these modifications were already identified decades ago (Davis and Allen, 1957; Desrosiers et al., 1974; Perry and Kelley, 1974), the recent development of methodological approaches have allowed their mapping and characterization. Several chemical mRNA modifications have been identified since the 60s, including N^6-methyadenosine (m^6A), N^6,2'-O-dimethyadenosine (m^6Am), N^1-methyladenosine (m^1A), N^7-methylguanosine (m^7G), 5-methylcytidine (m^5C), 5-hydroxymethylcytidine (hm^5C), N^4-acetylcytidine (ac^4C), pseudouridine (ψ) and 2'-O-methylated nucleotides (Seo and Kleiner, 2020).

Among these modifications, N^6-methyladenosine (m^6A) is the most prevalent in mammalian mRNA; and has been also detected in small non-coding RNA (sncRNA) and long non-coding RNA (lncRNA) in multiple eukaryotic species (Frye and Blanco, 2016). It has been estimated that there are 1-5 m^6A residues per mRNA molecule, preferentially located in long exons, near stop codons and in 3'UTRs. Most m^6A sites in mammals are found within the consensus motif RRm^6ACH (R=A or G, G>A; H=A, U or C, U>A>C), although only a small fraction of them are detectably methylated *in vivo*, as a consequence of the tissue- and cell type-specific deposition of this modification (Gilbert et al., 2016). The abundance and function of m^6A, which is a reversible modification, are determined by the interplay between its methyltransferases (writers), demethylases (erasers) and m^6A binding proteins (readers; Frye and Blanco, 2016).

4.1. m^6A decoration: writers, erasers and readers

m^6A is deposited by a multicomponent methyltransferase complex (MTC), composed of the core components methyltransferase-like 3 (METTL3) and methyltransferase-like 14 (METTL14); and additional regulatory factors, including Wilms tumor 1 associated protein (WTAP), KIAA1429/VIRMA, RBM15/15B, CBLL1/HAKAI, and ZC3H13 (Zhang et al., 2020). Within this complex, METTL3 is the catalytic subunit, whereas METTL14 acts as a scaffold for RNA binding. Both METTL3 and METTL14 are highly conserved in mammals and form a stable heterodimer that is essential for m^6A-mRNA methylation, causing the deletion of any of these two methyltransferases a 99% reduction in the levels of mRNA methylation (Gilbert et al., 2016; Yang et al., 2018).

The reversibility of m^{6}A modification relies on the existence of demethylases or erasers, including fat mass and obesity-associated protein (FTO) and alkB homolog 5 (ALKBH5), which are able to revert N^6-methyladenosine to adenosine through oxidative demethylation. These two enzymes are widely expressed both during embryonic development and in adult tissues, although they are particularly enriched in the brain and in testes, respectively, suggesting that additional tissue-specific demethylases may remain to be identified in the future (Seo and Kleiner, 2020; Yang et al., 2018).

The effects of m^{6}A on mRNA can be mediated either by affecting the secondary structure of the transcripts (structural switch) or by the direct interaction of this modification with specific reader proteins. On the one hand, m^{6}A sites tend to be unstructured due to the destabilization of A-U pairs caused by this modification (Engel and von Hippel, 1974; Roost et al., 2015; Spitale et al., 2015), which in turn modulates the accessibility of RNA binding proteins (Harcourt et al., 2017). On the other hand, m^{6}A can directly recruit proteins of the YTH domain family, including YTHDF1, YTHDF2, YTHDF3, YTHDC1 and YTHDC2 (Dominissini et al., 2012; Roundtree et al., 2017a). Additionally, other RNA binding proteins act as readers for these modification, including ELAV-like protein 1 (ELAVL1), eukaryotic translation initiation factor 3 (eIF3) or insulin-like growth factor 2 mRNA-binding proteins (IGF2BPs) among others (Seo and Kleiner, 2020).

4.2. The role of m^{6}A modification at the molecular and cellular level

Interestingly, the majority of mRNA-modifying enzymes exhibit a nuclear localization, allowing m^{6}A to influence mRNA biogenesis from the earliest steps (Gilbert et al., 2016). This modification has been shown to regulate nearly every aspect of mRNA metabolism, from transcription and pre-mRNA processing to translation and mRNA stability (Yang et al., 2018; **Figure 10**). Some of these regulatory effects are mediated by the m^{6}A-induced structural switch, as for instance in the case of splicing, which is enhanced by the increase accessibility for heterogeneous nuclear ribonucleoprotein C and G (HNRNPC/G) binding as a result of m^{6}A modification (Harcourt et al., 2017; Liu et al., 2015, 2017). On the other hand, other m^{6}A functions are mediated by its interaction with specific readers, as is the case for the regulation of mRNA nuclear export. In this case, part of m^{6}A-dependent regulation is mediated by YTHDC1, which, through the binding to this modification, recruits the export adaptor protein SRSF3 and the export receptor NXF1 to m^{6}A-methylated mRNAs, promoting their export to the cytoplasm (Roundtree et al., 2017b; Seo and Kleiner, 2020).

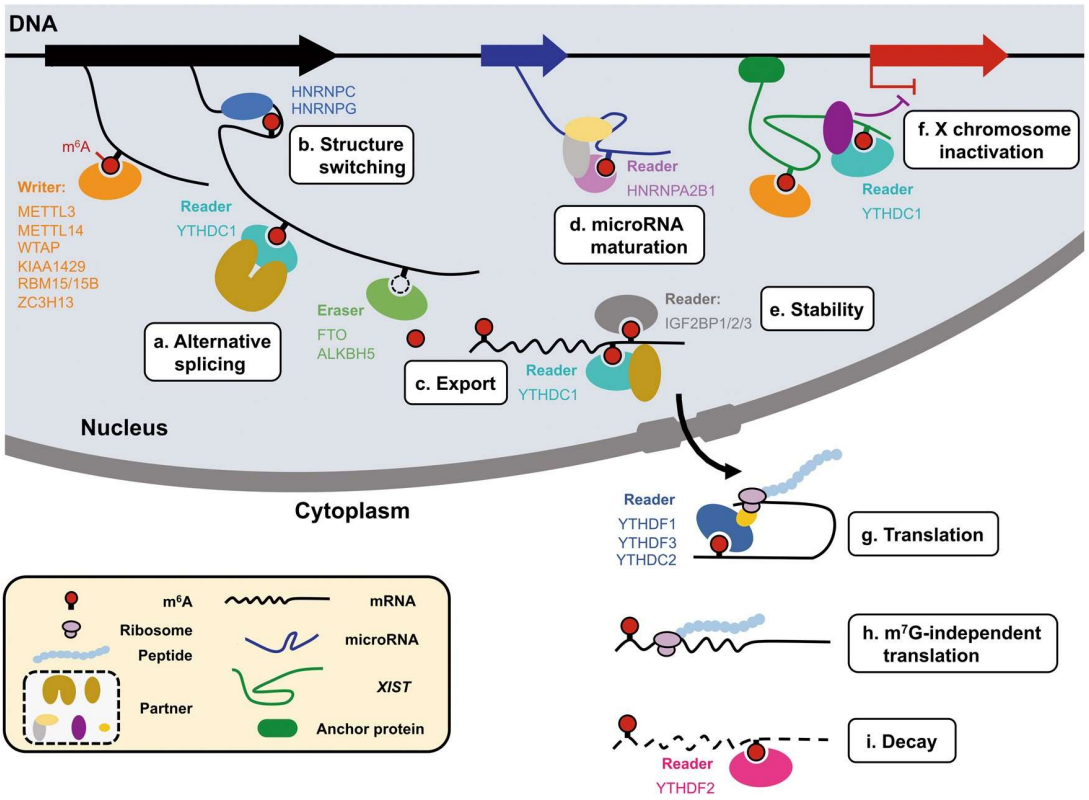

Figure 10| m^{6}A-mediated regulation of mRNA metabolism. Nascent transcripts can be co-transcriptionally modified by m^{6}A writer enzymes. At the molecular level, this modification has the potential to affect almost every step in gene expression, including splicing, nuclear export, translation and mRNA stability. Adapted from Yang et al., 2018.

The modulation of gene expression associated with m^{6}A modification has functional consequences on a variety of higher order biological processes, including early embryonic development, cell differentiation and immune response; and also in some pathological situations, such as cancer (Seo and Kleiner, 2020). For instance, m^{6}A mRNA modification is essential for the proper development of the nervous system, as well as for the maintenance of its function (Livneh et al., 2020; Noack and Calegari, 2018). In this sense, it has been recently shown that conditional depletion of either *Mettl3* or *Mettl14* during cortical development alters both neurogenesis and gliogenesis, due to defects in the m^{6}A-dependent decay of some transcripts associated with stemness, cell cycle regulation and differentiation (Wang et al., 2018; Yoon et al., 2017). Accordingly, the m^{6}A reader YTHDF2 has been involved in the degradation of transcripts related to neural development (Li et al., 2018b). In addition, several neural-specific m^{6}A-binding proteins have been identified, as is the case of fragile X mental retardation protein (FMRP), which promotes the nuclear export of m^{6}A-mRNAs during cortical development (Edens et al., 2019); and proline rich coiled-coli

2A (Prrc2a), which regulates both the proliferation of oligodendrocyte progenitor cells (OPCs) and the acquisition of oligodendrocyte fate through the stabilization of *Olig2* mRNA (Wu et al., 2019). On the other hand, m^6A modification is also linked to the regulation of adult neurogenesis, which is evidenced by the reduction adult NSCs proliferation and differentiation into neurons and glia produced by the loss of the demethylase FTO (Li et al., 2017).

Altogether these observations indicate that m^6A, as well as other post-transcriptional mRNA modifications, provide a mechanism to coordinately regulate the fate of groups of transcripts during a variety of biological process and in response to different cellular and environmental cues, contributing to the fine-tuning of both gene expression and protein translation (Frye et al., 2018; Roundtree et al., 2017a).

Objectives

Recent studies analyzing the transcriptomic dynamics that take place during NSC activation and differentiation have shown that lineage progression is tightly controlled during adult neurogenesis, both at the transcriptional and post-transcriptional levels. Moreover, thanks to the development of new technical approaches, which have enabled the availability of a large amount of high-throughput sequencing information, it has become increasingly evident that classically neglected regulatory mechanisms, such as intron retention or post-transcriptional mRNA modifications, have a pivotal role in the control of gene expression in a variety of biological processes.

General objective

The aim of this thesis is understanding the role of *Scratch* genes in adult neurogenesis.

Considering our preliminary data on the expression of *Scratch* genes in the adult brain (Marin and Nieto, 2006) and the described roles in neuronal survival and differentiation in zebrafish and mouse embryos (Rodriguez-Aznar and Nieto, 2011; Rodriguez-Aznar et al., 2013; Itoh et al., 2013; Paul et al., 2014), we wanted to assess their role in adult neurogenesis in the mouse.

Specific objectives

1. Characterizing the expression pattern of *Scratch1* in the adult neurogenic niche

2. Analyzing the function of Scratch1 transcription factor

3. Revealing the molecular mechanisms that regulate Scratch1 expression in the adult brain

Material and methods

1. Experimental animals

1.1. Mice

All experiments were performed using adult C57BL/6J wild-type mice between 2 and 4 months-old as a source of biological samples. All animal procedures were conducted in compliance with the European Community Council Directive (2010/63/EU) and Spanish legislation. The protocols were approved by the CSIC Ethical Committee and the Animal Welfare Committee at the Institute of Neurosciences (Alicante).

1.2. Zebrafish

All the experiments were performed using 6 months-old zebrafishes of the AB strain, which were maintained at 28ºC under standard conditions. All animal procedures were conducted in compliance with the European Community Council Directive (2010/63/EU) and Spanish legislation. The protocols were approved by the CSIC Ethical Committee and the Animal Welfare Committee at the Institute of Neurosciences (Alicante).

2. Perfusion and histological analysis

With the aim of preserving brain structure and cell integrity for subsequent histological analysis, adult mice were anesthetized using isofluorane and transcardially perfused with 0.1M Phosphate-buffered Saline pH 7.4 (PBS), followed by 4% paraformaldehyde (PFA) in diethyl pyrocarbonate (DEPC)-treated 0.1M PBS at a flow rate of 5.5 ml/min. Then, brains were extracted and post-fixed by immersion in the same fixative overnight (o/n). After washing the tissue with PBS, brains were serially sectioned into 30-50 µm coronal sections using a Leica VT1000 vibratome and subsequently processed according to the protocol for each particular technique.

3. *In situ* hybridization

In all the cases, *in situ* hybridization (ISH) was performed following a protocol adapted from that previously described by Acloque et al., 2008.

3.1. Probe synthesis

Labeled probes were synthesized by *in vitro* transcription of the DNA template in the presence of ribonucleotides labeled with digoxygenin (DIG). Probe constructs carrying each template (1 µg) were linearized with proper restriction enzymes. After checking that the linearization was complete, RNA probe transcription was performed using Promega kit containing 5x transcription buffer, 0.1M dithiothreitol (DTT), T3/T7/SP6 RNA polymerases and RNasin (40U/µl) plus nucleotide mix (Roche). The mix was incubated for 3h at 37ºC. Next, probes were purified by the addition of 1/10 3M sodium acetate and 2.5 volumes of ethanol and the subsequent incubation at -20ºC o/n. The product was then centrifuged 30 minutes at 13000 rpm at 4ºC, washed twice with 70% ethanol, air dried and re-dissolved in 1:1 volume of nuclease-free water and formamide. Finally, the quality of probes was checked by electrophoresis on 1% agarose/TAE gel and, if satisfactory, immediately used or stored at -80ºC.

Templates for probes that were not previously available were amplified by PCR from their respective cDNA (to generate probes for mature or total mRNA) or genomic DNA (to obtain intronic probes) and subcloned into the pGEMT-easy vector (Promega) or pCR-Blunt II-TOPO vector (Thermo Fisher).

3.2. Fluorescent *in situ* hybridization in mouse brain sections

After dissection and post-fixation of mouse brains and collection of serial coronal sections in a Leica VT1000 vibratome, the tissue was washed twice with ice-cold PBS-DEPC 0.1% Tween20 (PBS-T) and dehydrated through a series of PBS-T solutions with increasing concentrations of methanol (25%, 50%, 75% and 100%), then twice in methanol 100% and kept o/n at -20ºC. Next, sections were rehydrated through the reverse series of PBS-T/methanol solutions and washed twice in PBS-T. In order to inactivate endogenous peroxidase activity, sections were then incubated in 1% H_2O_2 for 40 minutes and then washed three times with PBS-T. Then, sections were treated with 10 µg/ml proteinase K in PBS-T for 3 minutes at room temperature (RT). After that, they were re-fixed with 4%PFA-DEPC for 20 min at RT and washed twice in PBS-T. Sections were then incubated in prehybridization solution (50% formamide, 5X SSC, 2% Roche blocking powder, 0.1% Tween20, 50 mg/ml heparin, 1mg/ml tRNA, 1mM EDTA, 0.1% CHAPS in DEPC-treated dH_2O) at 60ºC for 1 hour first, and then o/n after refreshing prehybridization solution. Sections were either used the next day for ISH or stored at -20ºC.

Next, prehybridized sections were incubated with 1 µg/ml of denatured DIG-labeled probes o/n at 60ºC. After that, they were washed twice with 2x SSC, 0.1% CHAPS, then twice with 0.2x SSC, 0.1% CHAPS at 60ºC and finally with KTBT washing buffer (50mM Tris-HCl pH7.5, 150mM NaCl, 10mM KCl, 0.1% Triton X-100 in H_2O). After the washes, sections were incubated in blocking solution (20% goat serum, 0.7% Roche blocking solution in KTBT) for 3h at 4ºC. For probe detection, sections were then incubated with 1:500 dilution of an anti-DIG peroxidase (POD)-conjugated antibody in blocking solution o/n at 4ºC. The whole next day, sections were washed many times in KTBT buffer and kept o/n in KTBT at RT. For developing, sections were incubated with Amplification solution (TSA® fluorescein detection kit, PerkinElmer) for 1 minute, following manufacturer's instructions. FITC or Cy3 (1:100) were added to the Amplification solution for developing green or red colors, respectively and sections were incubated in the mix for 45 minutes in dark at RT. Then, they were washed several times with KTBT, stained with DAPI and imaged with Olympus DV1200 confocal microscope.

For combination of ISH with immunofluorescence, primary antibodies (**Table 1**) were added to the sections with the antibody for probe detection. After developing, sections were incubated with the appropriate secondary antibodies (**Table 2**), washed several times with PBS, stained with DAPI and subjected to confocal microscope imaging.

Antibody	Host	Dilution	Application	Provider	Cat. no.
βIII-tubulin	Mouse	1:300	IF	Covance	PRB-435P
Cleaved-caspase3	Rabbit	1:1000	IF	Cell Signaling	9664S
Digoxigenin-POD	Sheep	1:500	FISH	Roche	11207733910
Doublecortin	Rabbit	1:1000	IF	Abcam	ab18723
GFAP	Chicken	1:600	IF	Millipore	ab5541
GFAP	Rabbit	1:300	IF	Dako	2033429-2
HuC/D	Mouse	1:1000	IF	Invitrogen	A21271
Ki67	Rabbit	1:150	IF	Abcam	ab15580
Nestin	Mouse	1:4	IF	Hybridoma Bank	Rat-401
NeuN	Rabbit	1:500	IF	Abcam	ab128886
Nucleoporin	Mouse	1:500	IF	Abcam	ab24609

Table 1| List of primary antibodies. IF, Immunofluorescence; FISH, Fluorescent *in situ* hybridization.

Antibody	Dilution	Application	Provider	Cat. no.
Alexa Fluor® 568 anti-chicken	1:500	IF	Thermo Fisher	A11041
Alexa Fluor® 568 anti-mouse	1:500	IF	Thermo Fisher	A11004
Alexa Fluor® 568 anti-rabbit	1:500	IF	Thermo Fisher	A11011
Alexa Fluor® 647 anti-rabbit	1:500	IF	Thermo Fisher	A27040
Alexa Fluor® 568 Streptoavidin-conjugated	1:500	FISH	Thermo Fisher	S11226

Table 2| List of secondary antibodies. FISH, Fluorescent *in situ* hybridization; IF, Immunofluorescence.

3.3. Fluorescent *in situ* hybridization in zebrafish brain

In the case of zebrafish, brains were obtained from 6 months-old wild-type animals from the AB strain. Heads were dissected, washed in PBS-T and fixed with 4% PFA prepared in PBS-DEPC o/n at 4ºC. Next day, brains were extracted, dehydrated through a series of PBS-T solutions with increasing concentrations of methanol (25%, 50%, 75% and 100%) and kept in methanol 100% o/n at 4ºC. After that, brains were rehydrated through methanol:PBS-T solutions in reverse order, washed twice in PBS-T, incubated in 1% H_2O_2 for 40 minutes and then washed again with PBS-T. Then, they were treated with 10 µg/ml proteinase K in PBS-T for 6 minutes at RT and re-fixed with 4% PFA-DEPC for 20 minutes. After that, brains were washed with PBS-T and incubated with prehybridization solution at 60ºC for 1 hour first, and then o/n after refreshing the solution. Brains were either used the next day for ISH or stored at -20ºC.

After that, prehybridized sections were incubated with 1 µg/ml of denatured DIG-labeled probes o/n at 60ºC and, next day, washed twice with 2x SSC, 0.1% CHAPS, then twice with 0.2x SSC, 0.1% CHAPS at 60ºC and finally with KTBT buffer. Next, brains were embedded in 2% agarose in PBS-DEPC and sectioned into 50 µm thickness coronal sections using a Leica VT1000 vibratome. After washing with PBS-T, sections were incubated with blocking solution for 3 hours at 4ºC and, then, with 1:500 dilution of POD-conjugated antibodies anti-DIG in blocking solution o/n at 4ºC. The corresponding primary antibodies for immunofluorescence (**Table 1**) were added at the same time when required. All the posterior steps were performed as previously described for mouse brain sections.

3.4. *In situ* hybridization in cultured cells

To perform *in situ* hybridization in cells in culture, cells were seeded on an adhesive matrix. For that, the day before seeding the cells, glass coverslips were incubated with 2% methylcellulose or 1% Matrigel® diluted in Control Medium (see **Table 3**), depending on the experiment, at 37ºC in a 5% CO_2 humidified incubator. The day after, the cells were plated at the desired density after washing the plates twice with sterile dH_2O.

In order to detect the mRNA by *in situ* hybridization, cells were fixed with 2% PFA prepared in PBS-DEPC 15 minutes at RT. After, they were washed three times with PBS-T and, in case the samples were prepared for fluorescent *in situ* hybridization, they were incubated with 1% H_2O_2 for 20 minutes and washed again three times with PBS-T. Cells were then incubated with prehybridization solution at 60ºC for 1 hour, and then o/n after refreshing prehybridization solution. Samples were either used the next day for ISH or stored at -20ºC.

Then, cells were incubated with 1 µg/ml of denatured DIG-labeled probes o/n at 60ºC and, next day, washed three times with the first washing solution (50% formamide, 5x SSC, 1% SDS in H_2O) at 60ºC, then three times with the second washing solution (50% formamide, 2x SSC in H_2O) at 60ºC and finally three times with TBST (140 mM NaCl, 2.7 mM KCl, 25 mM Tris-HCl pH7.5, 0.1% Tween20 in H_2O) at RT.

For visible *in situ* hybridization, cells were incubated with blocking solution (10% FBS in TBST) for 1 hour at RT. Then, they were incubated with 1:1000 alkaline phosphatase (AP)-conjugated anti-DIG antibody diluted in blocking solution o/n at 4ºC. Next day, cells were washed many times with TBST and kept in this buffer o/n. The following day, they were washed twice with TBST and then three times with NTMT (100mM Tris-HCl pH9.5, 59mM MgCl2, 100mM NaCl, 0.1% Tween-20, 1mM levamisole in H_2O). For developing, cells were incubated with NTMT containing freshly-added 3 µl NBT and 2.6 µl BCIP per 1ml (developing solution), in the dark at RT until the color reaction develops. In order to stop the developing reaction, cells were washed several times with TBST, fixed with 4% PFA and washed again with TBST. Samples were imaged using a Leica DMR microscope.

For fluorescent *in situ* hybridization, cells were incubated with blocking solution for 1 hour at RT and after with 1:500 dilution of an anti-DIG POD-conjugated antibody in blocking solution o/n at 4ºC. Cells were incubated also with primary antibodies for immunofluorescence (**Table 1**) at the same time when necessary. The whole next day,

sections were washed many times in TBST buffer and kept o/n in TBST at RT. The next day, after several washes with TBST, cells were incubated with Amplification Solution (Perkin Elmer) for 1 minute to adjust the pH and then with FITC or Cy3 (1:100) diluted in Amplification Solution for 15 minutes in dark at RT. Then, cells were washed several times with TBST, incubated with the corresponding secondary antibodies (**Table 2**), washed again with TBST, stained with DAPI and imaged with Olympus FV1200 confocal microscope.

3.5. DNA *in situ* hybridization in cell cultures

For DNA *in situ* hybridization, cells were plated on 0.2% gelatin-coated glass coverslips. After they attached to the matrix, cells were fixed with 2% PFA for 15 min at RT. Next, they were washed three times with PBS, incubated with 0.2% pepsin for 4 minutes at 37ºC and post-fixed with 4% PFA for 5 minutes at RT. After washing twice with PBS, cells were dehydrated by incubating them with 70%, 90% and 100% ethanol, 3 minutes each; and after the coverslips were air dried for several minutes. In the meantime, *chromosome 15* specific probe labeled with biotin (Chrombios®) was denatured by incubating it for 6 minutes at 72ºC. Then, cells were incubated with the denatured probe o/n at 60ºC. The day after, samples were washed once with 2x SSC at 60ºC, three times with 50% formamide 2x SSC at 60ºC and twice with Tris-Saline-Tween buffer (TST; 1x saline, 0.1M Tris, 0.05% Tween20 in H_2O) at RT. After that, cells were incubated with blocking solution (TSBSA; 1x saline, 0.1M Tris, 20% BSA in H_2O) for 1 hour at RT and then with 1:500 dilution of Alexa Fluor™ 568-conjugated Streptavidin (Thermo Fisher). Finally, samples were washed several times with TST, stained with DAPI and imaged with an Olympus FV1200 confocal microscope.

4. Neural Stem Cell cultures

Neural stem cells (NSCs) isolated from the adult SEZ can be cultured in medium containing basic fibroblast growth factor (bFGF) and epidermal growth factor (EGF). Under those conditions, NSCs proliferate and form clonal aggregates, called neurospheres. NSC cultures can be expanded and maintained for several passages thanks to their capacity to self-renew and generate new aggregates upon neurosphere dissociation (Belenguer et al., 2016; Ferrón et al., 2007).

4.1. Culture media

Reagent	Working concentration	Stock conc./ Storage T[a]	Provider	Cat. no.
D-Glucose	0.6%	30% (-20ºC)	Sigma	G7021
$NaHCO_3$	0.1%	7.5% (4ºC)	Sigma	S5761
HEPES	5 mM	1 M (4ºC)	Sigma	H3375
L-Glutamine	2 mM	200 mM (-20ºC)	Gibco	25030-024
Penicillin-Streptomycin	1x	100x (-20ºC)	Gibco	15140-122
Hormone mix	1x	10x (-20ºC)	Homemade (see **Table 4**)	
Heparin sodium salt	0.7 U/ml	350 U/ml (4ºC)	Sigma	H3149
BSA	4 mg/ml	Powder (4ºC)	Sigma	B4287
DMEM	0.5x	1x (4ºC)	Sigma	D6429
Nutrient mixture F12	0.5x	1x (4ºC)	Sigma	N6658

Table 3| Composition of Control medium. BSA, Bovine Serum Albumin; DMEM, Dulbecco's Modified Eagle Medium; F12, Ham's F12 Nutrient Mixture.

Reagent	Working concentration	Stock conc./ Storage T[a]	Provider	Cat. no.
D-Glucose	0.6%	30% (-20ºC)	Sigma	G7021
$NaHCO_3$	0.1%	7.5% (4ºC)	Sigma	S5761
HEPES	5 mM	1 M (4ºC)	Sigma	H3375
Apo-transferrin	0.8 mg/ml	Powder (-20ºC)	Sigma	T2252
Bovine insulin	500 nM	5 µM (-20ºC)	Sigma	I6634
Putrescine	0.1 mg/ml	1 mg/ml (-20ºC)	Sigma	P7505
Progesterone	0.2 nM	2 mM (-20ºC)	Sigma	P6149
Sodium selenite	0.3 µM	3 mM (-20ºC)	Sigma	S9133
DMEM	0.5x	1x (4ºC)	Sigma	D6429
Nutrient mixture F12	0.5x	1x (4ºC)	Sigma	N6658

Table 4| Composition of 10x Hormone mix. DMEM, Dulbecco's Modified Eagle Medium; F12, Ham's F12 Nutrient Mixture

Reagent	Working concentration	Stock conc./ Storage T[a]	Provider	Cat. no.
Control medium		Homemade (see **Table 1**)		
EGF	20 ng/ml	4 µg/ml (-20ºC)	Gibco	53003-018
bFGF	10 ng/ml	25 µg/ml (-20ºC)	Sigma	F0291

Table 5| Composition of Complete medium. EGF, Epidermal Growth Factor; bFGF, basic Fibroblast Growth Factor.

4.2. Establishment of primary NSC culture

In order to establish primary cultures of adult NSCs, mice from 2 to 4 months were sacrificed by cervical dislocation and brains were extracted and placed in a plate with ice-cold PBS. Then, both SEZs from each mouse were dissected, chop into small pieces and enzymatically digested by incubation in 1 ml of previously activated Papain solution (see **Table 6**) for 30 minutes at 37ºC. After the digestion, the reaction was stopped by the addition of Control medium (see **Table 3**) and the tissue was mechanically dissociated pipetting up and down the cellular suspension. Then, cells were washed in 10 ml of Control medium, centrifuged at 1000 rpm for 10 min and the pellet was resuspended in Complete medium (see **Table 5**).

Reagent	Working concentration	Stock conc./ Storage T[a]	Provider	Cat. no.
Papain	12 U/ml	384 U/ml (4ºC)	Sigma	P3125
L-Cystein hydrochloride	0.2 mg/ml	Powder (RT)	Sigma	C8277
EDTA	0.2 mg/ml	Powder (RT)	Sigma	E6511
EBSS	1x	1x (4ºC)	Gibco	24010-043

Table 6| Composition of Digestion solution. EBSS, Earle's Balanced Salt Solution.

For the establishment of the cultures, cells obtained from each brain (2 SEZs) were plated in 8 wells of a 48-well plate with 500 µl of Complete medium per well and incubated at 37ºC in a 5% CO_2 humidified incubator for between 7 and 10 days.

4.3. Subculture and bulk expansion of established NSC cultures

Once primary cultures were established, grown neurospheres were collected in 15 ml conical tubes and centrifuged 5-7 minutes at 700-1000 rpm, depending on their overall size. Neurospheres were then dissociated by incubation with Accutase® solution (Sigma) for 10 minutes at RT, in combination with mechanical disaggregation by pipetting up and down several times. After the digestion, Control medium was added to the tubes in order to stop the reaction and individual cells were collected by centrifugation at 1000 rpm for 10 minutes. After removing the supernatant, cells were resuspended in Complete medium. Then, the concentration of viable cells was estimated by Trypan Blue exclusion on a Neubauer chamber. Finally, for bulk expansion, cells were seeded in a density of 10,000 cells/cm^2 in Complete medium and incubated at 37ºC in a 5% CO_2 humidified incubator for 5-7 days, until new neurospheres were formed.

4.4. Cryopreservation of NSCs

Once neurosphere cultures were established and expanded, they were cryopreserved for future use. To do so, grown neurospheres were dissociated as previously described and the concentration of viable cells was estimated by Trypan Blue exclusion on a Neubauer chamber. Then, 2 x 10^6 cells were resuspended in fresh Complete medium supplemented with 10% dimethyl sulfoxide (DMSO), transferred to a cryotube and placed at -80ºC in a freezing container. For long-term storage, cryotubes were stored in a liquid nitrogen tank.

In order to thaw cells, vials were placed in a 37ºC water bath until they were completely thawed. Then, cells were transferred to a 15 ml tube with Control medium and centrifuged at 1000 rpm for 10 minutes. After that, cells were resuspended in Complete medium, plated and incubated at 37ºC in a 5% CO_2 humidified incubator until new neurospheres were formed.

4.5. Lentiviral infection for shRNA gene silencing

In order to perform loss of function experiments in NSCs, cultures of these cells were transduced with lentiviruses (LVs) carrying either control constructs or different specific shRNAs for the genes of interest. This LV-mediated gene delivery system allows the long-term transduction of the cells and the generation of stable cell cultures in which the expression of a given gene has been downregulated.

4.5.1. Lentiviral production and titration

LVs containing shRNA constructs were generated using HEK293T packaging cells, which were maintained in HEK293T medium (see **Table 7**). For that purpose, the day before transfection 8.5 x 10^6 HEK293T cells were plated in a 15 cm plastic dish and incubated at 37ºC in a 5% CO_2 humidified incubator with LV medium (DMEM supplemented with 10% FBS). Next day, cells were transfected with a solution containing 15 µg of psPAX2 plasmid, 10 µg of pmD2.G plasmid, 20 µg of the appropriate pGIPZ plasmid (see **Table 8**), 200 µl of 2.5 M $CaCl_2$ in a final volume of 2 ml. After 5 minutes of RT incubation, 2 ml of 2x HEPES Buffered Saline (HBS) were added dropwise and the solution was incubated for 20-30 minutes at RT, allowing the formation of a fine calcium phosphate-DNA precipitate. Subsequently, this solution was added to the HEK293T cells and cultures were incubated at 37ºC in a 5% CO_2 humidified incubator. After 16h, HEK293T medium was refreshed and cells were incubated for 24h before the collection of lentiviral particles. To do so, next day the medium of the cultures was collected, centrifuged 5 minutes at 2000 rpm and filtered through a 0.22 µm pore nitrocellulose filter. Then, a concentrated solution of lentiviral particles was obtained by ultracentrifugation for 90 min at 25,000 rpm with a SW-32Ti rotor in an Optima XL-100K ultracentrifuge (Beckman Coulter). Next, the supernatant was discarded and the pellet was resuspended in sterile PBS and kept at -80ºC until used.

For lentiviral titration, the day before infection HEK293T cells were plated at a density of 50,000 cells per well in a 6-well plate and incubated at 37ºC in a 5% CO_2 humidified incubator with HEK293T medium. Next day, HEK293T cells were infected with serial dilutions, from 10^{-3} to 10^{-8}, of the lentiviral stock prepared in HEK293T medium supplemented with 8 µg/ml Polybrene reagent (Sigma) and returned to the incubator for 72 additional hours. Then, cells were harvested, resuspended in fixing solution (0.5% PFA and 2% FBS in sterile PBS) and the percentage of GFP-positive cells in the cultures was quantified using a FACSAria III flow cytometer (BD Biosciencies). The titer of the lentiviral stocks was calculated using the following formula:

$$\text{Titer (TU/ml)} = \frac{\text{Percentage of GFP}^+ \text{ cells}}{100} \text{ x Number of cells infected x Dilution factor}$$

Only the cultures in which the percentage of GFP-positive cells was between 1% and 20% were consider in the analysis, in order to ensure the reliability of the measurements and to minimize the number of cells infected by multiple lentiviral particles in the samples.

Reagent	Working concentration	Stock conc./ Storage T[a]	Provider	Cat. no.
FBS (inactivated)	10%	Pure (-20ºC)		
Penicillin-Streptomycin	1x	100x (-20ºC)	Gibco	15140-122
L-Glutamine	2 mM	200 mM (-20ºC)	Gibco	25030-024
DMEM	1x	1x (4ºC)	Sigma	D6429

Table 7| Composition of HEK293T culture medium. DMEM, Dulbecco's Modified Eagle Medium; FBS, Fetal Bovine Serum.

Plasmid	Codified molecule	Reporter	Use	Provider	Cat. no.
psPAX2	Gag, Pol, Rev	None	Lentiviral packaging	Addgene	#12251
pmD2.G	Env	None		Addgene	#12253
pGIPZ non-silencing control vector	control shRNA	tGFP	Expression silencing	Open Biosystems	RHS4346
pGIPZ shRNA Scrt1 (shScrt1A)	shRNA *Scrt1*	tGFP		Open Biosystems	V3LMM_ 456558
pGIPZ shRNA Scrt1 (shScrt1B)	shRNA *Scrt1*	tGFP		Open Biosystems	V3LMM_ 456561

Table 8| Plasmids used for lentiviral production.

4.5.2. NSC transduction

For lentiviral transduction, neurospheres were dissociated by incubation with Accutase® solution (Sigma) for 10 minutes at RT and individual cells were incubated with $5x10^6$ TU/ml of lentiviral particles in Complete medium supplemented with 8 µg/ml Polybrene reagent (Sigma) for 1h. Then, 4 ml of Complete medium were added and cells were plated in 25 cm^2 flasks in the presence of the lentiviruses for 4-6h. Finally, transduced cells were washed, and incubated at 37ºC in a 5% CO_2 humidified incubator in Complete medium until new neurospheres were formed.

4.6. Induction of NSC differentiation

The day before seeding the cells, plates or coverslips were coated with Matrigel diluted 1:100 in Control medium and incubated for 24h at 37ºC in a 5% CO_2 humidified. Next day,

plates or coverslips were washed twice with sterile dH_2O prior the seeding of the cells.

In order to induce the differentiation of NSCs, neurospheres were dissociated and washed with Control medium to eliminate the remaining mitogens from Complete medium. Then, cells were seeded at a density of 80,000 cell/cm^2 on Matrigel coated plates with Differentiation medium I (Control medium supplemented with 10 ng/ml bFGF), which induces the initiation of the differentiation process. Two days later the Differentiation medium I was removed and replaced with Differentiation medium II (Control medium supplemented with 2% FBS) and cells were incubated for 5 additional days, allowing further differentiation.

For the experiments in which the cells were fixed less than 12 hours after the induction of differentiation, they were first seeded in Complete medium for 24 hours and then washed and incubated in Differentiation medium I for the time required.

4.7. Treatments with RNA methylation and EGF signaling inhibitors

When required for the experiments, NSC cultures were treated with different drugs. In order to block EGF signaling cells were treated either with Gefitinib (Selleck Chemicals; 2.5 μM) or Afatinib (Enzo Life Sciences; 2.5 μM), two different EGF receptor (EGFR) inhibitors that hinder its phosphorylation and, therefore, prevent signal transduction. On the other hand, NSCs were treated with 3-Deazaadenosine (DAA, Sigma; 100 μM), a strong inhibitor of m^6A RNA methylation (Fustin et al., 2013).

5. Embryonic Stem Cell culture

5.1. Maintenance of ESC cultures

The mouse embryonic stem cell (ESC) line 46C (Sox1-GFP-IRES-pac knock-in; PrimCells) was cultured on 0.1% gelatin-coated plates in ESC medium (see **Table 9**), which was refreshed every day. When confluence was reached, cells were detached from the plate by Trypsin/EDTA (Fisher) treatment, seeded in new gelatin-coated plates and incubated at 37ºC in a 5% CO_2 humidified incubator.

Induced pluripotent stem cells (iPSC) reprogrammed from NSC were kindly provided by Dr. Sacri Rodríguez Ferrón.

Reagent	Working concentration	Stock conc./ Storage T[a]	Provider	Cat. no.
FBS (ES tested)	10%	100% (-20ºC)	Capricorn	FBS-12A
L-Glutamine	2 mM	200 mM (-20ºC)	Gibco	25030-024
Sodium pyruvate	1mM	100 mM (4ºC)	Gibco	11360-070
NEAA	1x	100x (4ºC)	Gibco	11140-050
Penicillin-Streptomycin	1x	100x (-20ºC)	Gibco	15140-122
LIF	10 ng/ml	0.1mg/ml (-20ºC)	Prepotech	AF-300-05
B-Mercaptoethanol	0.1 mM	0.1 M (RT)	Sigma	M3148
GMEM	1x	1x (4ºC)	Sigma	G5154

Table 9| Composition of ES medium. FBS, Fetal Bovine Serum; GMEM, Glasgow Minimum Essential Medium; LIF, Leukemia Inhibitory Factor; NEAA, Non-Essential Amino Acids.

5.2. Generation of ESC-derived NSCs

NSC were derived from ESC as previously described in Conti et al., 2005. Briefly, 20,000 cells/cm^2 were seeded on gelatin-coated plates with N2B27 medium (see **Table 10**) and incubated at 37ºC in a 5% CO_2 humidified incubator for 7 days. The medium was refreshed every day. Under these conditions, a large proportion of the cells in the cultures underwent neural lineage specification during the firsts 4-5 days and exhibited clear features of neural differentiation from day 5 (5DIV) onwards. From day 6 on, cells were treated with 0.5 µg/ml puromycin (Calbiochem) for 48h, in order to select the cells that had undergone neural lineage specification (Sox1$^+$ cells).

Next, with the aim of obtaining homogenous NSC cultures, cells were collected and replated on uncoated culture dishes with NS medium (see **Table 12**) for 2-3 days, until neurosphere-like aggregates were formed. Then, aggregates were harvested and dissociated, and individual cells were plated on gelatin-coated plates with fresh NS medium. After some days, cell aggregates attached to the plate and acquired a bipolar morphology.

For the maintenance of ESC-derived NSC cultures, when confluence was reached, cells were trypsinized, replated on gelatin-coated plates with NS medium and incubated at 37ºC in a 5% CO_2 humidified incubator.

Reagent	Working concentration	Stock conc./ Storage T[a]	Provider	Cat. no.
N2	1x	10x (-20ºC)	Homemade (see **Table 11**)	
B27	0.5x	50x (-20º)	Gibco	17504-044
BSA (fraction V)	50 µg/ml	7.5% (4ºC)	Gibco	15260-037
Penicillin-Streptomycin	1x	100x (-20ºC)	Gibco	15140-122
Neurobasal media	0.5x	1x (4ºC)	Life technologies	21103-049
DMEM	0.25x	1x (4ºC)	Sigma	D6429
Nutrient mixture F12	0.25x	1x (4ºC)	Sigma	N6658

Table 10| Composition of N2B27 medium.

Reagent	Working concentration	Stock conc./ Storage T[a]	Provider	Cat. no.
Bovine insulin	250 µg/ml	1.25mg/ml (-20ºC)	Sigma	I6634
Apo-transferrin	1 mg/ml	Powder (-20ºC)	Sigma	T2252
Putrescine	160 µg/ml	1 mg/ml (-20ºC)	Sigma	P7505
Progesterone	60 ng/ml	2 mM (-20ºC)	Sigma	P6149
Sodium selenite	300 nM	3 mM (-20ºC)	Sigma	S9133
DMEM	0.25x	1x (4ºC)	Sigma	D6429
Nutrient mixture F12	0.25x	1x (4ºC)	Sigma	N6658

Table 11| Composition of N2 (10x).

Reagent	Working concentration	Stock conc./ Storage T[a]	Provider	Cat. no.
L-Glutamine	2 mM	200 mM (-20ºC)	Gibco	25030-024
N2	1x	10x (-20ºC)	Homemade (see **Table 11**)	
EGF	10 ng/ml	4 µg/ml (-20ºC)	Gibco	53003-018
bFGF	10 ng/ml	25 µg/ml (-20ºC)	Sigma	F0291
EuroMed-N media	1x	1x (4ºC)	Euroclone	

Table 12| Composition of NS medium.

6. Immunofluorescence in cultured cells

In order to obtain samples for immunofluorescence, the day before seeding, coverslips were incubated with Matrigel diluted 1:100 in Control medium incubated o/n at 37ºC in a 5% CO_2 humidified incubator. Coverslips were washed twice with dH_2O before the cells were seeded and, after incubation for the times required, they were fixed with 2% PFA at 37ºC for 15 minutes. After fixation, cells were washed 3 times with PBS and kept in PBS-0.05% azide at 4ºC until the analysis.

For immunolabelling, samples were washed three times with PBS and incubated with blocking solution (10% FBS and 1% Glycine in PBS) for 45 minutes at RT. Then, they were incubated with the indicated primary antibodies (see **Table 1**) diluted in blocking solution o/n at 4ºC. Next day, cells were incubated with the appropriate fluorescently-labeled secondary antibodies (see **Table 2**) diluted in blocking solution for 45 minutes at RT, counterstained with DAPI (Sigma; 1 µg/ml) and mounted with Mowiol.

Samples were imaged with a Leica DMR microscope (Leica) and analyzed with ImageJ software. Confocal images were obtained in an Olympus FV1200 confocal microscope (Olympus).

7. Molecular methods

7.1. Total RNA extraction, cDNA synthesis and qPCR analysis

For gene expression assays, total RNA was extracted using the Illustra RNAspin Mini isolation kit (GE healthcare), following manufacturer's instructions. Reverse transcription was carried out using the Maxima First Strand cDNA Synthesis kit (Thermo Scientific). Quantitative RT-PCR was performed in a Step One Plus machine (Applied Biosystems) using Fast SYBR Green Mastermix (Applied Biosystems) and the primers listed in **Table 13**. Relative levels of expression were calculated using the comparative Ct method normalized to the internal control TBP housekeeping transcript.

Gene	Sequence (5'→3')	Orientation
Actb-F	GCGAGCACAGCTTCTTTGC	Sense
Actb-R	CGACCAGCGCAGCGATA	Antisense
Bbc3-F	GCGGCGGAGACAAGAAGA	Sense
Bbc3-R	AGTCCCATGAAGAGATTGTACATGAC	Antisense
Cdkn1a-F	AACATCTCAGGGCCGAAA	Sense
Cdkn1a-R	TGCGCTTGGAGTGATAGAAA	Antisense
Gapdh-F	TGACCTCAACTACATGGTCTACA	Sense
Gapdh-R	CTTCCCATTCTCGGCCTTG	Antisense
Mdm2-F	TGTTTGGAGTCCCGAGTTTC	Sense
Mdm2-R	AGCCACTAAATTTCTGTAGATCATTG	Antisense
Nanog-F	CCTCCAGCAGATGCAAGAA	Sense
Nanog-R	GCTTGCACTTCATCCTTTGG	Antisense
Nestin-F	GAGAGGCGCTGGAACAGA	Sense
Nestin-R	TCTGACTCTGTAGACCCTGCTTC	Antisense
p53-F	AGTCACAGCACATGACGGA	Sense
p53-R	AGTCACAGCACATGACGGA	Antisense
Pouf5f1-F	CACGAGTGGAAAGCAACTCA	Sense
Pouf5f1-R	CTTCTGCAGGGCTTTCATGT	Antisense
Ptbp1-F	TGTGTGTATTCTGAGCTTCTATGTCC	Sense
Ptbp1-R	CCACCTGCAAGTTGGTCA	Antisense
Ptbp2-F	GCTCTGATACAGATGGCTGATG	Sense
Ptbp2-R	TCCATACATCTTCTGCCCATT	Antisense
TBP-F	CATGGACCAGAACAACAGCC	Sense
TBP-R	CGTAAGGCATCATTGGACT	Antisense
Scrt1(total)-F	CAGGAATCATGCCCAGGTCC	Sense
Scrt1(total)-R	TCGAGGTCTGCCGAAGAGAA	Antisense
Sox1-F	GCTTCCTAATGGTTTAGCGTTTT	Sense
Sox1-R	AACCACAGGAAAGAAATGCAA	Antisense
Zfp42-F	GGACTAAGAGCTGGGACACG	Sense
Zfp42-R	GCGATCCTGCTTTCTTCTGT	Antisense

Table 13| List of qPCR primers used.

7.2. RNA immunoprecipitation (RIP) assay

For sample preparation, the day before seeding the cells, 100 mm culture dishes were coated with Matrigel diluted 1:100 in Control medium. Next day, plates were washed twice with dH_2O and 60,000 cells/cm^2 were seeded and incubated at 37ºC in a 5% CO_2 humidified incubator in Complete medium. The day after, cultures were washed twice with Control medium and incubated in Differentiation medium I (Control medium supplemented with 10 ng/ml bFGF). When indicated, cells were washed with PBS and total RNA was extracted using mirVana miRNA Isolation Kit (Invitrogen).

m^6A RNA immunoprecipitation was carried out as described in Zeng et al., 2018, with minor modifications. Briefly, 60 µl of protein-A magnetic beads (BioRad) were washed twice with IP buffer (500 mM NaCl, 10 mM Tris-HCl, pH 7.5, 0.1% IGEPAL CA-630 in nuclease free H_2O) and blocked with a solution of 0.5 mg/ml BSA (Sigma) and 2 µg/ml salmon sperm DNA (Applied Biosystems) in IP buffer for 2 hours at 4ºC. Then, beads were incubated with 10 µg/ml anti-N^6-methyladenosine (m^6A) antibody (Sigma) or IgG control antibody (Diagenode; see Supplementary table 1) o/n at 4ºC with head-over-tail rotation. Next day, antibody-bound beads were washed twice with IP buffer and incubated with 2 µg of purified RNA for 4 hours at 4ºC, in the presence of 10 µl/ml RNasin ribonuclease inhibitor (Promega). Then, beads were washed twice in IP buffer, twice in low-salt IP buffer (50 mM NaCl, 10 mM Tris-HCl, pH 7.5, 0.1% IGEPAL CA-630 in nuclease free H_2O) and twice in high-salt IP buffer (500 mM NaCl, 10 mM Tris-HCl, pH 7.5, 0.1% IGEPAL CA-630 in nuclease free H_2O) for 10 minutes each at 4ºC. m^6A-enriched RNA was then eluted in TRIzol Reagent (Ambion) and isolated following manufacturer's instructions.

Reverse transcription and quantitative RT-PCR were performed as described above (see **Table 13** for the list of primers used). The expression percentage of a target gene in IP sample was calculated relative to that in input samples and normalized relative to *Gapdh* expression.

8. RNA-seq

Samples were prepared as described above for RIP assay. After RNA isolation, library preparation and high-throughput sequencing were performed by the Genomic Unit at the Centre for Genomic Regulation (CRG). Paired-end read (125 nt) libraries for assayed

conditions were produced using HiSeq v4 Chemistry kit (Illustra) and processed with the sequencer software HiSeq Control Software version 2.2.58. Sequencing quality was checked using FastQC (https://www.bioinformatics.babraham.ac.uk/projects/fastqc/).

Read alignment and gene count were performed using STAR version 2.5.3 [23104886] against Mus musculus genome assembly v10 (GRCm38 build; Ensembl). Differential gene expression analysis was performed with DESeq2 [25516281] using a Wald Test and p-values were adjusted for multiple testing using Benjamini-Hochberg FDR correction. Alternative splicing genome wide quantification was performed using VAST-TOOLS [28855263] against M. musculus v10 (GRCm38 build; Ensembl). Complementary analysis of intron retention was performed with ASpli R/Bioconductor package (http://bioconductor.org/packages/release/bioc/html/ASpli.html). Cluster analysis was performed using hierarchical and fuzzy c-means clustering using custom R scripts.

9. *In silico* analyses

9.1. Detection of potential m^{6}A sites

m^{6}A site prediction was performed using the primary Mus musculus *Scratch1* RNA sequence (ENSMUST00000096365.4, Ensembl) by applying TargetM6A method (Li et al., 2016; http://csbio.njust.edu.cn/bioinf/TargetM6A).

9.2. Analysis of *Scratch* intron sequences

Sequences of *Scratch* introns from different species were downloaded from Ensemble (http://www.ensembl.org/index.html). The annotation of the splicing sites, the branch point and the polypyrimidine tract was done manually.

9.3. Statistical analysis

All statistical analyses were carried out using Prism (GraphPad software, version 7.0). For cell counting and quantitative PCR experiments, treatments were compared to their corresponding controls using unpaired two-tailed Student's t- test. All bar graphs represent mean ± SEM (Standard Error of the Mean). Statistical significances were as follows: * = P≤0.05, ** = P≤0.01 and *** = P≤0.001.

Results

1. Scrtach1 in the adult neural stem cell niche

1.1. Characterization of *Scratch1* expression pattern in the SEZ

The expression pattern of *Scratch* genes in the mouse brain had been previously analyzed in the lab (Marín and Nieto, 2006), revealing that after embryonic development, when they are widely expressed, *Scratch1* expression is maintained in different regions during postnatal and adult stages, including the walls of the lateral ventricles (LVs). This area is of particular interest since it harbors the most active neurogenic niche in adult mammals, the SEZ (Obernier and Alvarez-Buylla, 2019). With this in mind, we decided to focus on this area and performed a more detailed characterization, in order to identify the specific cell types that expressed *Scratch1* within this niche (**Figure 11a)**. The combination of *in situ* hybridization for *Scratch1* with immunofluorescence for makers of different cell populations allowed us to determine that both GFAP-positive NSCs (**Figure 11b**) and DCX-positive neuroblasts express this gene (**Figure 11c**). In addition, we observed that *Scratch1* expression level appeared to be higher in neuroblasts than in NSCs, pointing to an upregulation associated with NSC differentiation.

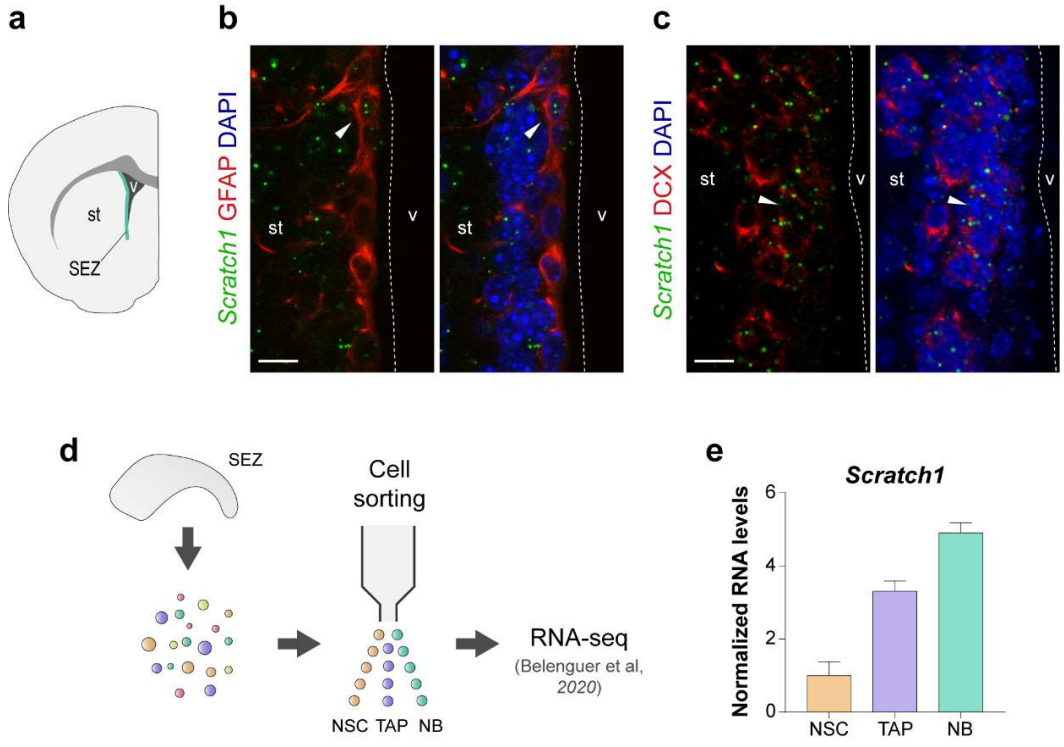

Figure 11| *Scratch1* expression increases as NSCs progress into the neurogenic lineage. (a) Schematic representation highlighting the location of the SEZ in a coronal section of an adult mouse

brain hemisphere. **(b-c)** *In situ hybridization* for *Scratch1* (green) in the SEZ (coronal section), combined with immunofluorescence for GFAP (red, **b**) or DCX (red, **c**). Arrowheads indicate double-positive cells. **(d)** Simplified representation of the strategy used to generate the RNA-seq samples. After SEZ dissociation, cells were FACS-sorted according to the expression of several surface markers and subjected to bulk RNA-seq. **(e)** Relative *Scratch1* expression in NSCs, TAPs and neuroblasts isolated from the adult SEZ. Data from Belenguer et al., 2020. Scale bars represent 10 μm. SEZ, subependymal zone, RMS, rostral migratory stream; st, striatum; v, ventricle; NSC, neural stem cells; TAP, transient amplifying progenitors; NB, neuroblasts.

To better follow the dynamics of *Scratch1* expression along the neurogenic lineage, we took advantage of RNA-seq data obtained from the different cell populations isolated from the *in vivo* niche (**Figure 11d**; Belenguer et al., 2020). This data also indicated that *Scratch1* is expressed at low levels in NSCs and that its expression gradually increases as these cells differentiate and progress into the neurogenic lineage, being moderate in TAPs and relatively high in neuroblasts (**Figure 11e**).

1.2. Scratch1 plays a pleiotropic role during adult neurogenesis

After characterizing the expression pattern of *Scratch1* in the SEZ, we then analyzed the role of this transcription factor during adult neurogenesis. For that purpose, we transduced primary cultures of NSCs with lentiviruses containing a non-silencing control or two different *Scratch1*-specific shRNAs, both of which efficiently downregulated its expression (**Figure 12**). The increase in *Scratch1* expression as NSCs progress into the neurogenic lineage (**Figure 11**) suggested that it might have a role related with the process of neurogenesis. Taking this into account, we aimed to recapitulate this process in culture by artificially inducing the differentiation of NSCs, and analyzed the effect of *Scratch1* downregulation at different time-points.

1.2.1. Scratch1 acts as a survival factor for differentiating neural progenitors

Scratch1 downregulation caused a significant increase in cell death in the cultures, which was already evident 2 days after de induction of differentiation (2DIV), when the cultures are known to be mainly composed by progenitor cells (Belenguer et al., 2016). The decrease in the survival of the cells was caused by an increased in apoptosis, as reflected by the increased in the proportion of cleaved-caspase 3-positive cells in the cultures were *Scracth1* was downregulated compared to the control condition (**Figure 13b,c**). Conversely, when NSCs were kept in proliferation conditions upon *Scracth1* downregulation, preventing

their differentiation, the survival of the cells was not affected by the reduction in the levels of *Scratch1* (**Figure 13b,c**), indicating that this transcription factor acts protecting cells from undergoing programmed cell death specifically during the process of differentiation, but appeared to be dispensable when they are maintained in an undifferentiated state.

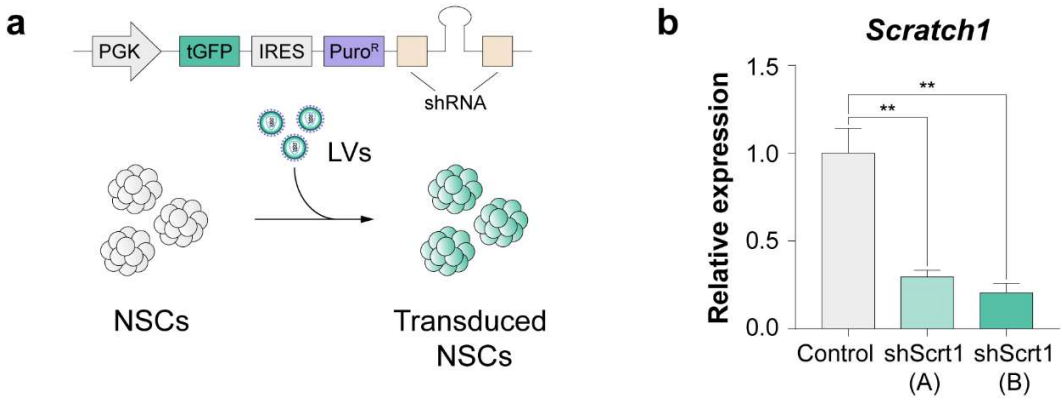

Figure 12| *Scratch1* is efficiently downregulated in NSCs transduced with lentiviruses carrying specific shRNAs. (a) Schematic drawing representing the transduction of the NSCs and the construct use for *Scratch1* loss of function experiments. **(b)** Analysis of *Scratch1* shRNAs efficiency by qPCR (n=3).

Previous work of the lab has shown that in the developing spinal cord of zebrafish scratch2 fulfills a similar role, conferring resistance to the newly formed neurons to cell death (Rodríguez-Aznar and Nieto, 2011). In the case of this system, scratch2 acts antagonizing p53-mediated apoptosis by repressing the transcription of some of its targets, such as *bbc3* (Puma), which is the main effector of cell death induced by p53 in vertebrates (Hafner et al., 2019). Considering that, we analyzed the levels of several components of the p53 pathways. First, we found that *Scratch1* downregulation did not affect p53 expression, neither at the mRNA (**Figure 13e**) or protein levels (**Figure 13f**). Consistently, we did not detect changes in the expression of *Mdm2* (**Figure 13g**), which encodes for a E3 ubiquitin ligase responsible for p53 degradation (Hafner et al., 2019). On the contrary, *Bbc3* (Puma) levels increased upon *Scratch1* downregulation (**Figure 13h**), indicating that, consistently with previous results in other systems (Rodríguez-Aznar and Nieto, 2011; Thellmann et al., 2003), Scratch1 promotes the survival of the differentiating NSCs acting downstream of p53 and repressing the transcription of its target *Bbc3* (Puma; **Figure 13d**).

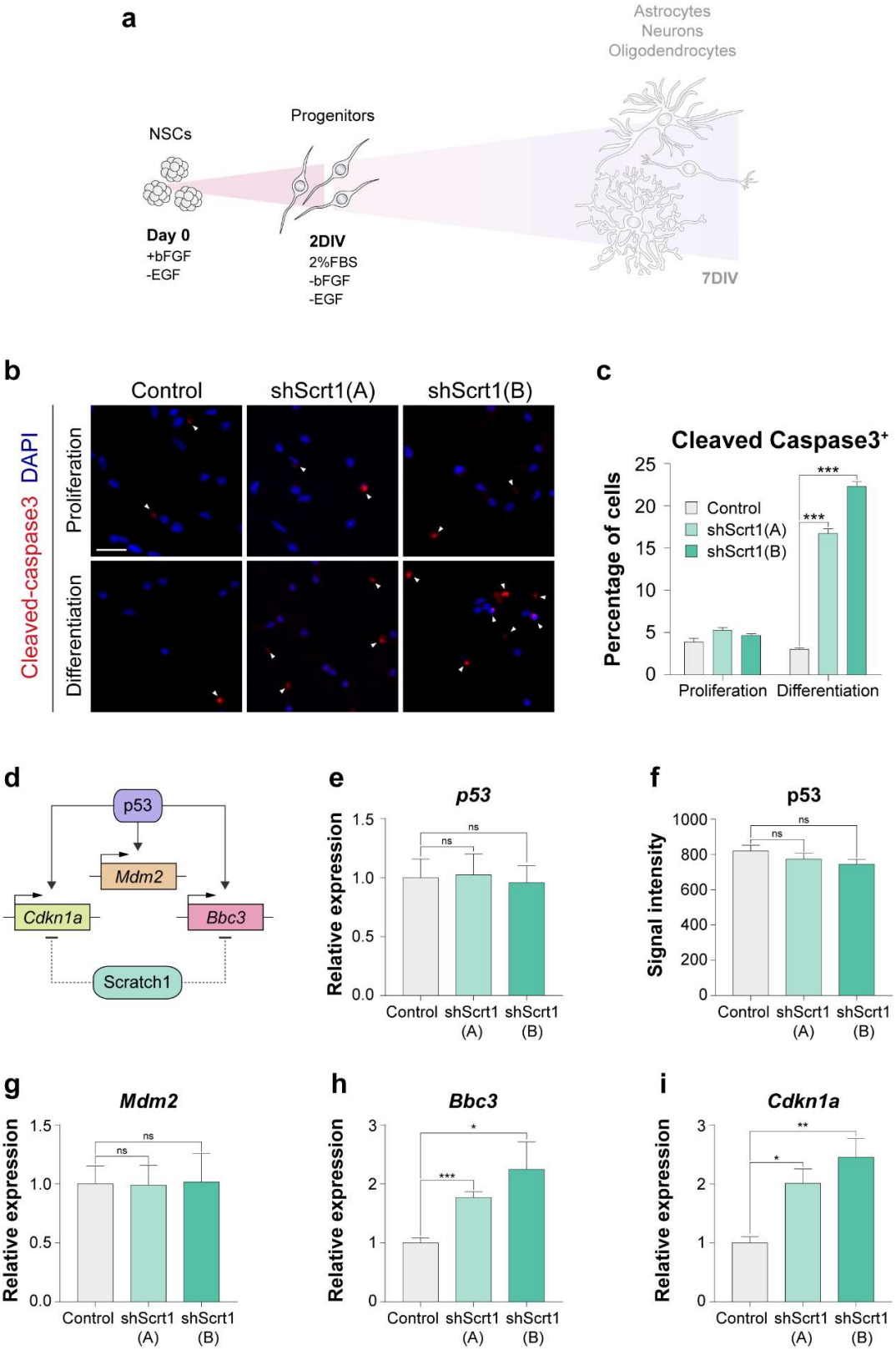

Figure 13| Scratch1 promotes the survival of differentiating neural progenitors by repressing

the transcription of p53 targets. (a) Schematic representation of the differentiation protocol. In order to initiate the process, neurospheres were disaggregated and seeded in Matrigel-coated plates in the absence of EGF. To study the effect of *Scracth1* downregulation in progenitor cells, samples were obtained 2 after the induction of differentiation (2DIV). **(b)** Immunodetection of cleaved-caspase 3 (red) in cells transduced with control or shScratch1 lentiviruses, cultured in the presence (proliferation) or the absence of EGF (differentiation) for 2 days. Arrowheads indicate positive cells. **(c)** Quantification of the percentage of cleaved-caspase 3^+ cells in the cultures (n=3). **(d)** Schematic representation of the proposed action of Scratch1 repressing the transcription of several p53 targets. **(e)** Relative *p53* mRNA levels in RNA extracts obtained 2 days after the induction of differentiation. **(f)** Quantification of signal intensity for p53 in cells fixed 2 days after the induction of differentiation. **(g-i)** Relative mRNA levels of **(g)** *Mdm2*, **(h)** *Bbc3* and **(i)** *Cdkn1a* relative to *TBP* in RNA extracts obtained 2 days after the induction of differentiation. Scale bars represent 25 µm.

Moreover, *Scracth1* downregulation also induced an increase in the levels of *Cdkn1a* (p21, **Figure 13i**), which is a cyclin-dependent kinase (CDK) inhibitor involved in p53-mediated cell cycle arrest (Hafner et al., 2019).

1.2.2. Scracth1 contributes to the appropriate proliferation of the progenitor cells

Taking into consideration the upregulation of *Cdkn1a* (p21) in response to *Scratch1* downregulation, we analyzed whether it had any effect on the proliferation of the progenitor cells (Nestin positive) and found that there was a significant decrease in the proportion of Ki67-positive cells in the cultures treated with both *Scratch1* shRNAs compared to the control (**Figure 14b,c**), suggesting that Scratch1 contributes to the maintenance of the normal proliferation of the progenitor cells by maintaining *Cdkn1a* (p21) levels low, also acting downstream of p53.

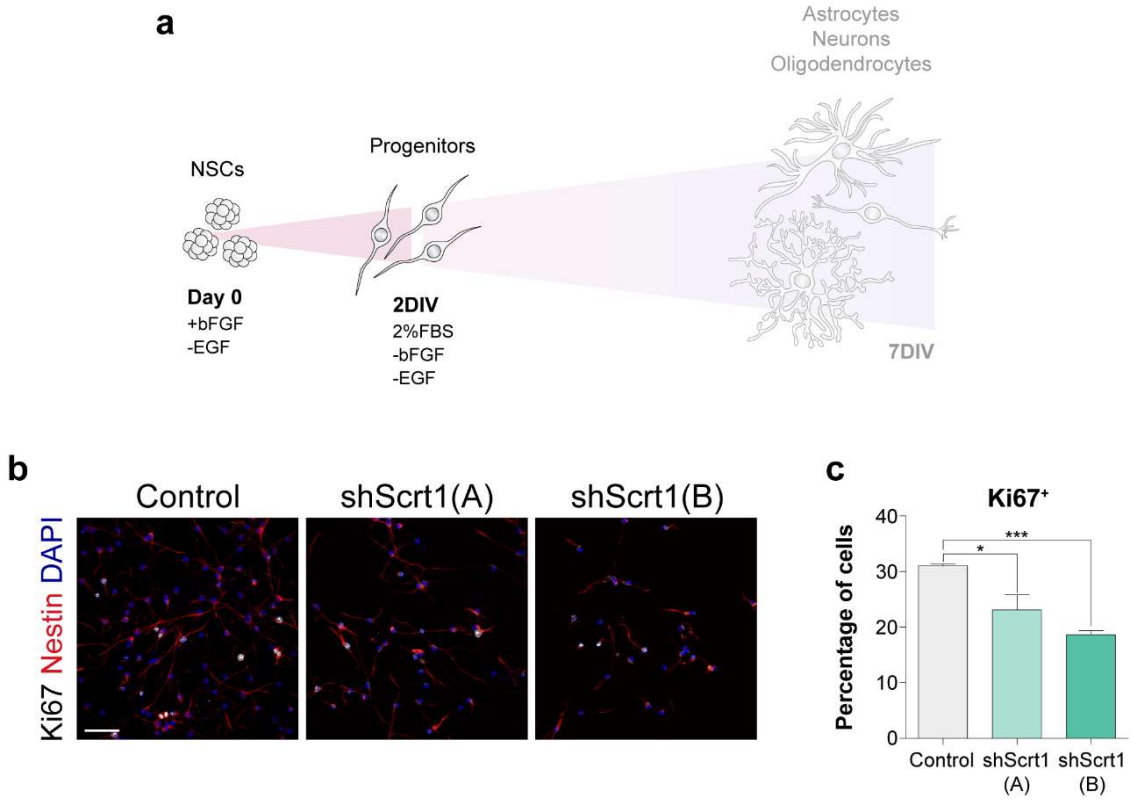

Figure 14| Scracth1 promotes the proliferation of the progenitor cells. (a) Schematic representation of the differentiation protocol. To study the effect of *Scracth1* downregulation in progenitor cells, samples were obtained 2 days after the induction of differentiation (2DIV). **(b)** Immunodetection of Ki67 (white) and Nestin (red) in cultures transduced with control or shScratch1 lentiviruses 2 days after the induction of differentiation. **(c)** Quantification of the percentage of Ki67^{+} cells in the cultures (n=3). Scale bars represent 25 µm.

1.2.3. Scracth1 favors the acquisition of the neuronal fate

Additionally, we analyzed the effect that *Scratch1* downregulation had on the final outcome of the differentiation culture. To do so, we quantified the proportion of astrocytes (GFAP^{+}), neurons (βIII-tubulin^{+}) and oligodendrocytes (O4^{+}) generated in the cultures 7 days after the induction of NSC differentiation (7DIV). The differentiation protocol that we applied leads to a massive production of astrocytes, with a small number of neurons and oligodendrocytes scattered among them (Belenguer et al., 2016), which was mainly what we observed both in control cultures and in the ones where *Scracth1* was downregulated. In the latter, we found that there was a slight increase in the proportion of astrocytes (**Figure 15b,c**, top panel; GFAP positive), and a significant decrease in the proportion of neurons present in the cultures (**Figure 15b,c**, middle panel; βIII-tubulin positive) which where even

more sparse than in control conditions. Regarding oligodendrocytes, their proportion remained unaffected upon *Scratch1* downregulation (**Figure 15b,c**, bottom panel; O4 positive).

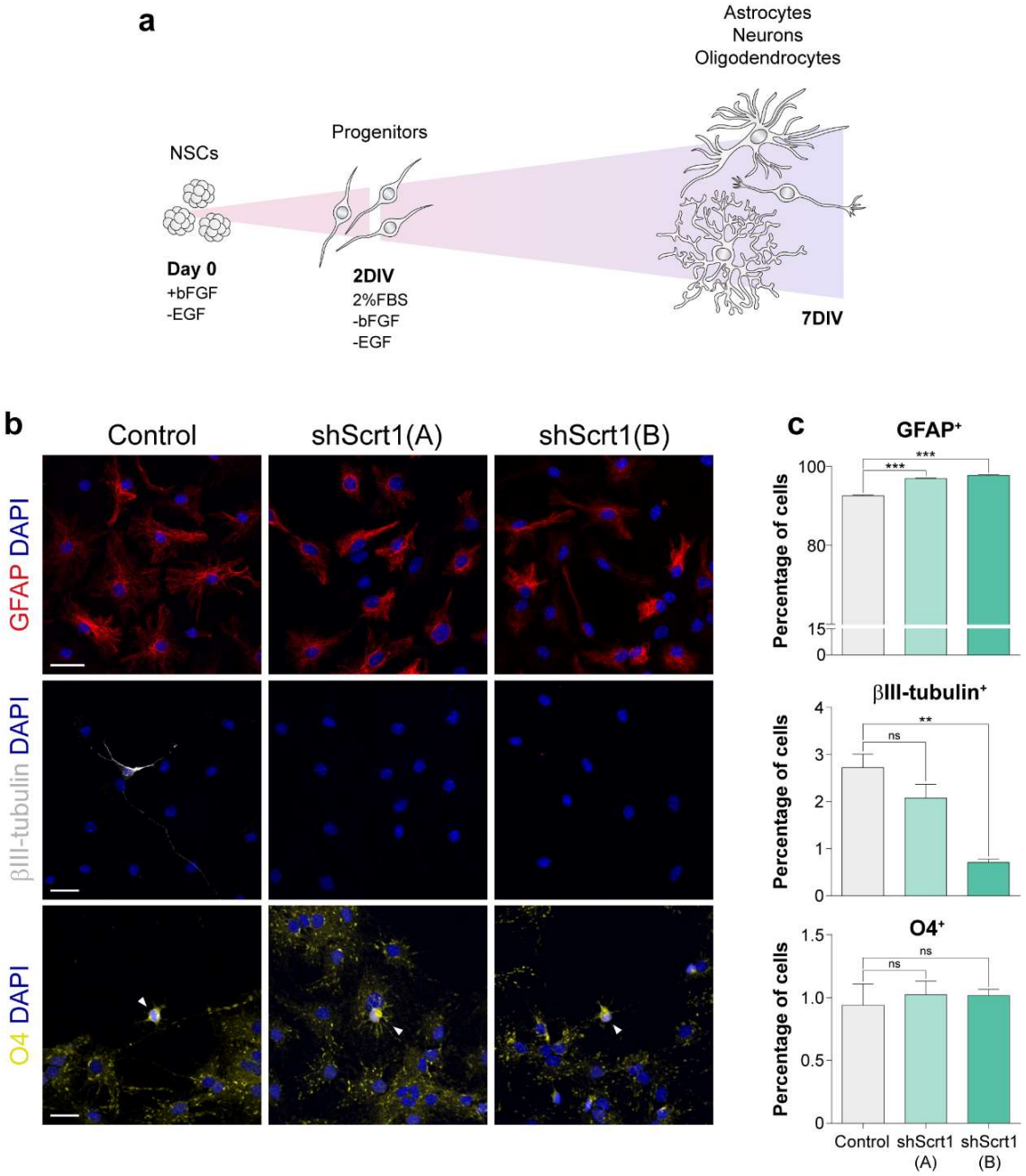

Figure 15| Scracth1 favors neurogenesis at the expense of gliogenesis. (a) Schematic representation of the differentiation protocol. To study the effect of *Scracth1* downregulation on the final outcome of the differentiation, cells were fixed 7 days after the initiation of the process (7DIV). **(b)** Immunodetection of GFAP (red), βIII-tubulin (white) and O4 (yellow) in cultures transduced with

control or shScratch1 lentiviruses 7 days after the induction of differentiation. Arrowheads in the bottom panel indicate $O4^+$ cells. **(c)** Quantification of the percentage of positive cells for GFAP (top), βIII-tubulin (middle) and O4 (bottom) in the cultures (n=3). Scale bars represent 25 μm.

These results show that the decrease in the levels of *Scracth1* causes a change in the fate of the differentiating cells, which tend to differentiate less into neurons and become astrocytes instead. Therefore, altogether these results indicate that Scratch1 also promotes neuronal differentiation in this context, as previously shown in other systems (Metzstein and Horvitz, 1999; Nakakura et al., 2001b; Paul et al., 2014; Roark et al., 1995), favoring neurogenesis at the expense of gliogenesis.

2. Post-transcriptional regulation of *Scrtach1* expression

The results obtained in the functional analyses indicated that Scratch1 plays several roles during neural differentiation (**Figure 13Figure 14**Figure 15). However, its downregulation did not seem to have any effect in NSCs, albeit we had observed that it is also expressed (**Figure 11b**).

2.1. *Scratch1* mRNA is not exported to the cytoplasm in NSCs

The absence of phenotype in NSCs upon *Scratch1* downregulation prompted us to examine more in detail its expression pattern in the SEZ and we noticed that the distribution of *Scratch1* mRNA in NSCs significantly differed from that observed in neuroblasts. In particular, *Scratch1* transcripts showed the expected wide distribution in the cytoplasm in neuroblasts, whereas it was much more restricted in NSCs (**Figure 16**).

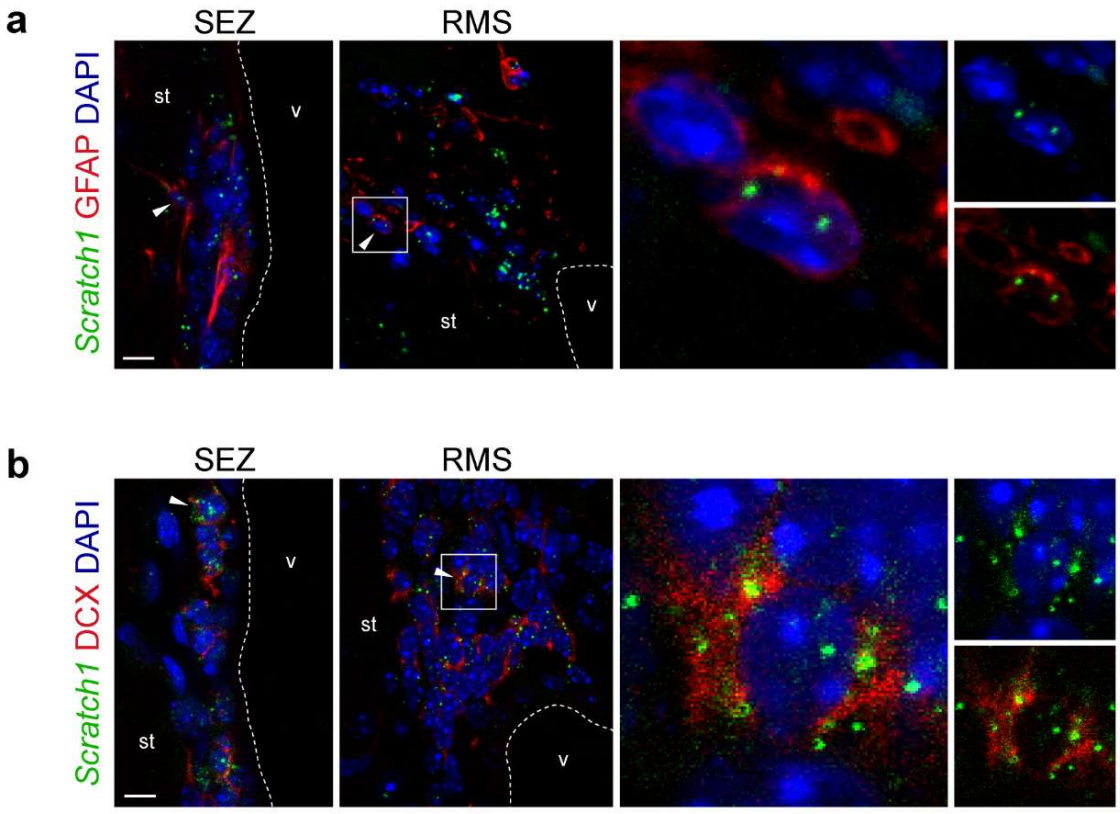

Figure 16| *Scratch1* mRNA is differentially distributed in NSCs and neuroblasts in the adult SEZ. (a) *In situ* hybridization for *Scratch1* (green) combined with immunofluorescence for GFAP (red). **(b)** *In situ* hybridization for *Scratch1* (green) combined with immunofluorescence for DCX (red). Arrowheads indicate double-positive cells. Scale bars represent 10 µm.

In order to gain resolution in the analysis of the subcellular localization of the transcripts, we decided to examine their distribution in NSC in culture (**Figure 17a**). We found that *Scratch1* mRNA was located inside the nucleus in NSCs, accumulating near the nuclear membrane (**Figure 17b**, left panel). By contrast, we observed that the transcripts of the other family member in mammals, *Scratch2*, presented the expected cytoplasmic distribution (**Figure 17b**, right panel), indicating that the subcellular localization of *Scratch1* transcripts were subjected to a special regulation in NSCs.

Considering that *Scratch1* transcripts accumulated in the nucleus in two foci, we hypothesized that the mRNA might be located close to its transcription sites. To study this possibility, we performed an *in situ* hybridization for chromosome 15, where the loci of *Scracth1* are located, which allowed us to identify the position of the region occupied by this chromosome during interphase. The position of the chromosome territories was indeed compatible with the localization of *Scratch1* mRNA foci in NSCs (**Figure 17c,d**), suggesting that the transcripts remain near its transcription sites when they accumulate in the nucleus.

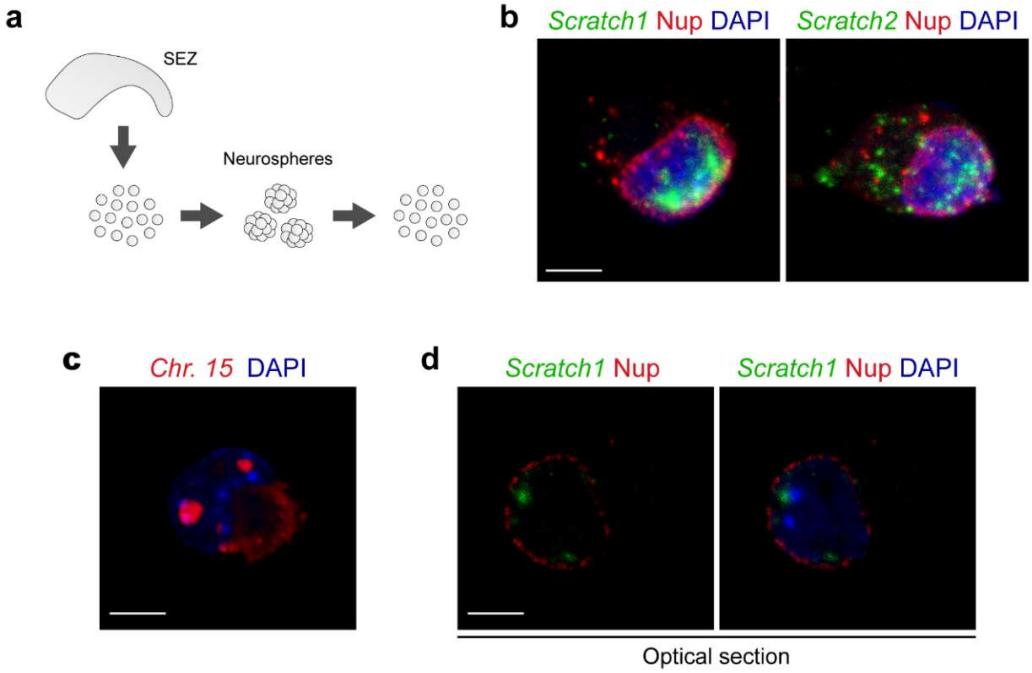

Figure 17| *Scracth1* mRNA accumulates inside the nucleus in NSCs. (a) Schematic representation of the strategy used to obtain SEZ-derived NSCs to study the subcellular distribution of the transcripts. After SEZ disaggregation, cells were plated in complete medium, allowing the formation of neurospheres. Those neurospheres were dissociated and plated on methylcellulose-coated coverslips. **(b)** *In situ* hybridization for *Scracth1* (left panel, green) and *Scratch2* (right panel, green) in primary cultures of NSCs. The nuclear membrane is labeled using a pan-nucleoporin antibody (Nup, red). **(c)** DNA *in situ* hybridization for chromosome 15 (red), where *Scratch1* loci are

located. **(d)** Optical section of an *in situ* hybridization for *Scratch1* (green) combined for immunofluorescence for nucleoporins (red) in cultured NSCs. Scale bars represent 5 µm

2.2. *Scratch1* mRNA accumulates in the nucleus of NSC due to inefficient splicing

The finding that *Scratch1* transcripts are sequestered inside the nucleus of NSCs pointed to an alteration in the process of mRNA export from the nucleus to the cytoplasm. Efficient mRNA export is achieved by coupling it to transcription, splicing and polyadenylation. In fact, the formation of export-competent complexes requires the previous processing of the nascent transcripts, since the splicing machinery is responsible for the recruitment of essential export factors, such as the TREX complex. This ensures that only mature transcripts are exported to the cytoplasm and can be translated into protein (Köhler and Hurt, 2007; Stewart, 2019). Therefore, splicing is a crucial step in the process of mRNA export.

Taking this into consideration, we wondered whether *Scratch1* transcripts were properly spliced when they accumulated in the nucleus of NSCs. We designed probes for *in situ* hybridization that specifically recognized the only intron of *Scratch1* or *Scratch2*. With those probes we could observe that, in the case of *Scratch2*, the pre-mRNA was only detected forming two small nuclear puncta at the transcription sites (**Figure 18b**), reflecting that its transcripts were co-transcriptionally spliced (Vargas et al., 2011), consistent with their cytoplasmic distribution. Conversely, in the case of *Scrtach1,* we were able to detect a large amount of pre-mRNA accumulated in the nucleus (**Figure 18a**), indicating its transcripts remained uspliced in NSCs, preventing their export to the cytoplasm.

As the decrease in the splicing efficiency is often caused by inefficient recognition of the canonical splicing sites (Sibley et al., 2016), we compared the sequence of *Scratch1* and *Scratch2* introns, focusing particularly in those regions that are known to be key for splicing. This analysis revealed a significant enlargement in *Scracth1* polypyrimidine tract (PPT, **Figure 18c**), a sequence enriched in pyrimidines and located between the branch point and the 3'-splicing site and whose recognition promotes the assembly of the spliceosome (Herzel et al., 2017). The length of this sequence typically ranges between 18 and 40 nt (Keren et al., 2010), as is the case for *Scratch2* PPT, and compatible with the co-transcriptional splicing and its cytoplasmic localization. By contrast, *Scratch1* PPT has an extension of 131 nt, substantially longer than the consensus. This enlargement hinders its

recognition by the splicing machinery (Vargas et al., 2011), generating a sub-optimal splicing site and, in turn, causing the uncoupling of splicing from transcription, and transcripts nuclear accumulation.

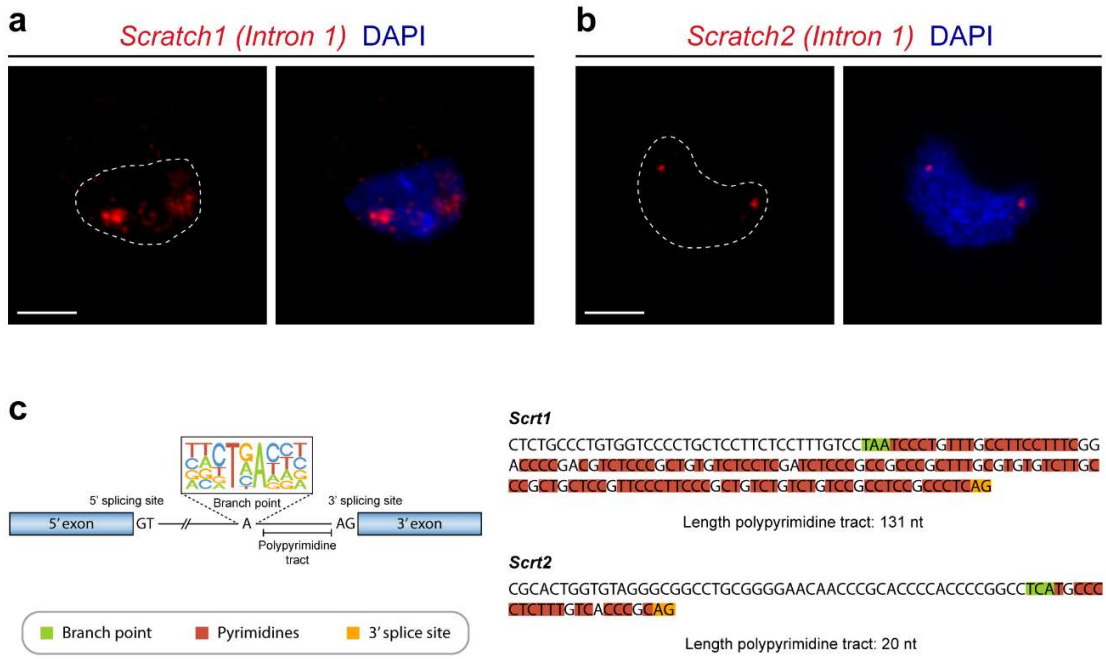

Figure 18| *Scratch1* mRNA is retained in the nucleus of NSCs due to inefficient splicing. (a) *In situ* hybridization for the only intron of *Scratch1* (red) in NSCs in culture. **(b)** *In situ* hybridization for the only intron of *Scratch2* (red) in NSCs in culture. **(c)** Comparison between the sequence of *Scratch1* and *Scratch2* polypyrimidine tracts. Scale bars represent 5 µm.

2.2.1. Evolutionary analysis of *Scratch* intronic sequences

In order to gain more insight from an evolutionary point of view, we analyzed the features of the PPT of *Scracth1* and *Scratch2* orthologues in different vertebrates (**Figure 19**). In all the species analyzed, the length of *Scratch2* PPT was within the consensus range. By contrast, in the case of *Scratch1,* we detected an enlargement of this region in all mammalian species analyzed, including humans, which did not occur in other vertebrates, suggesting that the enlargement of this sequence during evolution has led to the emergence of a sub-optimal splicing site specifically in mammals.

As a proof of concept, we decided to analyze the expression pattern of *Scratch1* in zebrafish, a non-mammalian vertebrate. In this species, due a whole genome duplication (Dehal and Boore, 2005), *Scratch1* has two orthologues: *scratch1a* and *scratch1b*.

Zebrafish presents adult neurogenesis in several areas (Than-Trong and Bally-Cuif, 2015), but we decided to focus particularly in the Pallial Germinal Zone (PGZ, **Figure 20a**), since this region is homologous to the main adult neurogenic niches in rodents (Dirian et al., 2014). There, NSCs present radial glial characteristics and are aligned along the ventricle, which in the case of teleost is exposed to the telencephalic surface (**Figure 20b**) due to a morphogenetic process called eversion (Folgueira et al., 2012). In that region, we observed that neither *scratch1a* or *scratch1b* were expressed in GFAP-positive NSCs, while both were expressed in HuC/D-positive early neurons, where the transcripts exhibited a cytoplasmic distribution (**Figure 20c,d**). Therefore, in the zebrafish, the onset of expression for *Scracth1* orthologues is later in the neurogenic lineage and the transcripts are exported to the cytoplasm as soon as they are transcribed, in contrast to what happens in the mouse SEZ.

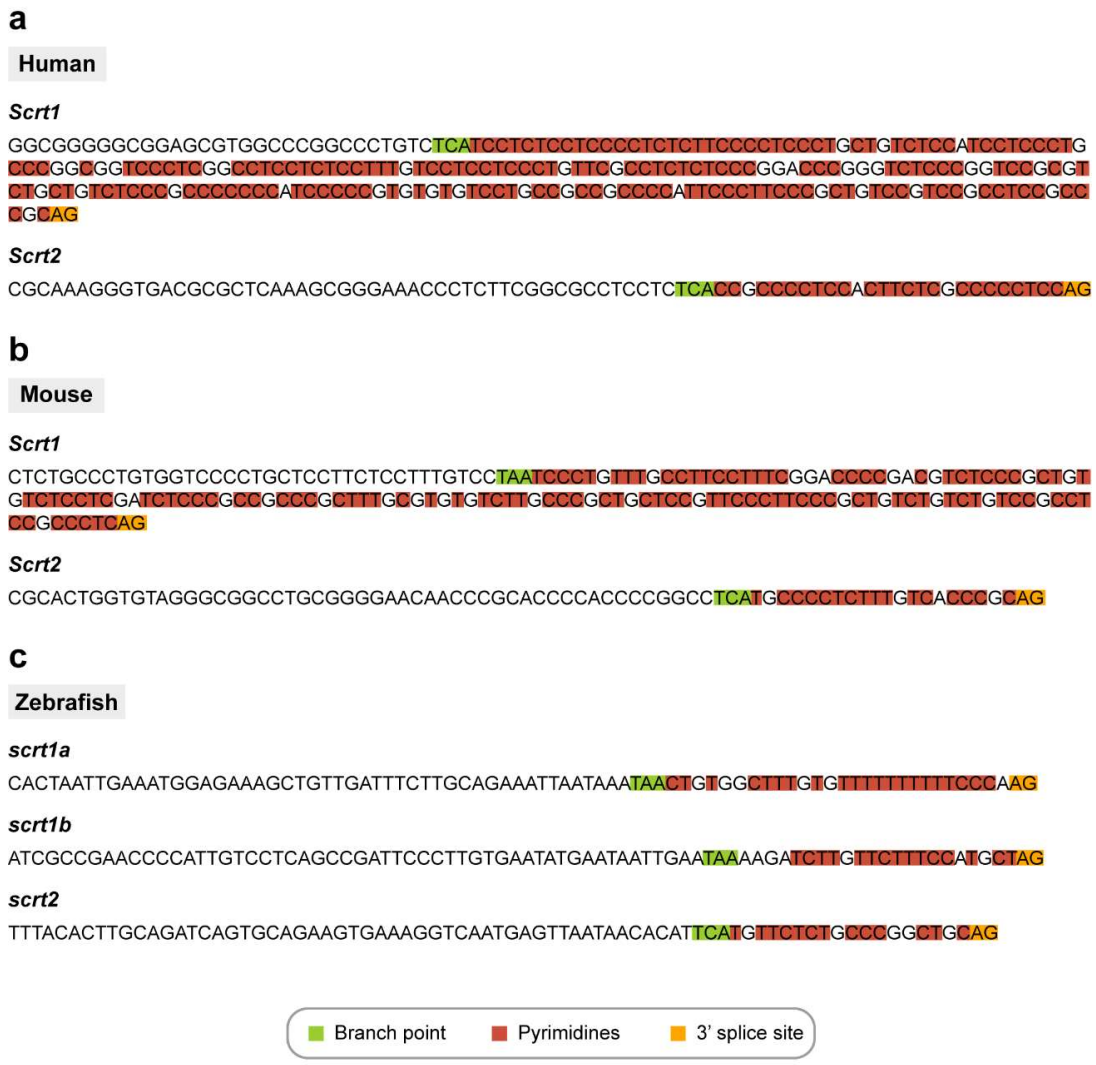

Figure 19| Sequence comparison of the polypyrimidine tract for *Scratch* family members in

different vertebrates. (a) Sequence of *Scratch1* and *Scratch2* intron polypyrimidine tracts in human. **(b)** Sequence of *Scratch1* and *Scratch2* intron polypyrimidine tracts in mouse. **(c)** Sequence of *scratch1a*, *scratch1b* and *scratch2* intron polypyrimidine tracts in zebrafish.

This observation suggested that the presence of a sub-optimal splicing site in the intron of mouse and human *Scratch1* has allowed the implementation of an additional regulatory mechanism in NSCs, contributing to a tighter control of *Scratch1* expression at the post-transcriptional level. As such, the inefficient splicing of *Scratch1* in NSCs that leads to the retention of the transcripts in the nucleus prevents its translation. By contrast, we know that in neuroblasts, *Scratch1* mRNA presents a cytoplasmic distribution and, consequently, the protein can be potentially produced. This situation is equivalent to what we have observed in zebrafish, where the onset of expression of *scracth1a* and *scracth1b* is later in the lineage, and the transcripts are not subjected to nuclear retention. Importantly, nuclear retention does not modify transcription but rather, it constitutes an additional regulatory step at the level of splicing and mRNA export that contributes to the refinement in the temporal control of *Scratch1* function during adult neurogenesis.

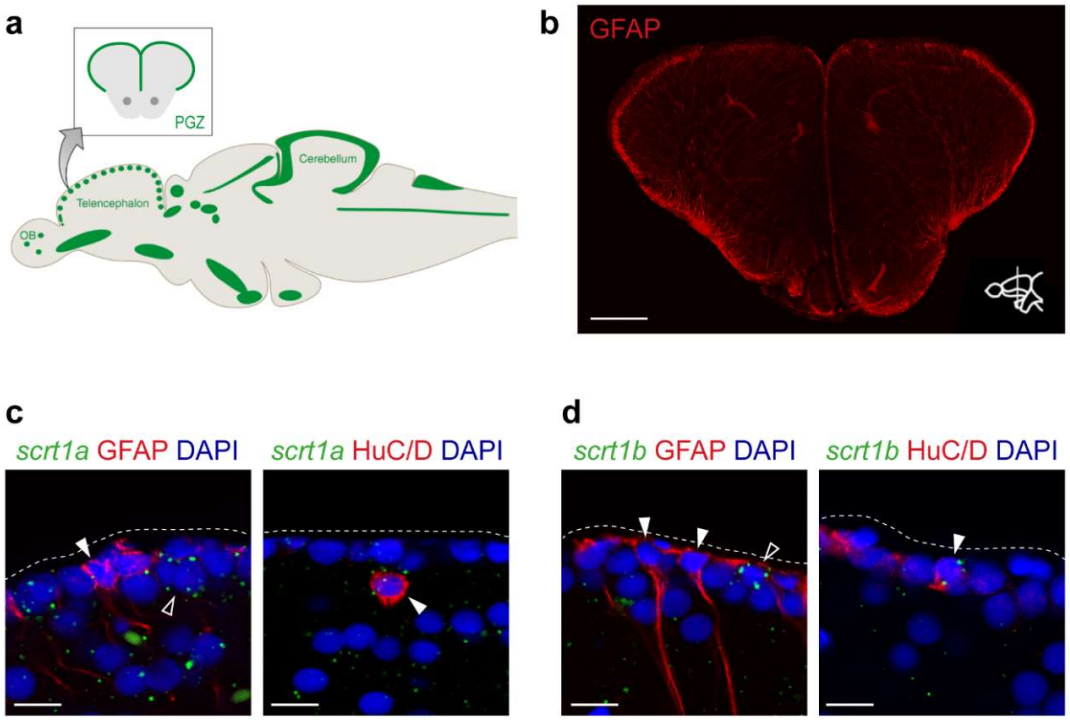

Figure 20| Zebrafish *Scratch1* orthologues do not present nuclear retention in the PGZ. (a) Schematic representation of the zebrafish adult brain in a sagittal view, highlighting the position of the neurogenic niches and the location of the PGZ in a coronal view. Adapted from Dimou and Götz, 2014. **(b)** Overview of GFAP immunostaining in a coronal section of the zebrafish telencephalon. **(c)**

In situ hybridization for *scrt1a* (green) combined with immunofluorescence for GFAP (left panel, red) or HuC/D (right panel, red) in the zebrafish PGZ. **(d)** A similar analysis for *scrt1b* (green). Arrowheads point to double-positive cells and empty arrowheads to single-positive cells in (**c**) and (**d**). Scale bars: (**b**) 100 µm; (**c-d**) 10 µm. PGZ, pallial germinal zone.

2.2.2. *Scracth1* nuclear retention is specific of SEZ-resident NSCs

Taking into account that the sub-optimal splicing site responsible for the retention of *Scratch1* intron in adult NSCs is only present in mammals, we sought to examine the expression pattern of this gene in the other main neurogenic niche in mammals, the SGZ of the dentate gyrus (DG) in the hippocampus. NSCs located in this region, give rise to neurons that differentiate in the hippocampus itself and integrate in the synaptic circuits of the DG (Ming and Song, 2005; **Figure 21a**). There, we observed that *Scracth1* mRNA was not detectable in NSCs (**Figure 21b**), whereas it starts to be moderately expressed in neuroblasts (**Figure 21c**) and presents high levels of expression in a sub-population of NeuN-positive mature neurons (**Figure 21c**), exhibiting a cytoplasmic distribution of the mRNA in all the cell types where it is transcribed. Therefore, as in the case of the zebrafish PGZ, in the SGZ of the mammalian hippocampus *Scratch1* starts to be expressed later in the neurogenic lineage and its transcripts do not present intron retention in any cell population resident in this niche.

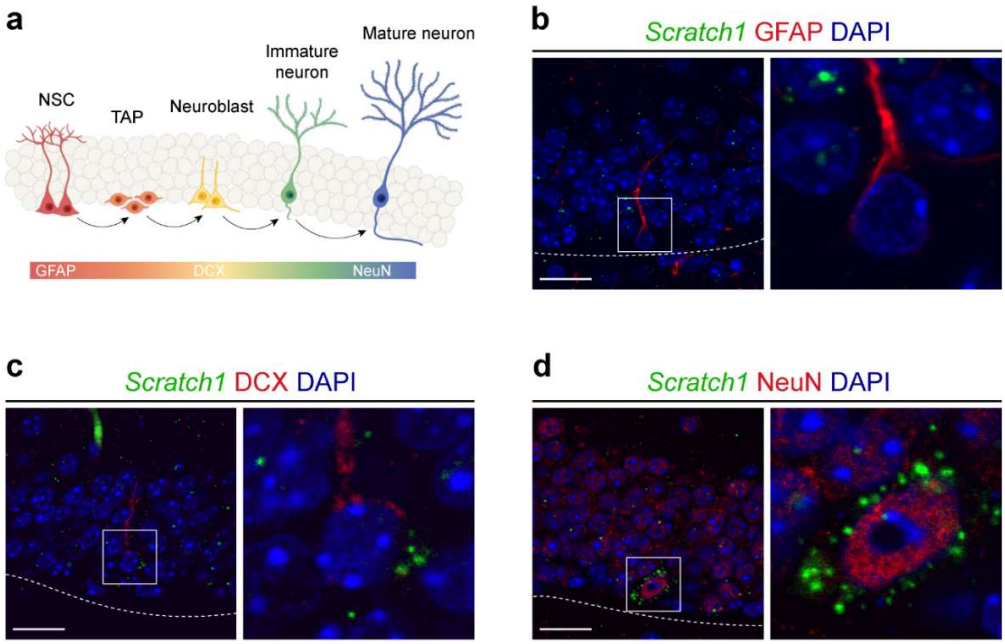

Figure 21| *Scratch1* expression pattern in the SGZ of the hippocampus. (a) Schematic

representation of the different neurogenic stages in the SGZ and the cell-specific markers used. **(b-d)** *In situ* hybridization for *Scratch1* (green) combined with immunofluorescence for GFAP (red) to specifically identify NSCs **(b)**, with immunofluorescence for DCX (red), labeling neuroblasts **(c)**, and with immunofluorescence for NeuN (red), a marker for mature neurons **(d)**. Scale bars represent 20 µm. SGZ, subgranular zone; NSC, neural stem cell; TAP, transit amplifying progenitor.

Hence, focusing on mammals, we have determined that *Scratch1* intron retention does not take place in all population of adult NSC present in the brain, but appears to be a specific trait of the SEZ, suggesting that the regulatory mechanism that we are characterizing has been exclusively implemented in this neurogenic niche.

2.3. *Scratch1* starts to be transcribed when stem cells acquire neural identity

The expression of *Scratch* genes is restricted to the nervous systems in all the species analyzed, from *Drosophila* to vertebrates (Barrallo-Gimeno and Nieto, 2009). Nevertheless, considering that in NSCs, although *Scratch1* is transcribed, the protein cannot be translated, we wonder whether the same happens in pluripotent stem cells. In order to assess this question, we analyzed the expression of *Scratch1* in embryonic stem cells (ESCs) and in induced pluripotent stem cells (iPSCs) reprogramed from NSCs isolated from the mouse SEZ, and observed that none of them express this gene (**Figure 22**).

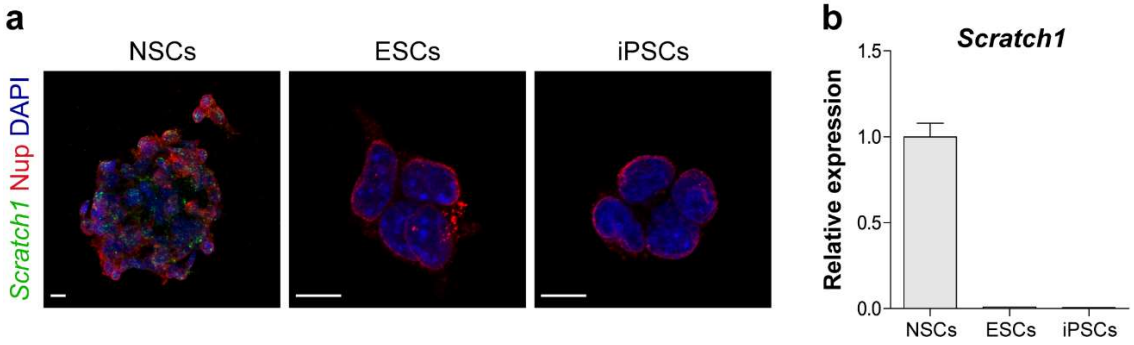

Figure 22| ESCs and iPSCs do not express *Scratch1*. (a) *In situ* hybridization for *Scratch1* (green) combined with immunofluorescence for nucleoporins (red) in cultured NSCs (left panel), ESCs (middle panel) and iPSCs (right panel). **(b)** Relative mRNA levels of *Scratch1* in RNA extracts obtained from NSCs, ESCs and iPSCs. Scale bars represent 10 µm. NSCs, neural stem cells; ESCs, embryonic stem cells; iPSCs, induced pluripotent stem cells.

With the aim of defining the onset of *Scratch1* transcription, we induced ESC-to-NSC differentiation and followed its expression during the process. To do so, we used a ESC line

that expresses GFP under the control of the *Sox1* promoter, an early marker of neural specification (Aubert et al., 2003). To generate ESC-derived NSCs we first cultured the cells as serum-free adherent monocultures, which induces the generation of neural progenitors that organize forming rosettes. After 7 days, cells were replated and cultured in the presence of FGF and EGF, leading to the formation of NS cells, which at first associate forming floating clusters and then attach to the substrate and acquire a bipolar morphology (Conti et al., 2005; **Figure 23a**). As expected, during this process we detected a progressive increase in the GFP signal, reflecting an upregulation in *Sox1* expression as the cells became committed to the neural lineage, which was followed by a posterior decrease in the fluorescence signal, as well as in endogenous *Sox1* expression, when cells differentiated into NSCs (**Figure 23b**).

The progression of the differentiation was assessed by analyzing the expression of several pluripotency (*Nanog*, *Pou5f1* and *Zfp42*) and neural specification (*Sox1* and *Nestin*) markers. During the generation of NSCs, we observed a progressive decrease in the expression of the pluripotency markers analyzed (**Figure 23c**), accompanied by a concomitant increase in the expression of neural markers (**Figure 23Figure 22d**). Within the course of the process, we found two different trends. On the one hand, as mention above, *Sox1* levels peaked 4 days after the onset of the differentiation process (4DIV) and then dropped progressively until the end of the process. On the other hand, *Nestin* expression continuously increased along the differentiation, although its upregulation was more gradual that in the case of *Sox1*.

Regarding the expression of *Scratch1*, it started to be detectable 5 days after de induction of the differentiation (5DIV), when the cells had already acquired the neural identity and were starting to downregulate *Sox1* (**Figure 23e**). After that, *Scratch1* expression continued to increase during the differentiation and showed a sharp increase when cells were converted into NSCs. Altogether, these data indicate that *Scratch1* is not expressed before neural specification, starting to be transcribed when cells are close to become NSC, confirming its neural-specific expression.

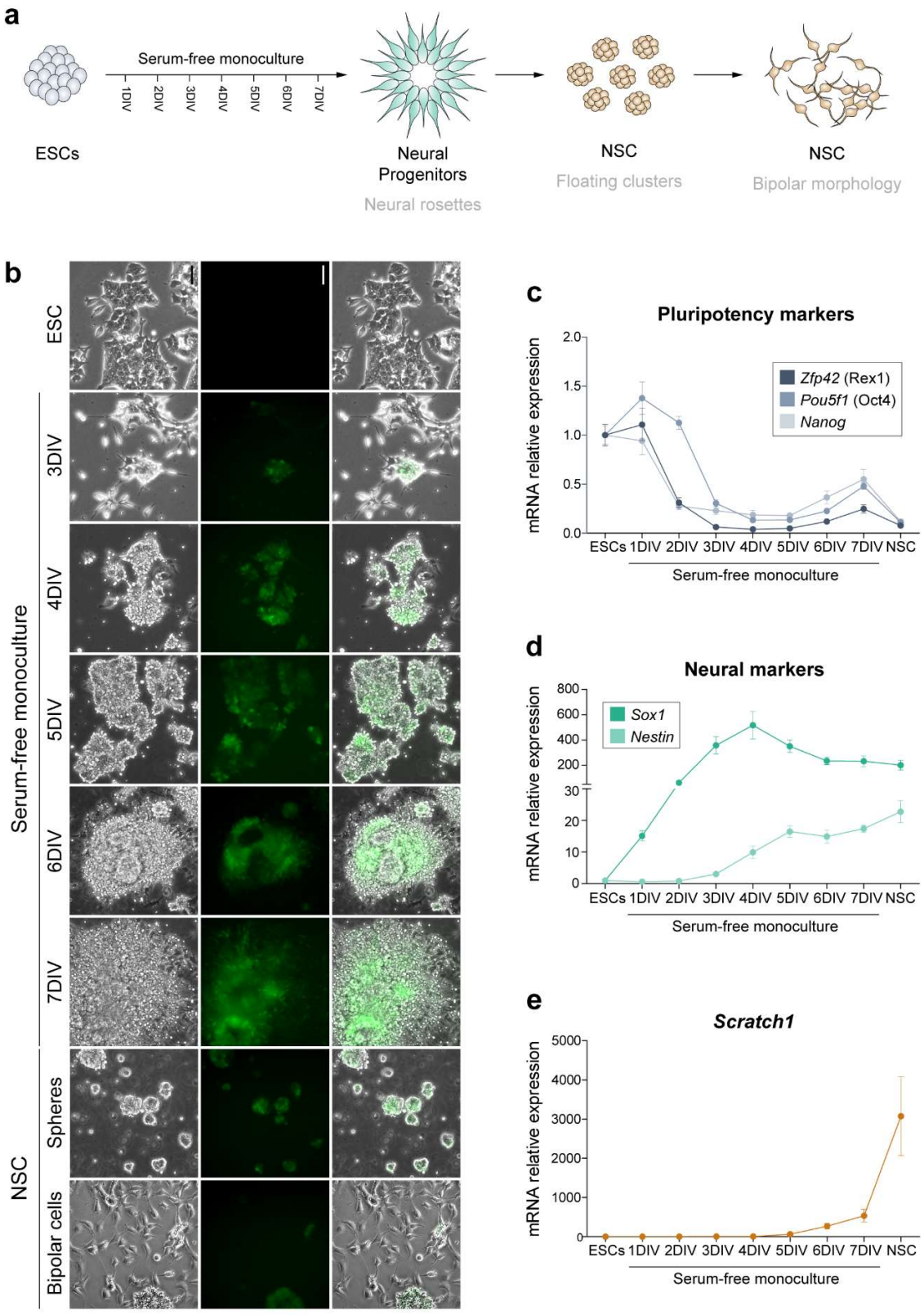

Figure 23| *Scratch1* expression is restricted to the neural lineage. (a) Schematic representation

of the protocol to obtain ESC-derived NSCs. **(b)** Cells at different time points in the process of ESC-to-NSC differentiation observed under phase contrast optics. GFP (green) labels the cells that express *Sox1*. **(c-e)** Relative mRNA levels of several pluripotency markers (*Nanog*, *Pou5f1* and *Zfp42*, **c**); neural markers (*Sox1* and *Nestin*, **d**); and *Scracth1* (**e**) in RNA extracts obtained at different time points during the differentiation of ESCs into NSCs (n=4). Scale bars represent 100 µm. ESC, embryonic stem cell; NSC, neural stem cell; DIV, days in vitro.

2.4. *Scratch1* mRNA is spliced and exported in response to the differentiation signal

We have determined that *Scratch1* mRNA is not exported to the cytoplasm in NSCs (**Figure 17**), although that we have also showed that the nuclear accumulation of the transcripts is not permanent, since in neuroblasts they present a cytoplasmic distribution (**Figure 16**). With this in mind, we sought to define more thoroughly the changes in mRNA distribution that takes place during the differentiation of NSCs.

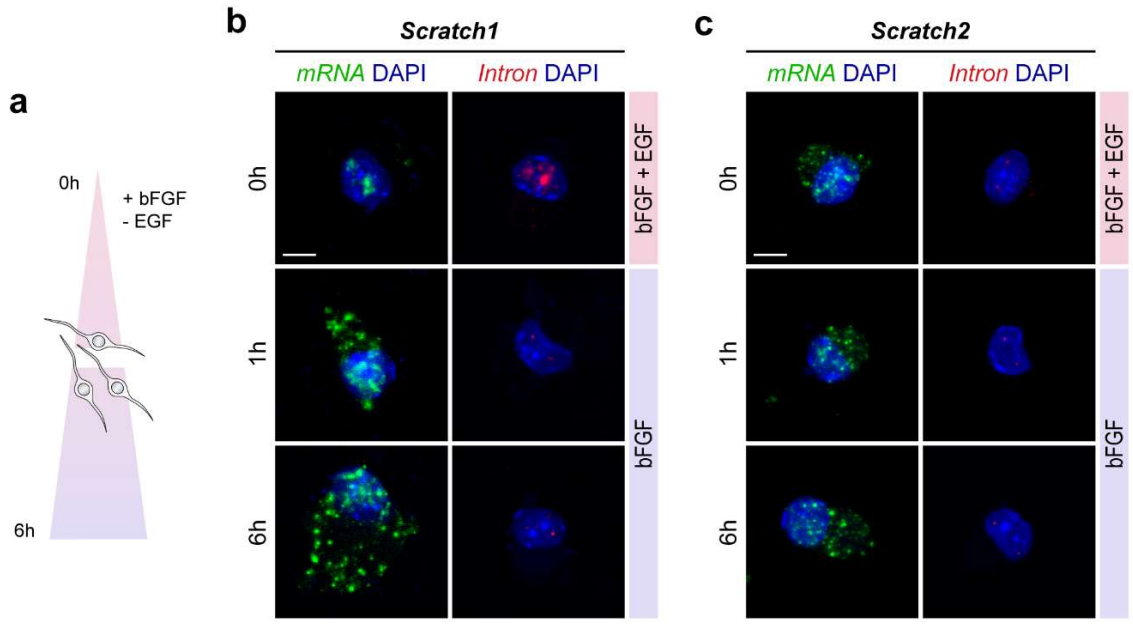

Figure 24| *Scratch1* mRNA is spliced and exported in reponse to the differentiation signal. (a) Schematic representation of the differentiation protocol. **(b)** *In situ* hybridization for *Scratch1* mRNA (green) and *Scratch1* intron (red) in NSCs 0h, 1h and 6h after the induction of differentiation. **(c)** *In situ* hybridization for *Scratch2* mRNA (green) and *Scratch2* intron (red) in similar conditions. Scale bars represent 5 µm.

To do so, cultures of SEZ-isolated NSCs were maintained in the absence of EFG, triggering their differentiation (Belenguer et al., 2016; **Figure 24a**). Contrary to what

happened in undifferentiated NSCs, where *Scratch1* mRNA could be detected unspliced and localized inside the nucleus, 1 hour after the induction of differentiation the transcripts were processed and already exhibited a canonical cytoplasmic distribution (**Figure 24b**), and this change in mRNA splicing and localization was maintained for 6 hours (**Figure 24b**, bottom panel). As a control, we analyzed the distribution of *Scratch2* mRNA during the process, which was normally spliced at all time points and, accordingly, always localized in the cytoplasm (**Figure 24c**).

Additionally, in order to confirm that the changes observed in the processing and distribution of *Scratch1* mRNA were triggered in response to EGF withdrawal, we treated the cells with either one of two different EGF receptor inhibitors (Gefitinib and Afatinib) to block its signaling into the cells (**Figure 25a**). As it happens when NSCs were cultured in the absence of EGF, the treatment with these inhibitors induced their differentiation and prompted *Scratch1* transcripts export to the cytoplasm (**Figure 25b**) as a result of their splicing (**Figure 25c**). These results indicate that *Scratch1* transcripts are rapidly spliced and exported in response to the differentiation signal, and also reveal that the retention of the intron in *Scratch1* mRNA is reversible. Thus, this can be considered an event of intron detention in NSC, as a result of regulated splicing rather than simply slow processing by reduced efficiency in the recognition of the splicing site (Boutz et al., 2015).

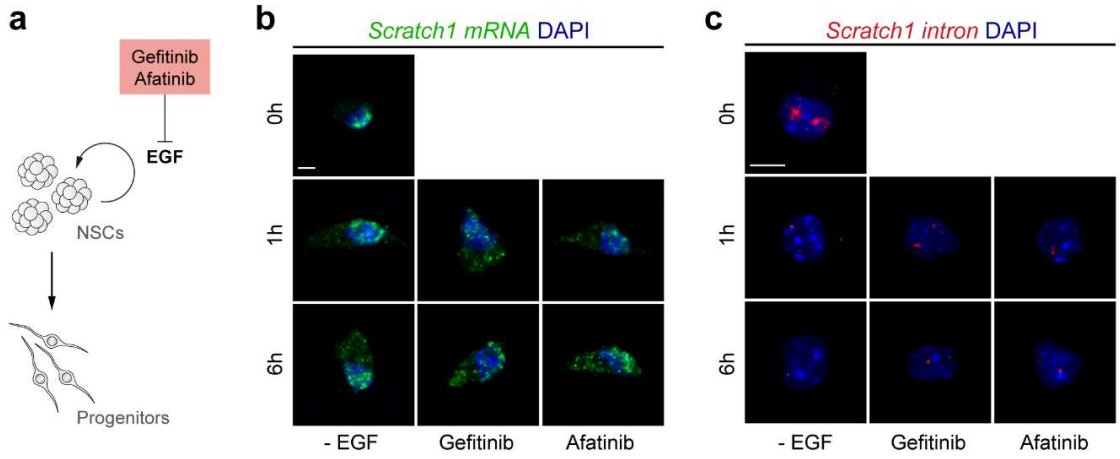

Figure 25| The splicing and export of *Scracth1* mRNA can be triggered by EGF withdrawal or EGF inhibition. (a) Schematic representation of the protocol used to induce the differentiation of NSCs in culture. **(b,c)** *In situ* hybridization for *Scratch1* mRNA (green, **b**) or *Scratch1* intron (red, **c**) in NSCs 0h, 1h and 6h after the induction of differentiation or the treatment with Gefitinib or Afatinib. Scale bars represent 5 µm.

2.5. Regulation of *Scratch1* mRNA splicing and export

Having determined that *Scrtatch1* mRNA splicing is detained until NSCs receive the differentiation signal, we then wanted to further investigate the mechanism that controlled this switch in the processing and subcellular localization of the transcripts.

2.5.1. *Scratch1* mRNA splicing is not induced in response to changes in PTB/nPTB expression

We have observed that *Sctratch1* PPT is a weak splice site due to its excessive length in mammals (**Figure 18c**). This sequence is susceptible to being bound by the polypyrimidine tract binding protein (PTB), which is a well-known negative regulator of splicing that preferentially binds to polypyrimidine-rich stretches (Sawicka et al., 2008). This class of sequence elements can be also bound by neural PTB (nPTB), a PTB paralog with different splicing regulator properties. PTB and nPTB protein expression is mutually exclusive, being PTB restricted to non-neuronal lineages and nPTB specifically expressed in post-mitotic neurons. During neuronal differentiation, PTB is downregulated and substituted by nPTB, and this switch generates significant changes in alternative splicing programs (Boutz et al., 2007; **Figure 26a**).

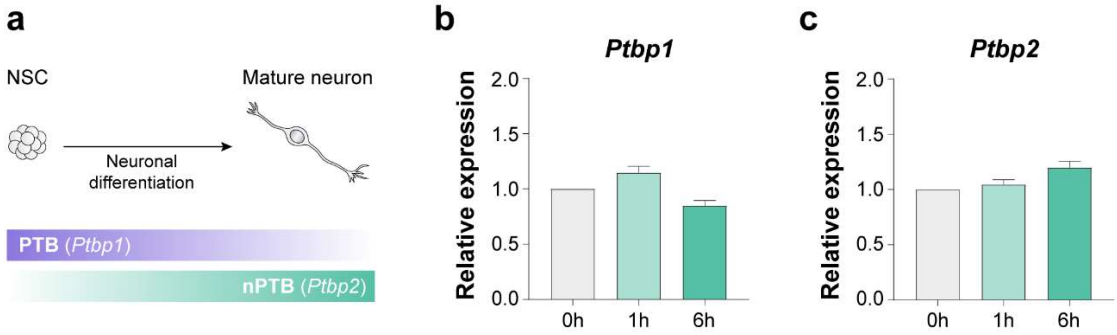

Figure 26| *Scracth1* mRNA processing and export do not involve a switch in PTB/nPTB expression (a) Schematic representation of the transition in the expression of PTB (*Ptbp1*) to nPTB (*Ptbp2*), known to take place during neuronal differentiation. **(b,c)** Relative mRNA levels of *Ptbp1* (b) and *Ptbp2* (c) in RNA extracts obtained from NSCs 0h, 1h and 6h after the induction of differentiation (n=3 per condition).

Taking this into account, we hypothesized that PTB could bind *Scratch1* PPT in NSCs, preventing the splicing of the transcripts; whereas the induction of differentiation might trigger a PTB/nPTB switch, allowing the processing of Scratch1 *mRNA* and their export to

the cytoplasm. In order to study this possibility, we checked the expression levels of these two splicing regulators in NSCs 1 hour and 6 hours after the induction of differentiation, when we have determined that *Scratch1* transcripts are already spliced and had a cytoplasmic distribution. However, we did not detect changes in the expression of PTB (*Ptbp1*) or nPTB (*Ptbp2*) at these short time-points of neural differentiation (**Figure 26b,c**), suggesting that the fast processing of *Scratch1* mRNA in response to the differentiation signal is not mediated by a switch in PTB/nPTB expression.

2.5.2. The splicing and export of *Scratch1* transcripts is controlled by the m^{6}A methylation of the mRNA

Additionally, we sought to investigate whether mRNA modifications, which have been involved in the regulation of multiple post-transcriptional events (Gilbert et al., 2016), regulate the switch in *Scratch1* mRNA splicing and export during neural differentiation. In particular, we focused on N^6-methyladenosine (m^{6}A), which is the most prevalent of these epitranscriptomic modifications and is known to be able to regulate splicing (Liu et al., 2015; Louloupi et al., 2018; Xiao et al., 2016) and mRNA export (Hsu et al., 2019; Lesbirel et al., 2018; Roundtree et al., 2017b; Zheng et al., 2013).

As a first approach, we performed an *in silico* analysis of *Scratch1* pre-mRNA sequence and found the RRm^{6}ACH consensus motif (Harcourt et al., 2017; **Figure 27a**) in numerous positions, some of which exhibited high probability of being methylated considering the features of the surrounding sequence (Li et al., 2016), especially in the intronic region and in the 3'UTR (**Figure 27b**).

m^{6}A is a dynamic modification that can be potentially added and removed in the lifetime of a single mRNA molecule, and, hence, the methylation of a given m^{6}A site is highly dependent on the cellular context (Harcourt et al., 2017). In order to analyze whether *Scratch1* mRNA is methylated during adult neurogenesis and whether there are changes in the level of methylation associated with NSC differentiation, we performed an m^{6}A-RNA immunoprecipitation assay (m^{6}A-RIP) and observed that there is an enrichment in *Scratch1* mRNA upon m^{6}A-RIP compared to the input, indicating that these transcripts were methylated (**Figure 27c,d**). We use *Actb* mRNA as a positive control, since it was known to be constitutively methylated. In addition, we observed an increase in *Scratch1* mRNA enrichment upon the induction of NSC differentiation, coinciding with the processing and the

export of the transcripts (**Figure 24b**), which suggested that RNA methylation might be involved in the regulation of these two processes in the context of adult neurogenesis.

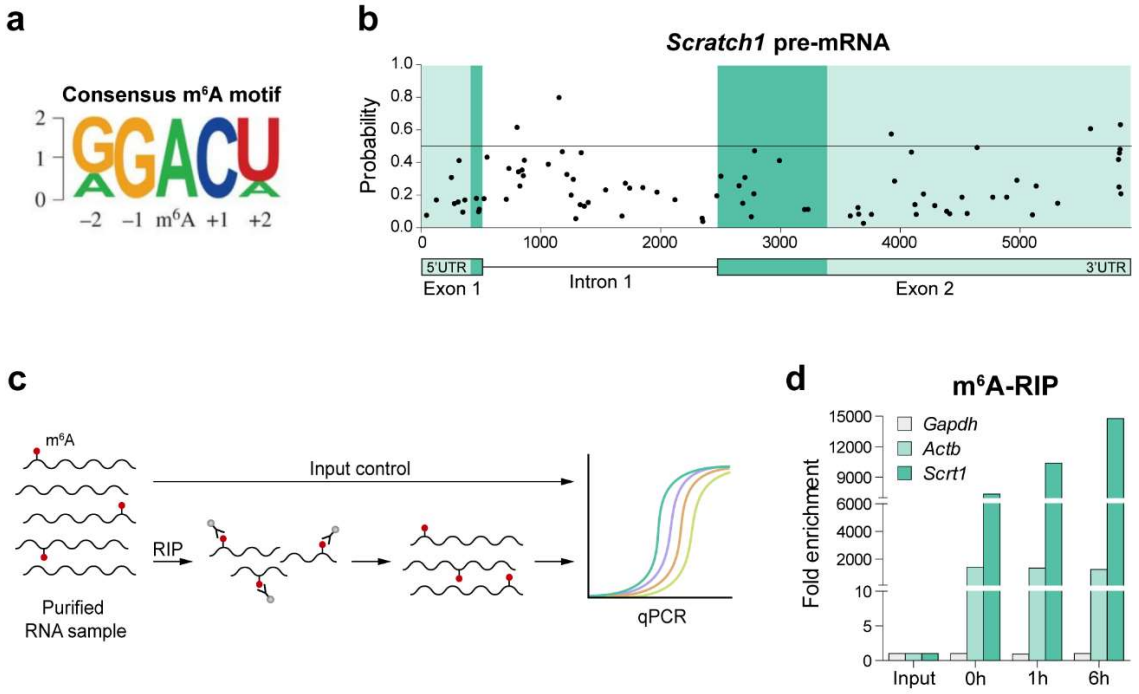

Figure 27| *Scratch1* mRNA m^{6}A-methylation levels increase during NSC differentiation. (a) Sequence logo representing the consensus motif for m^{6}A: RRm^{6}ACH (R=A or G, G>A; H=A, U or C, U>A>C). **(b)** *In silico* analysis of methyation probability in the different m^{6}A sites present in *Scratch1* pre-mRNA. **(c)** Schematic representation of the m^{6}A-RIP protocol. **(d)** m^{6}A-RIP-qPCR for *Gapdh*, *Actb* and *Scratch1* 0h, 1h and 6h after the induction of differentiation.

With the aim of analyzing the effect that *Scrtach1* mRNA methylation has on the subcellular localization of the transcripts, we treated NSCs with 3-deazaadenosine (DAA), a strong inhibitor of m^{6}A (Fustin et al., 2013). Under these conditions, *Scratch1* mRNA failed to be spliced and exported in response to the induction of NSC differentiation, whereas in control cultures the transcripts were processed and exhibited a cytoplasmic localization (**Figure 28**). Therefore, this indicates that RNA methylation promotes *Scratch1* mRNA splicing and export to the cytoplasm during NSC differentiation.

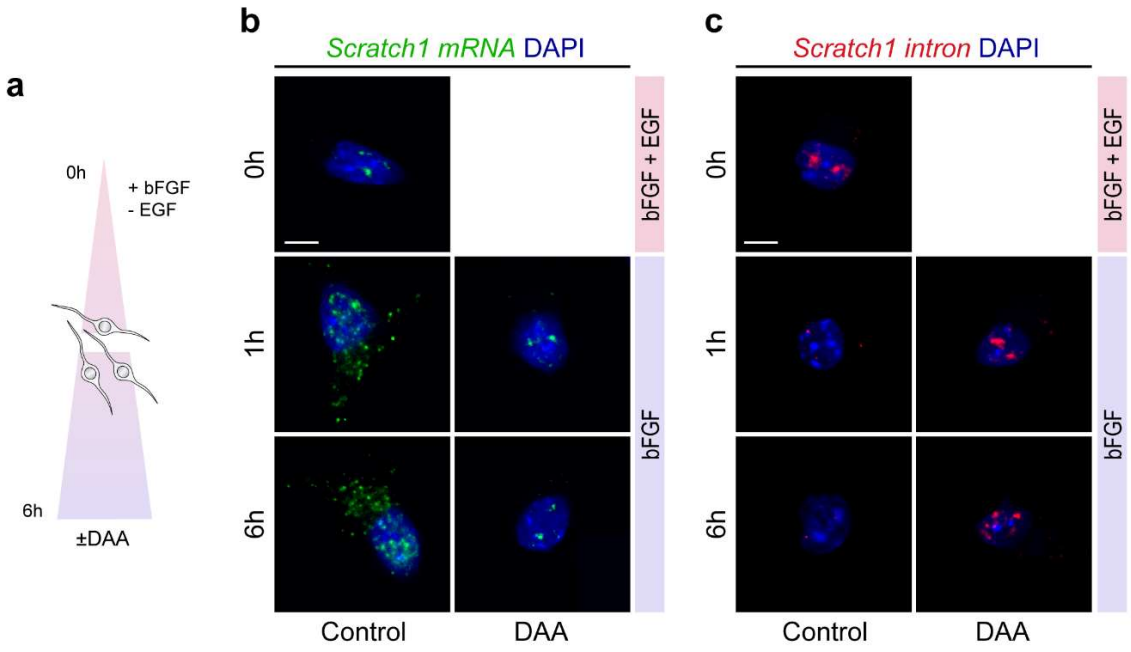

Figure 28| RNA m^{6}A-methylation promotes *Scratch1* mRNA splicing and export during NSC differentiation. (a) Schematic representation of the differentiation protocol. **(b, c)** *In situ* hybridization for *Scratch1* mRNA (green, **b**) and *Scratch1* intron (red, **c**) in control NSCs and in NSCs treated with 3-deazaadenosine. Scale bars represent 5 µm. DAA, 3-deazaadenosine.

3. Intron detention as a general mechanism for the regulation of translation during adult neurogenesis

We have uncovered that intron detention and mRNA methylation regulate the subcellular localization of *Scratch1* transcripts, controlling their availability for translation. In order to study whether other transcripts were post-transcriptionally regulated by the same mechanism, we performed RNA-seq on samples from different time-points of NSC differentiation and analyzed the data following a specific pipeline to detect splicing isoforms (**Figure 29a**), allowing us to identify numerous events of intron retention (IR).

3.1. Differential gene expression analysis at the initial stages of NSC differentiation

First, in order to validate that NSC differentiation was efficiently induced, we analyzed changes in gene expression at the transcriptional level. RNA-seq data indicated that there was an upregulation of genes associated with glial and neuronal differentiation, accompanied by a downregulation in the expression of genes associated with NSC self-renewal and proliferation (**Figure 29b**).

Furthermore, we performed a clustering analysis based on differentially expressed genes (DEG) aimed at identifying trends in gene expression during the differentiation process. This analysis generated 3 groups of genes, with the vast majority of them in Groups 1 or 3, including those that showed low expression at the beginning of the differentiation (0h and 1h) and were upregulated later, or those that present higher levels of expression in the early time-points and were downregulated with differentiation, respectively (**Figure 29c,e**). On the one hand, in Group 1 we found genes such as *Ascl1*, *Olig2*, *Elavl3* and *Dbx2* and, performing a functional enrichment analysis, as expected, we found terms related to neural differentiation (**Figure 29c**). On the other hand, Group 3 was enriched in terms related to the regulation of cell proliferation and cell cycle, including the regulation of telomerase activity, and containing genes such as *Myc*, *Id2*, *Mcm2* and *Pcna* (**Figure 29e**). Additionally, we also identified a small cluster of genes (Group 2) whose expression peaks 1 hour after the induction of NSC differentiation, and then decreases in the latest time-point, suggesting that they might be required at the very beginning of the process, but are dispensable later. This cluster was functionally enriched in terms associated with several signaling pathways,

including MAPK and Wnt signaling, and with mRNA binding-mediated regulation (**Figure 29d**).

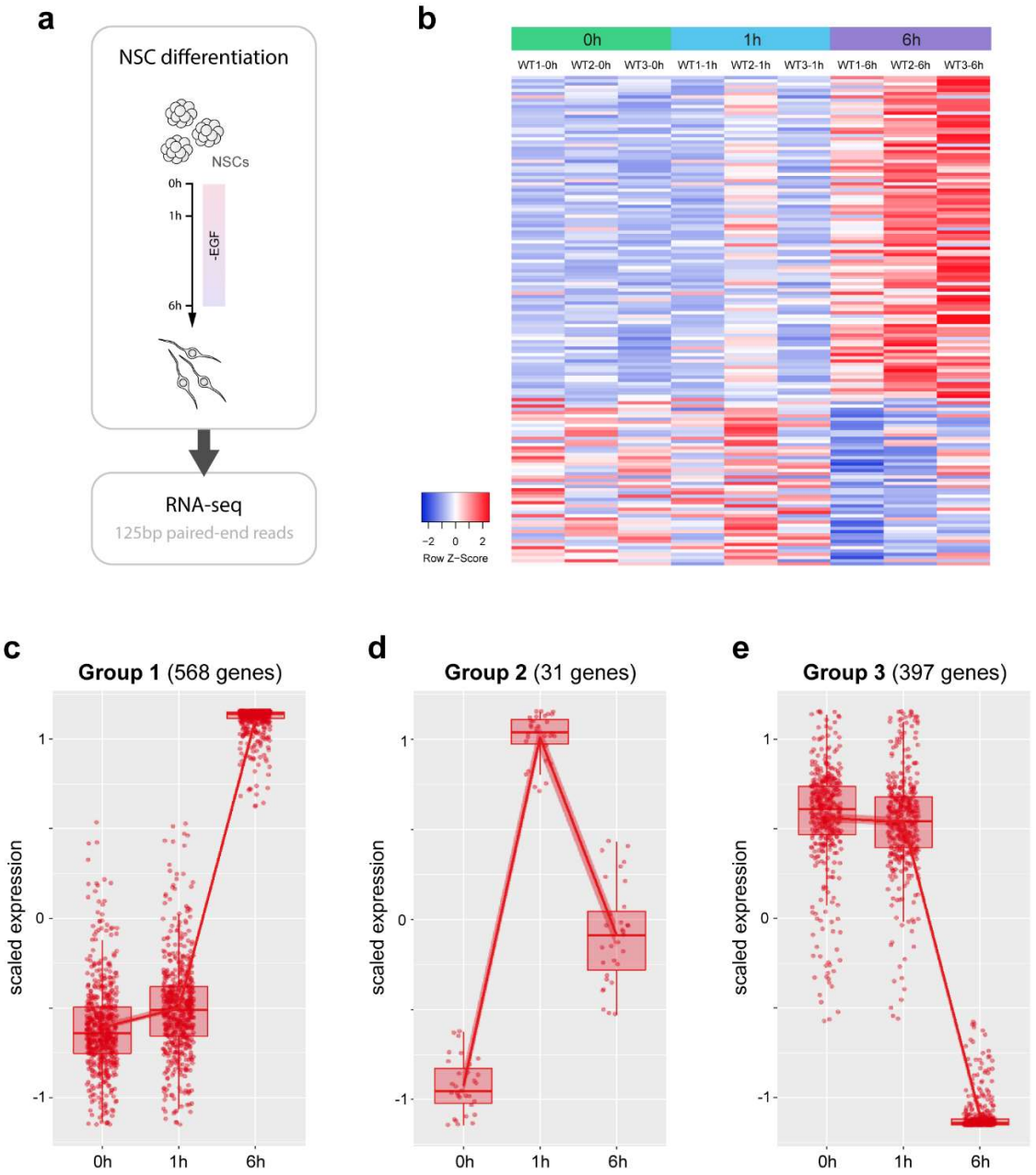

Figure 29| Changes in gene expression during the first stages of NSC differentiation. (a) Schematic representation of the protocol followed for the generation of RNA-seq samples. **(b)** Heatmap representing the expression of DEGs associated with glial and neuronal differentiation and with SC population maintenance 0h, 1h and 6h after the induction of differentiation. **(c-e)** Trends in gene expression detected by DEG clustering analysis: **(c)** Group 1, **(d)** Group 2 and **(e)** Group 3.

On the other hand, we also performed an Integrated System for Motif Activity Response Analysis (ISMARA), which enables the identification of key transcription factors responsible for expression changes across the samples using RNA-seq data as input (Balwierz et al., 2014; **Figure 30a**). This analysis revealed that the expression trend of the genes belonging to Group 1 might be closely related to the activity of SIX5, which is involved in the regulation of the formation of the retina, as well as other organs (Winchester et al., 1999); of KLF16, which is a transcription factor involved in the modulation of dopaminergic transmission in the brain (Hwang et al., 2001); and of SMARCC2, a subunit of the neural progenitor-specific chromatin remodelling complex (npBAF complex) and the neuron-specific chromatin remodelling complex (nBAF complex), which are essential for the chromatin remodelling that takes place during neural development when the cells switch from a stem/progenitor to a post-mitotic state (Lessard et al., 2007; **Figure 30b**). On the other hand, regarding Group 3, ISMARA results indicated that the changes in gene expression across the samples were associated with the activity of KLF4, which is a transcription factor involved in the maintenance of embryonic stem cells that has been also shown to promote NSC self-renewal (Moon et al., 2018); of Znf711, known to regulate the expression of genes involved in neural development (Kleine-Kohlbrecher et al., 2010); and of TFDP1 and E2F1, both associated with cell cycle regulation and DNA replication (Wu et al., 1995; **Figure 30c**).

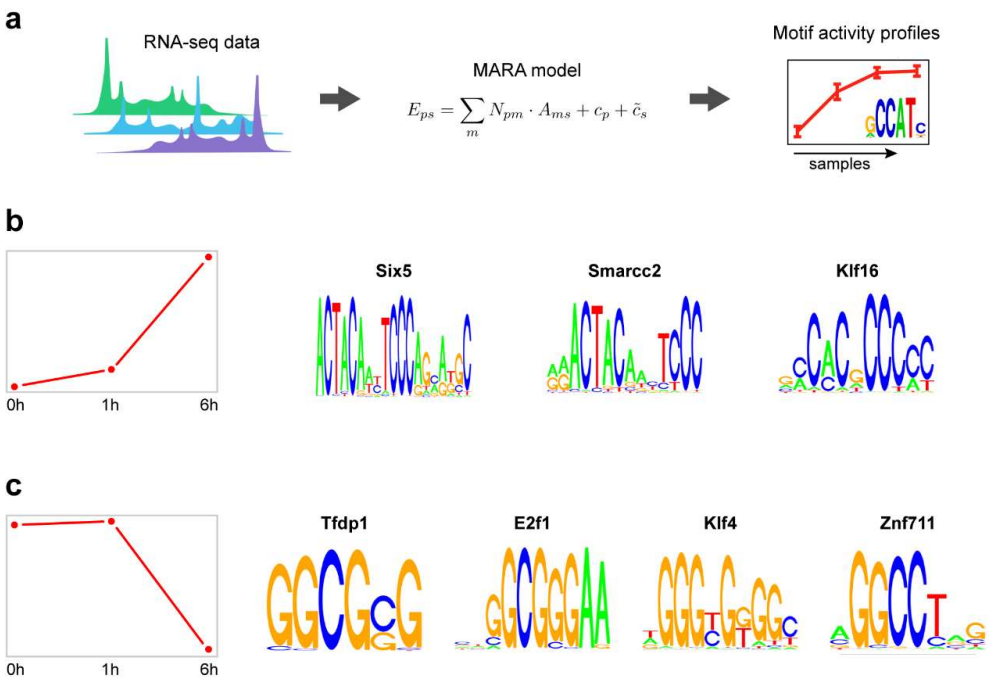

Figure 30| Prediction of the key transcription factors responsible for the changes in gene expression detected during the first 6 hours of NSC differentiation. (a) Schematic representation

of the Integrated System for the Motif Activity Response Analysis (ISMARA) pipeline. **(b)** Motif activity profile for the genes upregulated during NSC differentiation. **(c)** Motif activity profile for the genes downregulated during NSC differentiation.

Altogether, these analyses revealed that, at the transcriptional level, the samples isolated 1 hour after the induction of NSC differentiation were closer to the ones obtained from undifferentiated NSCs (0h) than to the ones obtained 6 hours after the onset of the differentiation process. In order to gain more insight into this, we performed a hierarchical cluster analysis based on the differentially expressed genes (DEGs). We observed that, although the samples obtained 6 hours after the induction of NSC differentiation clustered together, the samples obtained from undifferentiated NSCs (0h) and cells after 1 hour of differentiation did not clustered according to their time-point (**Figure 31b**), indicating that 1 hour was not enough time to generate significant changes at the transcriptional level in this system. Nonetheless, when the hierarchical cluster analysis was performed based on the IR events that we were able to detect, the samples clustered in agreement with their differentiation time (**Figure 31c**), suggesting that, in response to the differentiation signal, changes in the splicing pattern are more rapidly implemented that changes in the transcriptional pattern.

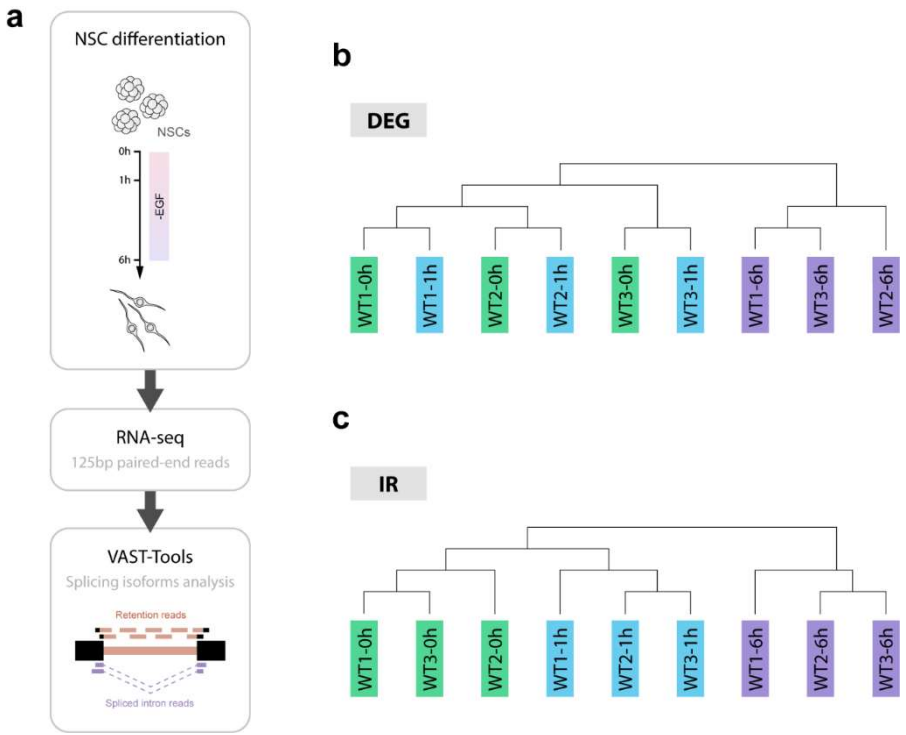

Figure 31| Hierarchical clustering analysis based on DEG and IR events (a) Schematic

representation of the strategy used for the identification of intron retention events during NSC differentiation. **(b)** Samples grouped using hierarchical clustering based on differentially expressed genes (DEG). **(c)** Samples grouped using hierarchical clustering based on intron retention events (IR).

3.2. Intron detention regulates the subcellular localization of multiple transcripts related to NSC self-renewal and differentiation

With the aim of identifying other genes whose expression is post-transcriptionally regulated by intron detention, as we have described for *Scratch1*, we performed an analysis of splicing variants using VAST-Tools (Vertebrate Alternative Splicing and Transcription Tools; Braunschweig et al., 2014). This toolset enables the detection of IR events by aligning RNA-seq reads to comprehensive sets of exon–intron and exon–exon junctions (**Figure 31a**), which in our system led to the detection of thousands of IR events. Then, in order to identify mRNAs that presented differential IR during NSC differentiation, we performed a k-means clustering analysis of the IR events identified, which revealed several patterns of splicing across the samples (**Figure 32**).

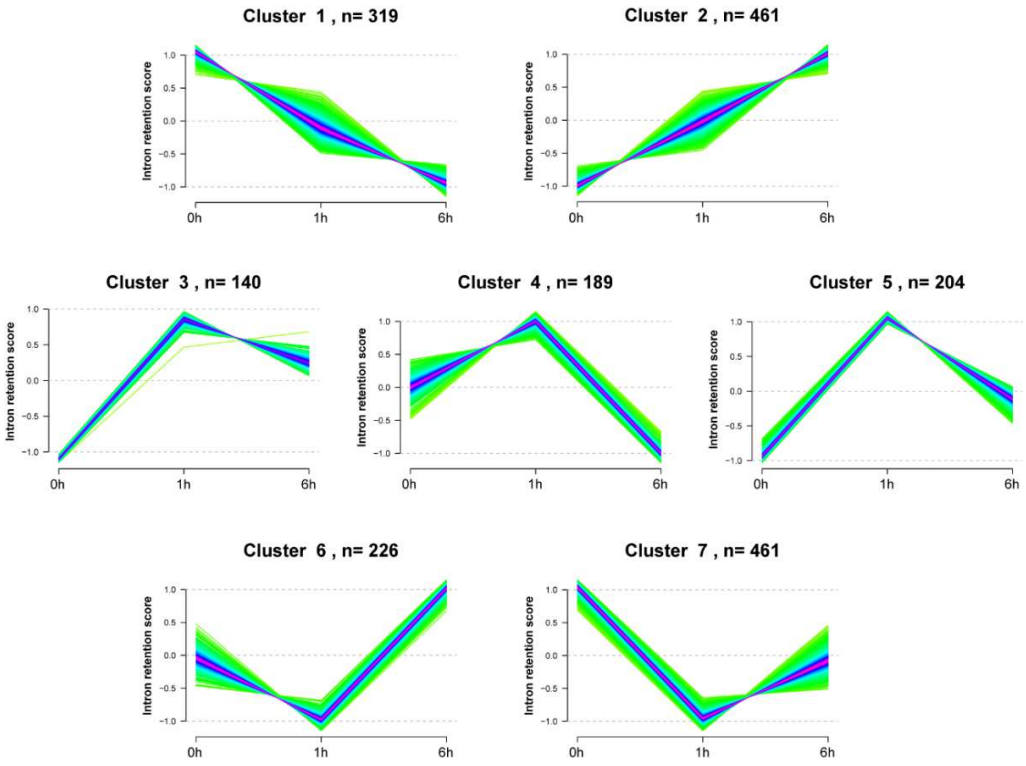

Figure 32| Trends in intron retention during the process of NSC differentiation. Plots depicting the different splicing patterns identified for all the intron retention events detected, grouped using k-means clustering.

For further analysis, we decided to focus particularly on Cluster 1, which included genes that presented the same splicing pattern than *Scratch1* mRNA (i.e. intron detention in NSCs and splicing in response to the differentiation signal; **Figure 33b,c**); and on Cluster 2, which was composed by genes with the opposite pattern (i.e. normal processing of the transcripts in NSCs and intron detention upon the induction of differentiation; **Figure 33d,e**). Performing a functional enrichment analysis, we found that Cluster 1 contained genes related with both neuronal and glial differentiation, as well as axonogenesis and axon guidance (**Figure 33b**); Cluster 2 contained genes associated with stem cell maintenance and the regulation of proliferation (**Figure 33d**). Moreover, we noticed that the genes and enriched functional terms associated with Cluster 1 were related to the ones of Group 3 (genes downregulated upon the induction of NSC differentiation) in the expression trends clustering analysis (**Figure 29e**), whereas those that were assigned to Cluster 2 were more related to Group 1 (genes upregulated along the differentiation process; **Figure 29c**), suggesting that these events of IR might be involved in the post-transcriptional silencing of the affected genes.

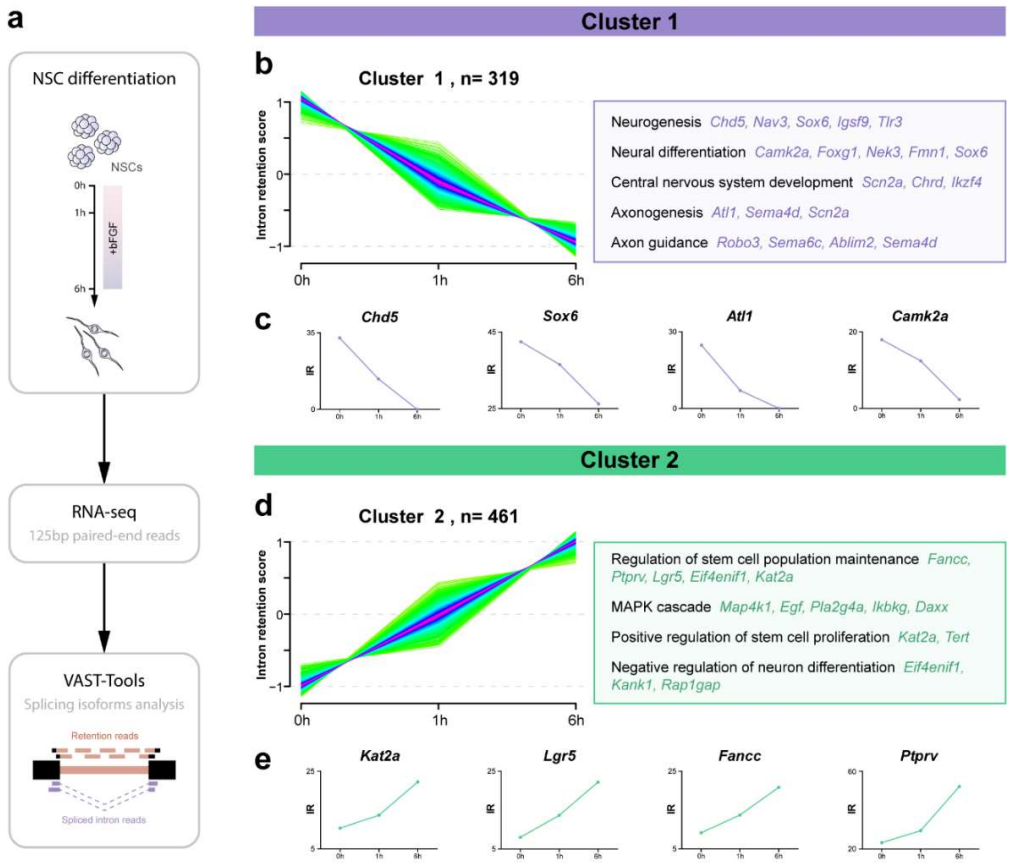

Figure 33| Intron retention is present in multiple transcripts related to NSC self-renewal and differentiation. (a) Schematic representation of the pipeline followed for the identification of splicing

variants during NSC differentiation. **(b)** Plot illustrating time point-specific changes in intron retention for genes belonging to Cluster 1 (left), and representative Gene Ontology (GO) terms of the biological process categories enriched in this cluster (rigth). **(c)** Intron retention score for several representative genes belonging to Cluster 1: *Chd5*, *Sox6*, *Atl1* and *Camk2a*. **(d)** Plot illustrating time point-specific changes in intron retention for genes belonging to Cluster 2 (left) and representative Gene Ontology (GO) terms of the biological process categories enriched in this cluster (rigth). **(e)** Intron retention score for several representative genes belonging to Cluster 2: *Kat2a*, *Lgr5*, *Fancc* and *Ptprv*.

In order to characterize the effect that intron detention had on the subcellular localization of the transcripts of these genes, we selected several candidates from each cluster and examined the distribution of their mRNA in response to NSC differentiation in culture. On the one hand, among the candidates selected from Cluster 1 there was *Chd5*, which encodes for a chromatin-remodeling protein that induces the expression of genes that favor terminal neuronal differentiation and represses that of genes involved in cell proliferation (Egan et al., 2013; Potts et al., 2011; Vestin and Mills, 2013). In the case of this gene, as was also the case for the other Cluster 1 genes selected for validation, its mRNA was unspliced and consistently accumulated in the nucleus in NSCs, whereas it was processed and exported upon the induction of differentiation (**Figure 34c**), as predicted by the RNA-seq data (**Figure 34a,b**). Moreover, when cells where treated with DAA, transcripts did not undergo splicing and remained in the nucleus, indicating that, as observed for *Scratch1* transcripts, mRNA methylation promoted the splicing and export of the transcripts included in Cluster 1.

On the other hand, as an example of Cluster 2 we selected *Ptprv*, which encodes a tyrosine phosphatase involved in stem cell maintenance (Lee et al., 1997). In the case of *Ptprv*, as well as for the rest of Cluster 2 genes analyzed, we observed that its mRNA was normally spliced in NSCs, while intron retention was detected when differentiation was induced (**Figure 35c**), as the RNA-seq data indicated (**Figure 35a,b**). Consequently, *Ptprv* transcripts exhibited a canonical cytoplasmic distribution in NSC and accumulation in the nucleus during the differentiation process. Furthermore, although the treatment of differentiating NSC with DAA had no additional effect on the processing and export of *Ptprv* mRNA, which was already unspliced and accumulated in the nucleus in response to the differentiation signal, it was enough to prevent the splicing and export of the mRNA in undifferentiated NSCs, indicating that the subcellular localization of the transcripts that present intron detention upon the induction of differentiation (Cluster 2) is also regulated by mRNA methylation.

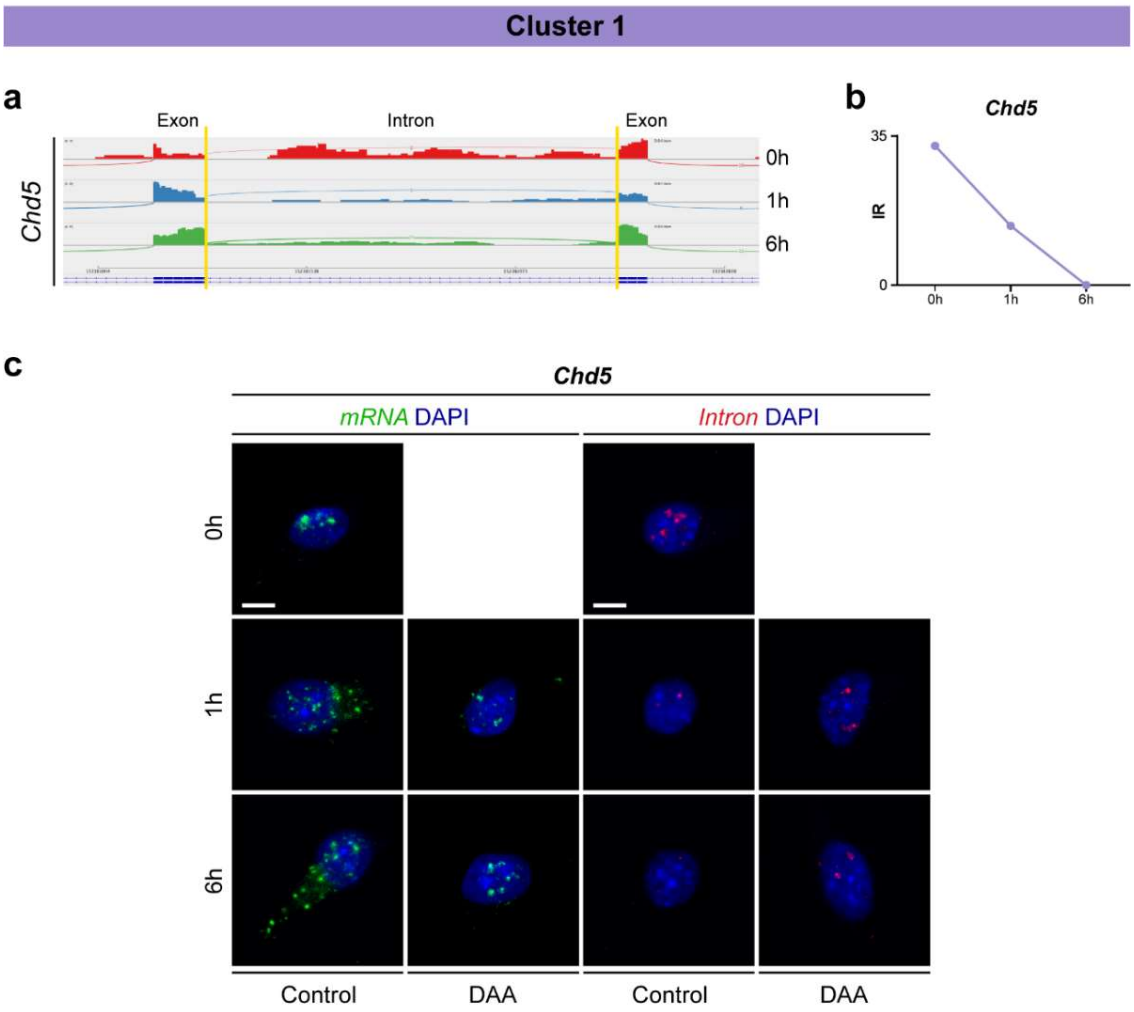

Figure 34| Intron retention associates with the nuclear accumulation of Cluster 1 transcripts in NSCs. (a) Sashimi plots depicting read density and number of splice junctions for Chd5 (Cluster 1) at different time-points during the differentiation process, showing intron detention which decreases with differentiation. **(b)** Intron retention score for *Chd5* (intron 33) 0h, 1h and 6h after the induction of NSC differerntiation. **(c)** *In situ* hybridization for *Chd5* mRNA (green) or intron (red) in control NSCs and in NSCs treated with DAA, as an example of a Cluster 1 gene. Scale bars represent 5 μm.

Therefore, these results indicate that intron detention controls the subcellular localization and, therefore, the availability for translation of numerous transcripts relevant for the regulation of both NSC self-renewal and differentiation in the context of adult neurogenesis.

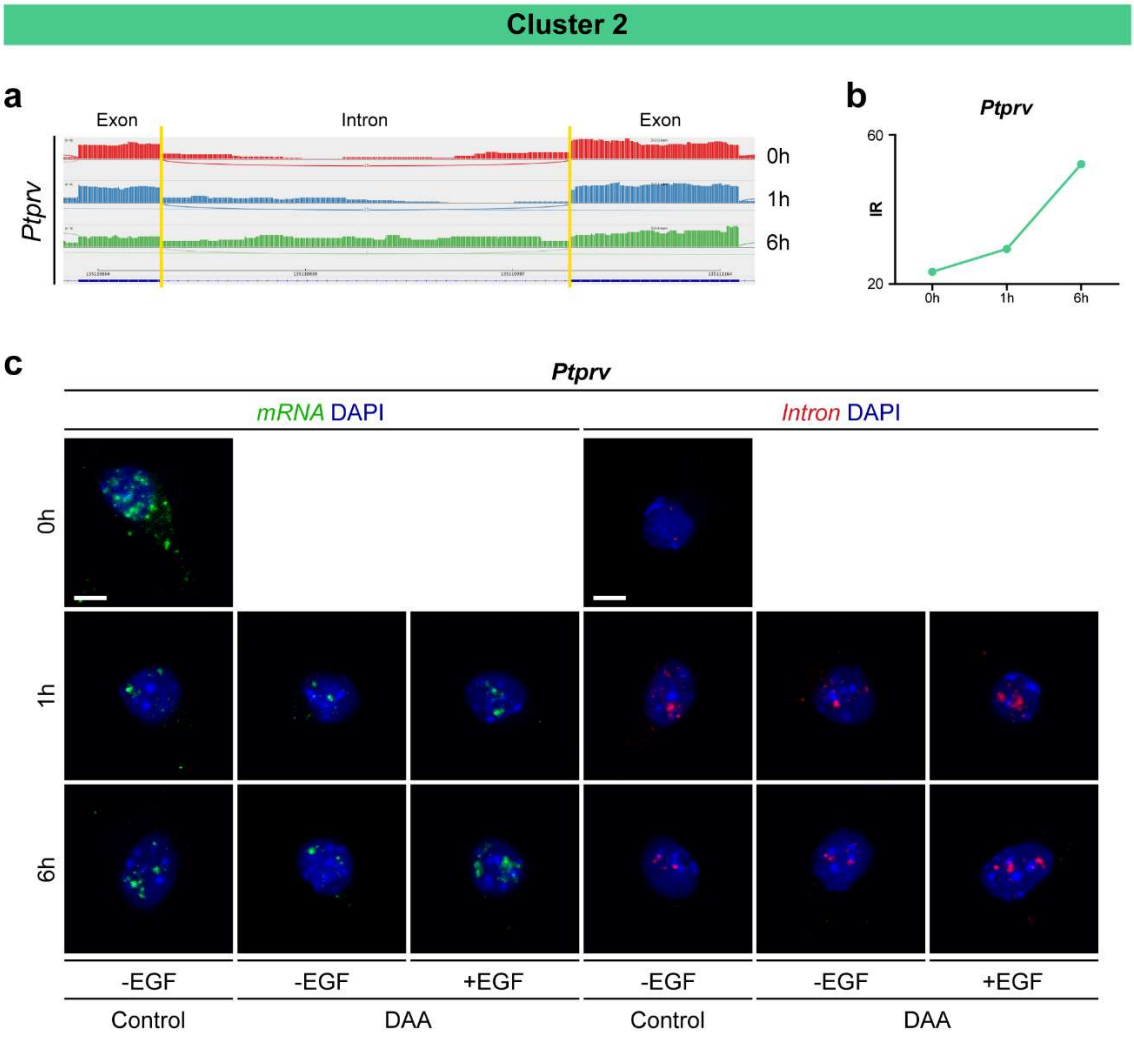

Figure 35| Intron retention induces the nuclear retention of Cluster 2 transcripts during NSC differentiation. (a) Sashimi plots depicting read density and number of splice junctions for *Ptprv* (Cluster 2) at different time-points of the differentiation process, showing an increase in intron retention with differentiation. **(b)** Intron retention score for *Ptprv* (intron 28) 0h, 1h and 6h after the induction of NSC differerntiation. **(c)** *In situ* hybridization for *Ptprv* mRNA (green) or intron (red) in control NSCs and in NSCs treated with DAA, as an example of a Cluster 2 gene. Scale bars represent 5 µm.

Discussion

The life-long persistence of adult NSCs requires the accurate balance between their self-renewal, proliferation and differentiation. This is achieved through the implementation of a plethora of regulatory mechanisms that tightly control the biology and function of NSCs. In this work, we describe a novel regulatory mechanism that controls the availability of transcripts for translation in the adult subependymal neurogenic niche. We started with the study of *Scratch1* confirming its role in promoting the survival of the differentiating neural cells, as well as favoring their terminal differentiation into neurons. Its study has allowed us to unveil a novel molecular mechanism used by genes involved in the control of either stemness or differentiation in the murine adult nervous system. It involves nuclear retention of transcripts, favored by an acquired sequence that impairs mRNA splicing in a manner that can be relieved by m^6A mRNA methylation. Importantly, this epitranscriptomics event that always triggers mRNA nuclear export occurs in NSCs in genes involved in the maintenance of stemness and in genes that promote differentiation only after NSCs received the neural differentiation signal. Thus, switch in the set of methylated transcripts controls the balance between stemness and differentiation in the adult subependymal stem cell niche.

1. Scratch1 and its role during NSC differentiation

In mammals, *Scratch1* is expressed in several regions of the adult brain (Marín and Nieto, 2006), including the two main neurogenic niches: the SEZ of the LVs (**Figure 11**) and the SGZ in the DG of the hippocampus (**Figure 21**). As it is the most active germinal region, we have focused in the SEZ, where we have determined that *Scratch1* is expressed along the entire neurogenic lineage, from NSCs to immature neurons. Nevertheless, its expression progressively increases as NSC differentiate, pointing to a role for Scratch during this process. In fact, we have found that *Scratch1* downregulation caused a decreased in the proportion of neurons differentiated from NSCs (**Figure 15**), indicating that Scratch1 also favors the acquisition of the neuronal fate in the adult brain, as it has been previously described for several members of the Scratch family, during mouse cortical development (Nakakura et al., 2001a; Paul et al., 2014) and in other species, including *Drosophila* (Roark et al., 1995) and *C. elegans* (Metzstein and Horvitz, 1999). Accordingly, *Scratch1* is among the very first genes that are expressed when microglia cells are artificially transformed into neurons, and contributes to this conversion by the transcriptional repression of microglial-associated genes, promoting the acquisition of neuronal properties (Matsuda et al., 2019).

This closely resembles the mechanism by which *Scratch* genes promote neuronal differentiation in physiological conditions, fulfilling their role as transcriptional repressors and blocking the expression of genes associated with non-neuronal fates (Metzstein and Horvitz, 1999; Nakakura et al., 2001b; Paul et al., 2014; Roark et al., 1995).

On the other hand, *Scratch1* downregulation in differentiating NSCs also produced a significant increase in apoptosis (**Figure 13**), indicating that it acts as a survival factor during this process, similarly to what has been described for Scratch homologs in *C. elegans* (Metzstein and Horvitz, 1999; Thellmann et al., 2003) and in zebrafish embryos (Rodríguez-Aznar and Nieto, 2011). As it is the case of scratch2 in the developing zebrafish spinal cord, we have determined that Scratch1 protects the differentiating NSCs from undergoing apoptosis by acting downstream of p53 and repressing the transcription of its target *Bbc3* (Puma), which is the main effector of cell death induced by p53 in vertebrates (Hafner et al., 2019). Moreover, in differentiating NSCs Scratch1 also inhibits the expression of *Cdkn1a* (**Figure 13i**), which encodes for p21, a cyclin-dependent kinase (CDK) inhibitor that is involved in p53-mediated cell cycle arrest (Hafner et al., 2019). Consistently, the reduction in *Scratch1* expression led to a significant reduction in the proliferation of differentiating progenitor cells (**Figure 14b,c**), contributing to the maintenance of their normal proliferation. Altogether, these results indicate that Scratch1 contributes to the homeostasis of neuronal populations during NSC differentiation acting downstream of p53, both in the adult SEZ and during embryonic development (Van Lookeren Campagne and Gill, 1998; Meletis et al., 2006). Interestingly, it has been recently described that the loss of p53 in human iPSC-derived NSCs induces their premature differentiation into neurons (Marin Navarro et al., 2020), pointing towards a role for this transcription factor in the regulation of neuronal differentiation. Assuming a similar function in the SEZ-resident NSC lineage, one could speculate that Scratch1 may favor neuronal differentiation not only by blocking the expression of non-neuronal genes (Metzstein and Horvitz, 1999; Nakakura et al., 2001b; Paul et al., 2014; Roark et al., 1995), but also through the repression of p53 transcriptional targets.

2. Regulation of Scratch1 translation: A matter of splicing

Splicing has been identified as one of the most relevant process for SEZ neurogenesis, whereas it does not appear to be that prominent in non-neurogenic regions (Lim et al., 2006), even though alternative splicing is known to be particularly active in the adult central

nervous system (Raj and Blencowe, 2015). Here, we describe that in SEZ-resident NSCs, *Scratch1* mRNA is retained in the nucleus due to inefficient splicing (**Figure 18**). Decreased splicing efficiency most often arises from the deficient recognition of canonical splicing sites and usually associates with the presence of weak consensus sequences in this positions (Kornblihtt et al., 2013; Sibley et al., 2016). In this sense, we have observed that in the case of *Scracth1,* the PPT, one of the intronic regions recognized by the spliceosome (Herzel et al., 2017) is significantly enlarged, generating a weak slice site. This deviation from the consensus likely affects its recognition by the splicing machinery and has as a consequence the reduction in its splicing efficiency (Sibley et al., 2016; Vargas et al., 2011), which without fully blocking its processing, allows the implementation of an additional layer of regulation.

By analyzing the PPT sequences of *Scratch1* orthologues in different vertebrate species, we found that the enlargement observed in mouse is present in all mammals analyzed (n=8), including humans, whereas the length of this sequence does not diverge from the consensus in the rest of the vertebrates (n=12). In agreement with this observations, in zebrafish, with *scratch1a* and *scracth1b* introns bearing consensus splicing sites, their transcripts are exported to the cytoplasm as soon as they are transcribed (**Figure 20**). By contrast, in the mouse, although *Scratch1* starts to be transcribed as soon as stem cells acquire neural identity (**Figure 23**), its mRNA remains in the nucleus in SEZ-resident NSCs (**Figure 17**), unavailable for translation (**Figure 36**). As expected form this, we found that *Scratch1* downregulation did not cause any phenotype in undifferentiated NSCs, reflecting that, although the gene is transcribed, Scratch1 is not functional in these cells, and therefore, it is dispensable until NSCs engage into the differentiation process. On the other hand, similar to the situation in zebrafish, we have observed that in the SGZ of the hippocampus, the other main neurogenic niche in mammals, *Scratch1* mRNA always presents a canonical cytoplasmic distribution (**Figure 21**), indicating that the enlargement in *Scratch1* PPT is not necessarily associated with the retention of the intron in every context. This is in agreement with the observation that intron detention events, although associated with the presence of weak splice sites, are in most cases tissue- or even cell type-specific (Braunschweig et al., 2014). Moreover, as happens in the zebrafish PGZ, *Scratch1* expression is not detectable in SGZ-resident NSCs, but instead starts to be transcribed later in the lineage when it is already required to fulfill its function. This reveals a differential regulation of *Scratch1* expression between the SEZ and the SGZ. Although these two neurogenic niches present multiple similarities, they also differ in important aspects, including (i) their anatomy, with the SGZ located away from the ventricles and the SEZ in

direct contact with them; and (ii) the fate of the neurons derived from their resident NSCs, becoming glutamatergic excitatory neurons in the SGZ that integrate in the DG itself, or migrating from the SEZ niche to the OB, to give rise to different inhibitory neurons (Obernier and Alvarez-Buylla, 2019). Additionally, the SEZ and the SGZ also differ in the kinetics of the neurogenic process. It has been estimated that, in the SEZ, the generation of neuroblast from NSCs takes 3-4 days (Ponti et al., 2013b) and their migration to the OB and their terminal differentiation, about 15 additional days (Petreanu and Alvarez-buylla, 2002). By contrast, in the SGZ the differentiation of NSCs into neuroblast lasts for approximately 2 weeks and their subsequent maturation, 1-2 additional months (Bischofberger, 2007). Thus, even though neuroblasts do not need to migrate far from the niche prior their terminal differentiation, neurogenesis constitutes a substantially slower process in the SGZ when compared to the SEZ. Taking this into account, we propose that in the SEZ, due to its fastest kinetics, Scratch1 protein might be required at the very first stages of NSC differentiation, and its translation would be more efficiently accomplished by having the gene already transcribed and its transcripts retained in the nucleus. By contrast, the slower kinetics of the SGZ would allow enough time for *Scratch1* to be transcribed, processed and translated when cells have already left the stem cell state. In this sense, *Scratch1* intron detention in the SEZ would allow the generation of a reservoir of transcripts that accumulate in the nucleus until they are required, “priming” NSCs for further differentiation, which will require the production of Scratch1 protein.

Consistently, we have shown that *Scratch1* mRNA is rapidly spliced and exported in response to the differentiation signal, being available for translation one hour after the cells received the extracellular input (**Figure 24**). Furthermore, we have determined that the processing of the detained intron and *Scracth1* mRNA nuclear export in response to NSC differentiation signals is promoted by the m^{6}A-modification of the transcripts (**Figure 28** and **Figure 36**). At the molecular level, m^{6}A can function both as a recognition element for specific RNA binding proteins or as a structural switch (Harcourt et al., 2017). The latter is due to the fact that the addition of the methyl group destabilizes A-U pairs (Engel and von Hippel, 1974; Roost et al., 2015), which hinders the formation of RNA duplexes (Spitale et al., 2015) and exposes binding sites to RNA binding proteins. In particular, it has been already described that the unstructured conformation of the transcripts as a result of m^{6}A deposition facilitates the binding of HNRNPC/G, promoting the splicing (Liu et al., 2015, 2017). In the case of *Scratch1* intron, its enlarged PPT might be involved in the generation of secondary structures, which has been described to reduce splicing efficiency (Vargas et

al., 2011), and the methylation of the mRNA might contribute to the destabilization of those duplexes, favoring its recognition by the splicing machinery. Alternatively, the m^{6}A mark might be recognized by a specific reader that recruits additional factors to stimulate the splicing of *Scratch1* intron.

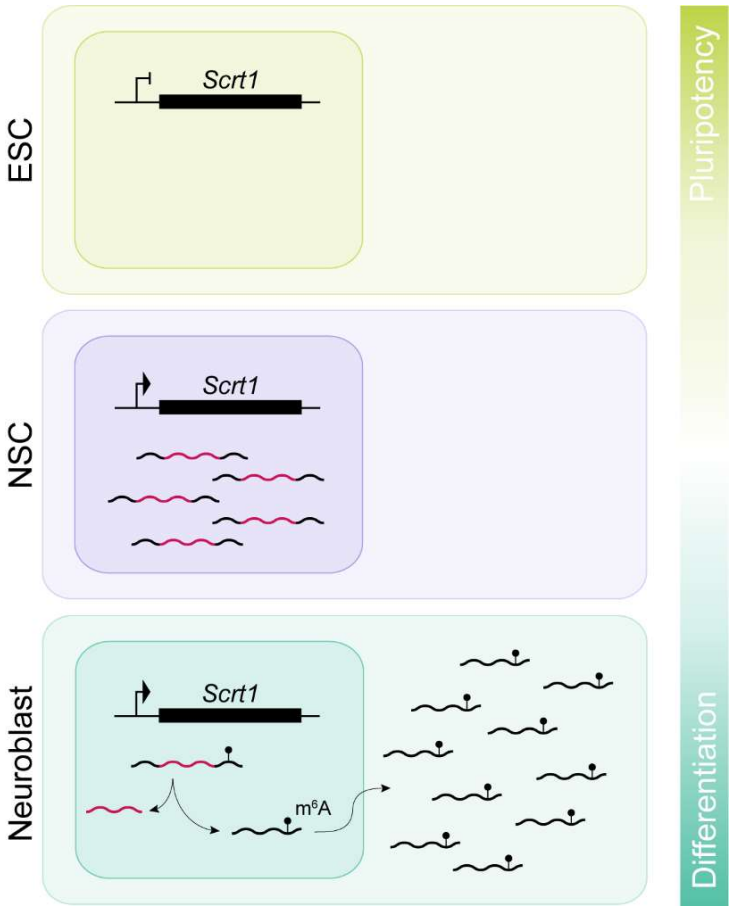

Figure 36| *Scratch1* mRNA splicing and nuclear export are dependent on m^{6}A deposition in response to the differentiation signal. *Scratch1* starts to be expressed when SCs acquire neural identity, but its transcripts are retained in the nucleus due to inefficient splicing. NSC, upon receiving the differentiaion signal, bear *Scratch1* mRNA methylated and, hence, spliced and exported to the cytoplasm, where the protein is translated to protect differentiating cells from undergoing apoptosis and to promote neuronal differentiation.

3. Intron detention as a mechanism to fine-tune adult neurogenesis

Several transcriptomic analyses performed during the progression of NSCs into the differentiation process have revealed that mRNAs typically associated with more differentiated cells can be already detected in NSCs (Beckervordersandforth et al., 2010; Dulken et al., 2017; Llorens-Bobadilla et al., 2015). Moreover, it has been recently shown that some transcripts are translated less efficiently than expected considering their mRNA levels (Baser et al., 2019). Altogether, these observations point to an important influence of

post-transcriptional regulation in the control of adult neurogenesis, that had remained elusive. Here we describe the regulatory mechanism that controls the subcellular localization of a large number of transcripts associated with both the maintenance of NSC in an undifferentiated state and their differentiation. This mechanism has the potential to tightly regulate the time in which these mRNAs are available for translation, contributing to the precise control of neural differentiation.

We find that intron detention regulates the post-transcriptional expression of transcripts related to (i) NSCs self-renewal and proliferation (Cluster 2) and (ii) differentiation (Cluster 1). On the one hand, genes belonging to Cluster 1 present intron detention in NSCs, where consequently accumulate in the nucleus, showing a rapid splicing and nuclear export in response to the differentiation signal. By contrast, Cluster 2 genes are properly spliced in NSCs, and the differentiation signal triggers intron retention and prevents their export from the nucleus. Detained introns can be spliced in response to different stimuli (Denis et al., 2005; Gill et al., 2017; Mauger et al., 2016; Naro et al., 2017; Ninomiya et al., 2011; Wong et al., 2013). However, little is known about how the extracellular signals are transduced in order to trigger the post-transcriptional processing of the transcripts. We have shown that, in the context of adult neurogenesis, the splicing of detained introns and the subsequent export to the cytoplasm of the different subsets of transcripts is promoted by the methylation of the mRNAs, revealing that m^6A modification might act as a connection between external stimuli and the processing of detained introns in response to them. In fact, the majority of mRNA-modifying enzymes reside in the nucleus (Gilbert et al., 2016), where they have access to DI-mRNAs, and their activity is known to be responsive to extracellular inputs. For instance, TGFβ signaling triggers the recruitment of the m^6A methylation complex by SMAD2/3 in hPSCs, stimulating the co-transcriptional methylation of given mRNAs (Bertero et al., 2018). YTHDF2, a m^6A reader that usually localizes in the cytoplasm, accumulates in the nucleus in response to heat shock stress, where it competes with the demethylase FTO, modulating the pattern of m^6A and promoting the translation of specific transcripts (Zhou et al., 2015). Furthermore, METTL3 and METTL14 can be post-translationally modified, which affects their capacity to interact with other components of the methylation complex and modulates their methylation activity (Du et al., 2018; Wang et al., 2016). In the adult SEZ, the balance between NSC self-renewal and differentiation is tightly regulated by both intrinsic and extrinsic factors. In this work, we have used an *in vitro* system in which NSC differentiation is triggered in response to EGF withdrawal (Belenguer et al., 2016). However, i*n vivo*, this process is regulated by a myriad of stimuli, such as BMPs present in the CSF

or released within the niche, the interaction with resident microglia or the synaptic inputs of dopaminergic neurons (Obernier and Alvarez-Buylla, 2019). Nevertheless, it remains to be determined whether these factors directly modulated the activity of the methylation machinery and how this impacts on the m^{6}A pattern.

Moving from the adult organism to the embryo, several studies connect m^{6}A with the regulation of the balance between retinal ganglion cells (RGC) self-renewal and differentiation during cortical development (Edens et al., 2019; Li et al., 2018b; Wang et al., 2018; Yoon et al., 2017), either by stimulating the decay of labelled transcripts or by promoting the nuclear export of m^{6}A-mRNAs through the CRM1-dependent pathway. Additionally, since RGC and adult NSCs are ontogenetically related, it is possible that m^{6}A also regulates the subcellular localization of specific transcripts during cortical development, as we have described in the case of SEZ-derived NSC differentiation. Moreover, it is noteworthy that both intron detention and m^{6}A have been shown to be relevant in processes such as spermatogenesis (ID: Naro et al., 2017; m^{6}A: Bailey et al., 2017; Hsu et al., 2017; Jain et al., 2018; Lin et al., 2017; Wojtas et al., 2017; Xu et al., 2017; Zheng et al., 2013) and hematopoiesis (ID: Cho et al., 2014; Edwards et al., 2015; Ni et al., 2016; Pimentel et al., 2016; Wong et al., 2013; m^{6}A: Lee et al., 2019; Li et al., 2018a, 2018c; Vu et al., 2017; Weng et al., 2018; Zhang et al., 2017). Therefore, the connection between the m^{6}A modification and intron detention might exist also in other systems.

Regardless of the context, the generation of reservoirs of mRNAs in the nucleus thought intron detention allows the rapid translation of these transcripts in the precise moment in which they are required, accelerating the response of the cells to external stimuli. Remarkably, immediately-early genes transcripts are shorter than the average (Tullai et al., 2007), which allow a faster transcription reducing the time they need to be ready for translation. Conversely, intron detention has been associated with longer transcripts (Braunschweig et al., 2014; Mauger et al., 2016). Thus, intron detention may provide a mechanism to generate rapid changes in gene expression, regardless of the length of the genes. Moreover, in the case of transcripts associated with the maintenance of NSCs in an undifferentiated state, the fast switch in their splicing pattern in response to the differentiation signal and the consequent events of intron detention in those mRNAs, rapidly block their translation, buffering the residual transcription and sharpening the response of the cells. Additionally, intron detention may also constitute a mechanism to synchronize the release from the nucleus of functionally related transcripts, allowing a coordinated and

robust response to changes in the extracellular environment and contributing to the establishment of what has been called 'RNA regulons' (Keene, 2007). Similarly, it has been proposed that m^{6}A methylation, being such a dynamic modification, might act selecting groups of functionally related transcripts to be coordinately regulated in response to changes in the external stimuli (Roundtree et al., 2017a). Altogether, these findings emphasize the relevance of post-transcriptional regulation in the control of numerous biological processes, highlighting the concept that transcription not necessarily implies translation and consequently, function.

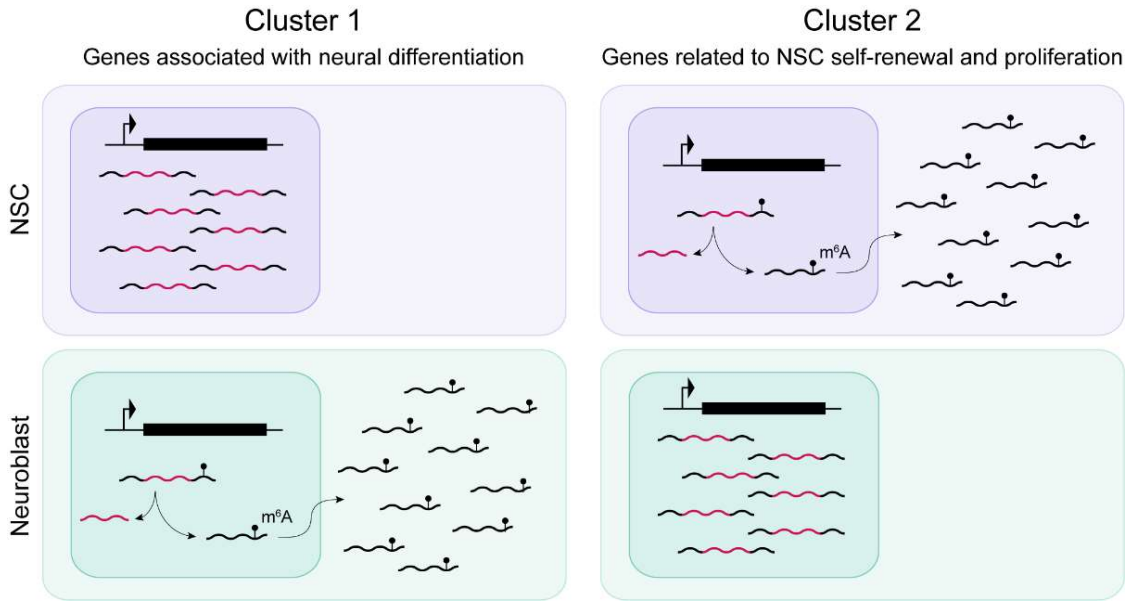

Figure 37| Intron detention regulates the translational availability of multiple mRNAs related with NSC self-renewal, proliferation and differentiation.

In summary, here we describe mRNA methylation as a mechanism that allows the rapid production of proteins in response to external stimuli and that operates like a switch on transcripts belonging to antagonistic functional groups, allowing a tight control in the timing of neural differentiation in the adult subependymal neural stem cell niche.

Conclusions

1. We have found that the Scratch1 transcription factor is expressed in the adult SEZ, where it plays several functions. It acts as a survival factor downstream of p53, repressing the transcription of its targets *Bbc3* (Puma) and *Cdkn1a* (p21). In addition, Scratch1 promotes neuronal differentiation, favoring neurogenesis at the expense of gliogenesis.

2. Although Scratch1 acts in response to the neural differentiation signal, it is constitutively transcribed in the NSCs of the SEZ. It is maintained inactive due to a deficient splicing that leads to the detention of its transcripts in the nucleus.

3. Upon receiving the neural differentiation signals, *Scratch1* mRNA is rapidly methylated and immediately spliced and exported to be translated in the cytoplasm.

4. We describe intron detention and subsequent mRNA methylation as a mechanism that allows an immediate cell response to the neural differentiation signal.

5. We also find that this mechanism is not *Scratch1*-specific but rather a general mechanism used to tightly control the response to neural differentiation signals in the adult subependymal neural stem cell niche.

6. Finally, we show that intron detention also operates preventing the translation of genes related to the maintenance of stemness during neural differentiation. Thus, a switch in the methylation status of gene transcripts related to stemness or differentiation regulates the activity of the neural stem cell niche.

1. Hemos encontrado que el factor de transcripción Scratch1 se expresa en la SEZ adulta, donde lleva a cabo varias funciones. Por una parte, actúa como factor de supervivencia por debajo de p53, reprimiendo la transcripción de sus dianas *Bbc3* (Puma) and *Cdkn1a* (p21). Además, Scratch1 promueve la diferenciación neuronal, favoreciendo la neurogénesis a expensas de la gliogénesis.

2. Aunque Scratch1 actúa en respuesta a la señal de diferenciación neural, se expresa de forma constitutiva en las NSCs de la SEZ, manteniéndose inactivo debido a un procesamiento deficiente que lleva a la detención de sus tránscritos en el núcleo.

3. En respuesta a las señales de diferenciación neural, el mRNA de *Scratch1* es rápidamente metilado e inmediatamente sufre *splicing* y es exportado para ser traducido en el citoplasma.

4. Hemos descrito la detención de intrones y la subsecuente metilación de mRNA como un mecanismo que permite una respuesta celular inmediata a la señal de diferenciación neural.

5. Hemos determinado que este mecanismo no es específico de *Scratch1*, sino que es un mecanismo general usado para controlar de forma precisa la respuesta a las señales de diferenciación neural en la SEZ adulta.

6. Finalmente, hemos mostrado que la detención de intrones también actúa previniendo la traducción de genes asociados con el mantenimiento de las propiedades de célula madre durante la diferenciación neural. Por tanto, un cambio en el patrón de metilación de mRNAs relacionados con el mantenimiento o la diferenciación de las células madre regula la actividad del nicho neurogénico.

Bibliography

Abad, M., Mosteiro, L., Pantoja, C., Cañamero, M., Rayon, T., Ors, I., Graña, O., Megías, D., Domínguez, O., Mertínez, D., et al. (2013). Reprogramming in vivo produces teratomas and iPS cells with totipotency features. Nature *502*, 340–345.

Acloque, H., Wilkinson, D.G., and Nieto, M.A. (2008). Chapter 9 In Situ Hybridization Analysis of Chick Embryos in Whole-Mount and Tissue Sections. Methods Cell Biol. *87*, 169–185.

Akef, A., Lee, E.S., and Palazzo, A.F. (2015). Splicing promotes the nuclear export of β-globin mRNA by overcoming nuclear retention elements. Rna *21*, 1908–1920.

Altman, J., and Das, G.D. (1965). Autoradiographic and histological evidence of postnatal hippocampal neurogenesis in rats. J. Comp. Neurol. *124*, 319–335.

Aubert, J., Stavridis, M.P., Tweedie, S., Reilly, M.O., Vierlinger, K., Li, M., Ghazal, P., Pratt, T., Mason, J.O., Roy, D., et al. (2003). Screening for mammalian neural genes via fluorescence-activated cell sorter purification of neural precursors from Sox1–gfp knock-in mice Jerome.

Avgustinova, A., and Benitah, S.A. (2016). Epigenetic control of adult stem cell function. Nat. Rev. Mol. Cell Biol. *17*, 643–658.

Bailey, A.S., Batista, P.J., Gold, R.S., Grace Chen, Y., de Rooij, D.G., Chang, H.Y., and Fuller, M.T. (2017). The conserved RNA helicase YTHDC2 regulates the transition from proliferation to differentiation in the germline. Elife *6*.

Balwierz, P.J., Pachkov, M., Arnold, P., Gruber, A.J., Zavolan, M., and Van Nimwegen, E. (2014). ISMARA: automated modeling of genomic signals as a democracy of regulatory motifs. Genome Res. *24*, 869–884.

Barrallo-Gimeno, A., and Nieto, M.A. (2005). The Snail genes as inducers of cell movement and survival: Implications in development and cancer. Development *132*, 3151–3161.

Barrallo-Gimeno, A., and Nieto, M.A. (2009). Evolutionary history of the Snail/Scratch superfamily. Trends Genet. *25*, 248–252.

Baser, A., Skabkin, M., Kleber, S., Dang, Y., Gülcüler Balta, G.S., Kalamakis, G., Göpferich, M., Ibañez, D.C., Schefzik, R., Lopez, A.S., et al. (2019). Onset of differentiation is post-transcriptionally controlled in adult neural stem cells. Nature *566*, 100–104.

Beckervordersandforth, R., Tripathi, P., Ninkovic, J., Bayam, E., Lepier, A., Stempfhuber, B., Kirchhoff, F., Hirrlinger, J., Haslinger, A., Lie, D.C., et al. (2010). In vivo fate mapping and expression analysis reveals molecular hallmarks of prospectively isolated adult neural stem cells. Cell Stem Cell *7*, 744–758.

Belenguer, G., Domingo-Muelas, A., Ferrón, S.R., Morante-Redolat, J.M., and Fariñas, I. (2016). Isolation, culture and analysis of adult subependymal neural stem cells. Differentiation *91*, 28–41.

Belenguer, G., Duart-Abadia, P., Jordán-Pla, A., Domingo-Muelas, A., Blasco-Chamarro, L., Ferrón, S.R., Morante-Redolat, J.M., and Fariñas, I. (2020). Adult Neural Stem Cells Are Alerted by Systemic Inflammation through TNF-alpha Receptor Signaling. Cell Stem Cell 1–15.

Bertero, A., Brown, S., Madrigal, P., Osnato, A., Ortmann, D., Yiangou, L., Kadiwala, J., Hubner, N.C., Ruiz de los Mozos, I., Sadee, C., et al. (2018). The SMAD2/3 interactome

reveals that TGFβ controls m6 A mRNA methylation in pluripotency. Nature *555*, 256–259.

Bischofberger, J. (2007). Young and excitable: New neurons in memory networks. Nat. Neurosci. *10*, 273–275.

Biteau, B., Hochmuth, C.E., and Jasper, H. (2011). Maintaining tissue homeostasis: Dynamic control of somatic stem cell activity. Cell Stem Cell *9*, 402–411.

Bond, A.M., Ming, G.L., and Song, H. (2015). Adult Mammalian Neural Stem Cells and Neurogenesis: Five Decades Later. Cell Stem Cell *17*, 385–395.

Boutz, P.L., Stoilov, P., Li, Q., Lin, C.H., Chawla, G., Ostrow, K., Shiue, L., Ares, M., and Black, D.L. (2007). A post-transcriptional regulatory switch in polypyrimidine tract-binding proteins reprograms alternative splicing in developing neurons. Genes Dev. *21*, 1636–1652.

Boutz, P.L., Bhutkar, A., and Sharp, P.A. (2015). Detained introns are a novel, widespread class of post-transcriptionally spliced introns. Genes Dev. *29*, 63–80.

Braunschweig, U., Barbosa-Morais, N.L., Pan, Q., Nachman, E.N., Alipanahi, B., Gonatopoulos-Pournatzis, T., Frey, B., Irimia, M., and Blencowe, B.J. (2014). Widespread intron retention in mammals functionally tunes transcriptomes. Genome Res. *24*, 1774–1786.

Chaker, Z., Codega, P., and Doetsch, F. (2016). A mosaic world: puzzles revealed by adult neural stem cell heterogeneity. Wiley Interdiscip. Rev. Dev. Biol. *5*, 640–658.

Chambers, I., and Smith, A. (2004). Self-renewal of teratocarcinoma and embryonic stem cells. Oncogene *23*, 7150–7160.

Cho, V., Mei, Y., Sanny, A., Chan, S., Enders, A., Bertram, E.M., Tan, A., Goodnow, C.C., and Daniel Andrews, T. (2014). The RNA-binding protein hnRNPLL induces a T cell alternative splicing program delineated by differential intron retention in polyadenylated RNA. Genome Biol. *15*, 1–17.

Conti, L., Pollard, S.M., Gorba, T., Reitano, E., Toselli, M., Biella, G., Sun, Y., Sanzone, S., Ying, Q.L., Cattaneo, E., et al. (2005). Niche-independent symmetrical self-renewal of a mammalian tissue stem cell. PLoS Biol. *3*, 1594–1606.

Dam, T.M.T., Kim, H.T., Moon, H.Y., Hwang, K.S., Jeong, Y.M., You, K.H., Lee, J.S., and Kim, C.H. (2011). Neuron-specific expression of scratch genes during early zebrafish development. Mol. Cells *31*, 471–475.

Davis, F., and Allen, F.W. (1957). Ribonucleic acids from yeast which contain a fifth nucleotide. J. Biol. Chem. *227*, 907–915.

Dehal, P., and Boore, J.L. (2005). Two rounds of whole genome duplication in the ancestral vertebrate. PLoS Biol. *3*.

Denis, M.M., Tolley, N.D., Bunting, M., Schwertz, H., Lindemann, S., Yost, C.C., Rubner, F.J., Kurt, H., Swoboda, K.J., Fratto, C.M., et al. (2005). Signal-Dependent Pre-mRNA Splicing in Anucleate Platelets Melvin. Cell *122*, 379–391.

Desrosiers, R., Friderici, K., and Rottman, F. (1974). Identification of methylated nucleosides in messenger RNA from Novikoff hepatoma cells. Proc. Natl. Acad. Sci. U. S. A. *71*, 3971–3975.

Dirian, L., Galant, S., Coolen, M., Chen, W., Bedu, S., Houart, C., Bally-Cuif, L., and

Foucher, I. (2014). Spatial Regionalization and Heterochrony in the Formation of Adult Pallial Neural Stem Cells. Dev. Cell *30*, 123–136.

Dominissini, D., Moshitch-Moshkovitz, S., Schwartz, S., Salmon-Divon, M., Ungar, L., Osenberg, S., Cesarkas, K., Jacob-Hirsch, J., Amariglio, N., Kupiec, M., et al. (2012). Topology of the human and mouse m6A RNA methylomes revealed by m6A-seq. Nature *485*, 201–206.

Du, Y., Hou, G., Zhang, H., Dou, J., He, J., Guo, Y., Li, L., Chen, R., Wang, Y., Deng, R., et al. (2018). SUMOylation of the m 6 A-RNA methyltransferase METTL3 modulates its function. Nucleic Acids Res. *46*, 5195–5208.

Dulken, B.W., Leeman, D.S., Boutet, S.C., Hebestreit, K., and Brunet, A. (2017). Single-Cell Transcriptomic Analysis Defines Heterogeneity and Transcriptional Dynamics in the Adult Neural Stem Cell Lineage. Cell Rep. *18*, 777–790.

Edens, B.M., Vissers, C., Su, J., Arumugam, S., Xu, Z., Shi, H., Miller, N., Rojas Ringeling, F., Ming, G. li, He, C., et al. (2019). FMRP Modulates Neural Differentiation through m6A-Dependent mRNA Nuclear Export. Cell Rep. *28*, 845-854.e5.

Edwards, C.R., Middleton, R., An, X., Mishra, T., Mohandas, N., Hardison, R.C., Rasko, J., and Blobel, G.A. (2015). A Dynamic Intron Retention Program in the Mammalian Megakaryocyte and Erythrocyte Lineages. Blood *126*, 2380–2380.

Egan, C.M., Nyman, U., Skotte, J., Streubel, G., Turner, S., O'Connell, D.J., Rraklli, V., Dolan, M.J., Chadderton, N., Hansen, K., et al. (2013). CHD5 is required for neurogenesis and has a dual role in facilitating gene expression and polycomb gene repression. Dev. Cell *26*, 223–236.

Ellis, R.E., and Horvitz, H.R. (1991). Two C. elegans genes control the programmed deaths of specific cells in the pharynx. Development *112*, 591–603.

Engel, J.D., and von Hippel, P.H. (1974). Effects of methylation on the stability of nucleic acid conformations: Studies at the monomer level. Biochemistry *13*, 4143–4158.

Ermolaeva, M., Neri, F., Ori, A., and Rudolph, K.L. (2018). Cellular and epigenetic drivers of stem cell ageing. Nat. Rev. Mol. Cell Biol. *19*, 594–610.

Evans, M.J., and Kaufman, M. (1981). Establishment in culture of pluripotential cells from mouse embryos. Nature *292*, 154–156.

Ferrón, S.R., Andreu-Agulló, C., Mira, H., Sánchez, P., Ángeles Marqués-Torrejón, M., and Fariñas, I. (2007). A combined ex/in vivo assay to detect effects of exogenously added factors in neural stem cells. Nat. Protoc. *2*, 849–859.

Fica, S.M., and Nagai, K. (2017). Cryo-electron microscopy snapshots of the spliceosome: Structural insights into a dynamic ribonucleoprotein machine. Nat. Struct. Mol. Biol. *24*, 791–799.

Folgueira, M., Bayley, P., Navratilova, P., Becker, T.S., Wilson, S.W., and Clarke, J.D.W. (2012). Morphogenesis underlying the development of the everted teleost telencephalon. Neural Dev. *7*.

Frye, M., and Blanco, S. (2016). Post-transcriptional modifications in development and stem cells. Dev. *143*, 3871–3881.

Frye, M., T. Haranda, B., Behm, M., and He, C. (2018). RNA modifications modulate gene expression during development. Science (80-.). *361*, 1346–1349.

Fuchs, E., Tumbar, T., and Guasch, G. (2004). Socializing with the neighbors: Stem cells and their niche. Cell *116*, 769–778.

Fuentealba, L.C., Rompani, S.B., Parraguez, J.I., Obernier, K., Romero, R., Cepko, C.L., and Alvarez-Buylla, A. (2015). Embryonic Origin of Postnatal Neural Stem Cells. Cell *161*, 1644–1655.

Furutachi, S., Miya, H., Watanabe, T., Kawai, H., Yamasaki, N., Harada, Y., Imayoshi, I., Nelson, M., Nakayama, K.I., Hirabayashi, Y., et al. (2015). Slowly dividing neural progenitors are an embryonic origin of adult neural stem cells. Nat. Neurosci. *18*, 657–665.

Fustin, J.M., Doi, M., Yamaguchi, Y., Hida, H., Nishimura, S., Yoshida, M., Isagawa, T., Morioka, M.S., Kakeya, H., Manabe, I., et al. (2013). XRNA-methylation-dependent RNA processing controls the speed of the circadian clock. Cell *155*, 793.

Gilbert, W. V., Bell, T.A., and Schaening, C. (2016). Messenger RNA modifications: Form, distribution, and function. Science (80-.). *352*, 1408–1412.

Gill, J., Park, Y., McGinnis, J.P., Perez-Sanchez, C., Blanchette, M., and Si, K. (2017). Regulated Intron Removal Integrates Motivational State and Experience. Cell *169*, 836-848.e15.

Graf, T., and Stadtfeld, M. (2008). Heterogeneity of Embryonic and Adult Stem Cells. Cell Stem Cell *3*, 480–483.

Hafner, A., Bulyk, M.L., Jambhekar, A., and Lahav, G. (2019). The multiple mechanisms that regulate p53 activity and cell fate. Nat. Rev. Mol. Cell Biol. *20*, 199–210.

Harcourt, E.M., Kietrys, A.M., and Kool, E.T. (2017). Chemical and structural effects of base modifications in messenger RNA. Nature *541*, 339–346.

Hatzold, J., and Conradt, B. (2008). Control of apoptosis by asymmetric cell division. PLoS Biol. *6*, 771–784.

Herzel, L., Ottoz, D.S.M., Alpert, T., and Neugebauer, K.M. (2017). Splicing and transcription touch base: Co-transcriptional spliceosome assembly and function. Nat. Rev. Mol. Cell Biol. *18*, 637–650.

Hsu, P.J., Zhu, Y., Ma, H., Guo, Y., Shi, X., Liu, Y., Qi, M., Lu, Z., Shi, H., Wang, J., et al. (2017). Ythdc2 is an N6 -methyladenosine binding protein that regulates mammalian spermatogenesis. Cell Res. *27*, 1115–1127.

Hsu, P.J., Shi, H., Zhu, A.C., Lu, Z., Miller, N., Edens, B.M., Ma, Y.C., and He, C. (2019). The RNA-binding protein FMRP facilitates the nuclear export of N6-methyladenosine–containing mRNAs. J. Biol. Chem. *294*, 19889–19895.

Hwang, C.K., D'Souza, U.M., Eisch, A.J., Yajima, S., Lammers, C.H., Yang, Y., Lee, S.H., Kim, Y.M., Nestler, E.J., and Mouradian, M.M. (2001). Dopamine receptor regulating factor, DRRF: A zinc finger transcription factor. Proc. Natl. Acad. Sci. U. S. A. *98*, 7558–7563.

Itoh, Y., Moriyama, Y., Hasegawa, T., Endo, T.A., Toyoda, T., and Gotoh, Y. (2013). Scratch regulates neuronal migration onset via an epithelial-mesenchymal transition-like mechanism. Nat. Neurosci. *16*, 416–425.

Jacob, A.G., and Smith, C.W.J. (2017). Intron retention as a component of regulated gene expression programs. Hum. Genet. *136*, 1043–1057.

Jain, D., Puno, M.R., Meydan, C., Lailler, N., Mason, C.E., Lima, C.D., Anderson, K. V., and Keeney, S. (2018). Ketu mutant mice uncover an essential meiotic function for the ancient RNA helicase YTHDC2. Elife *7*, 1–41.

Keene, J.D. (2007). RNA regulons: Coordination of post-transcriptional events. Nat. Rev. Genet. *8*, 533–543.

Keren, H., Lev-Maor, G., and Ast, G. (2010). Alternative splicing and evolution: Diversification, exon definition and function. Nat. Rev. Genet. *11*, 345–355.

Kim, J., and Koo, B. (2020). Human organoids: model systems for human biology and medicine. Nat. Rev. Mol. Cell Biol. *21*.

Kippin, T.E., Martens, D.J., and Kooy, D. Van Der (2005). p21 loss compromises the relative quiescence of forebrain stem cell proliferation leading to exhaustion of their proliferation capacity. 756–767.

Kleine-Kohlbrecher, D., Christensen, J., Vandamme, J., Abarrategui, I., Bak, M., Tommerup, N., Shi, X., Gozani, O., Rappsilber, J., Salcini, A.E., et al. (2010). A Functional Link between the Histone Demethylase PHF8 and the Transcription Factor ZNF711 in X-Linked Mental Retardation. Mol. Cell *38*, 165–178.

Köhler, A., and Hurt, E. (2007). Exporting RNA from the nucleus to the cytoplasm. Nat. Rev. Mol. Cell Biol. *8*, 761–773.

Kornblihtt, A.R., Schor, I.E., Alló, M., Dujardin, G., Petrillo, E., and Muñoz, M.J. (2013). Alternative splicing: A pivotal step between eukaryotic transcription and translation. Nat. Rev. Mol. Cell Biol. *14*, 153–165.

Kriegstein, A., and Alvarez-Buylla, A. (2009). The glial nature of embryonic and adult neural stem cells. Annu. Rev. Neurosci. *32*, 149–184.

Langer, E.M., Feng, Y., Zhaoyuan, H., Rauscher, F.J., Kroll, K.L., and Longmore, G.D. (2008). Ajuba LIM proteins are snail/slug corepressors required for neural crest development in Xenopus. Dev. Cell *14*, 424–436.

Lee, H., Bao, S., Qian, Y., Geula, S., Leslie, J., Zhang, C., Hanna, J., and Ding, L. (2019). Stage-specific requirement for Mettl3-dependent m6 A mRNA methylation during haematopoietic stem cell differentiation Heather. Nat. Cell Biol. *21*, 700–709.

Lee, K., Nichols, J., and Smith, A. (1997). Identification of a developmentally regulated protein tyrosine phosphatase in embryonic stem cells that is a marker of pluripotential epiblast and early mesoderm (Mech. Dev. 59 (1996) 153-164). Mech. Dev. *61*, 213–215.

Lesbirel, S., Viphakone, N., Parker, M., Parker, J., Heath, C., Sudbery, I., and Wilson, S.A. (2018). The m6A-methylase complex recruits TREX and regulates mRNA export. Sci. Rep. *8*, 1–12.

Lessard, J., Wu, J.I., Ranish, J.A., Wan, M., Winslow, M.M., Staahl, T., Wu, H., Aebersold, R., Graef, I.A., and Crabtree, G.R. (2007). An Essential Switch in Subunit Composition of a Chromatin Remodeling Complex during Neural Development. Neuron *55*, 201–215.

Li, G.-Q., Liu, Z., Shen, H.-B., and Yu, D.-J. (2016). TargetM6A: Identifying N6-

Methyladenosine Sites From RNA Sequences via Position-Specific Nucleotide Propensities and a Support Vector Machine. IEEE Trans. Nanobioscience *15*, 674–682.

Li, H., Tong, J., Zhu, S., Batista, P.J., Duffy, E.E., Zhao, J., Bailis, W., Cao, G., Kroehling, L., Chen, Y., et al. (2018a). m6A mRNA methylation controls T cell homeostasis by targeting IL-7/STAT5/SOCS pathway. Nature *548*, 338–342.

Li, L., Zang, L., Zhang, F., Chen, J., Shen, H., Shu, L., Liang, F., Feng, C., Chen, D., Tao, H., et al. (2017). Fat mass and obesity-associated (FTO) protein regulates adult neurogenesis. Hum. Mol. Genet. *26*, 2398–2411.

Li, M., Zhao, X., Wang, W., Shi, H., Pan, Q., Lu, Z., Perez, S.P., Suganthan, R., He, C., Bjørås, M., et al. (2018b). Ythdf2-mediated m6A mRNA clearance modulates neural development in mice. Genome Biol. *19*, 1–16.

Li, Z., Qian, P., Shao, W., Shi, H., He, X.C., Gogol, M., Yu, Z., Wang, Y., Qi, M., Zhu, Y., et al. (2018c). Suppression of m6A reader Ythdf2 promotes hematopoietic stem cell expansion. Cell Res. *28*, 904–917.

Lim, D.A., and Alvarez-Buylla, A. (2016). The adult ventricular–subventricular zone (V-SVZ) and olfactory bulb (OB) neurogenesis. Cold Spring Harb. Perspect. Biol. *8*, 1–33.

Lim, D.A., Suárez-Fariñas, M., Naef, F., Hacker, C.R., Menn, B., Takebayashi, H., Magnasco, M., Patil, N., and Alvarez-Buylla, A. (2006). In vivo transcriptional profile analysis reveals RNA splicing and chromatin remodeling as prominent processes for adult neurogenesis. Mol. Cell. Neurosci. *31*, 131–148.

Lin, Z., Hsu, P.J., Xing, X., Fang, J., Lu, Z., Zou, Q., Zhang, K.J., Zhang, X., Zhou, Y., Zhang, T., et al. (2017). Mettl3-/Mettl14-mediated mRNA N 6-methyladenosine modulates murine spermatogenesis. Cell Res. *27*, 1216–1230.

Liu, N., Dai, Q., Zheng, G., He, C., Parisien, M., and Pan, T. (2015). N6-methyladenosine-dependent RNA structural switches regulate RNA-protein interactions. Nature *176*, 139–148.

Liu, N., Zhou, K.I., Parisien, M., Dai, Q., Diatchenko, L., and Pan, T. (2017). N6-methyladenosine alters RNA structure to regulate binding of a low-complexity protein. Nucleic Acids Res. *45*, 6051–6063.

Livneh, I., Moshitch-Moshkovitz, S., Amariglio, N., Rechavi, G., and Dominissini, D. (2020). The m6A epitranscriptome: transcriptome plasticity in brain development and function. Nat. Rev. Neurosci. *21*, 36–51.

Llorens-Bobadilla, E., Zhao, S., Baser, A., Saiz-Castro, G., Zwadlo, K., and Martin-Villalba, A. (2015). Single-Cell Transcriptomics Reveals a Population of Dormant Neural Stem Cells that Become Activated upon Brain Injury. Cell Stem Cell *17*, 329–340.

Van Lookeren Campagne, M., and Gill, R. (1998). Tumor-suppressor p53 is expressed in proliferating and newly formed neurons of the embryonic and postnatal rat brain: Comparison with expression of the cell cycle regulators p21(Waf1/Cip1), p27(Kip1), p57(Kip2), p16(Ink4a), cyclin G1, and the proto-oncoge. J. Comp. Neurol. *397*, 181–198.

Louloupi, A., Ntini, E., Conrad, T., and Ørom, U.A.V. (2018). Transient N-6-Methyladenosine Transcriptome Sequencing Reveals a Regulatory Role of m6A in Splicing Efficiency. Cell Rep. *23*, 3429–3437.

Manzanares, M., Locascio, A., and Nieto, M.A. (2001). The increasing complexity of the Snail gene superfamily in metazoan evolution. Trends Genet. *17*, 178–181.

Marín, F., and Nieto, M.A. (2006). The expression of Scratch genes in the developing and adult brain. Dev. Dyn. *235*, 2586–2591.

Marin Navarro, A., Pronk, R.J., van der Geest, A.T., Oliynyk, G., Nordgren, A., Arsenian-Henriksson, M., Falk, A., and Wilhelm, M. (2020). P53 Controls Genomic Stability and Temporal Differentiation of Human Neural Stem Cells and Affects Neural Organization in Human Brain Organoids. Cell Death Dis. *11*.

Marqués-torrejón, M.Á., Porlan, E., Banito, A., Gómez-ibarlucea, E., Fernández-capetillo, Ó., Vidal, A., Gil, J., Torres, J., and Fariñas, I. (2013). Cyclin-dependent kinase inhibitor p21 controls adult neural stem cell expansion by regulating Sox2 gene expression. Cell St *12*, 88–100.

Matsuda, T., Irie, T., Katsurabayashi, S., Hayashi, Y., Nagai, T., Hamazaki, N., Adefuin, A.M.D., Miura, F., Ito, T., Kimura, H., et al. (2019). Pioneer Factor NeuroD1 Rearranges Transcriptional and Epigenetic Profiles to Execute Microglia-Neuron Conversion. Neuron *101*, 472-485.e7.

Mauger, O., Lemoine, F., and Scheiffele, P. (2016). Targeted Intron Retention and Excision for Rapid Gene Regulation in Response to Neuronal Activity. Neuron *92*, 1266–1278.

Meletis, K., Wirta, V., Hede, S.M., Nistér, M., Lundeberg, J., and Frisén, J. (2006). P53 Suppresses the Self-Renewal of Adult Neural Stem Cells. Development *133*, 363–369.

Menn, B., Garcia-Verdugo, J.M., Yaschine, C., Gonzalez-Perez, O., Rowitch, D., and Alvarez-Buylla, A. (2006). Origin of oligodendrocytes in the subventricular zone of the adult brain. J. Neurosci. *26*, 7907–7918.

Metzstein, M.M., and Horvitz, H.R. (1999). The C. elegans cell death specification gene ces-1 encodes a Snail family zinc finger protein. Mol. Cell *4*, 309–319.

Middleton, R., Gao, D., Thomas, A., Singh, B., Au, A., Wong, J.J.L., Bomane, A., Cosson, B., Eyras, E., Rasko, J.E.J., et al. (2017). IRFinder: Assessing the impact of intron retention on mammalian gene expression. Genome Biol. *18*, 1–11.

Ming, G. li, and Song, H. (2011). Adult Neurogenesis in the Mammalian Brain: Significant Answers and Significant Questions. Neuron *70*, 687–702.

Ming, G.L., and Song, H. (2005). Adult neurogenesis in the mammalian central nervous system. Annu. Rev. Neurosci. *28*, 223–250.

Mirzadeh, Z., Merkle, F.T., Soriano-navarro, M., and Garcia-verdugo, J.M. (2008). Article Neural Stem Cells Confer Unique Pinwheel Architecture to the Ventricular Surface in Neurogenic Regions of the Adult Brain. 265–278.

Mizrak, D., Levitin, H.M., Delgado, A.C., Crotet, V., Yuan, J., Chaker, Z., Silva-Vargas, V., Sims, P.A., and Doetsch, F. (2019). Single-Cell Analysis of Regional Differences in Adult V-SVZ Neural Stem Cell Lineages. Cell Rep. *26*, 394-406.e5.

Monteuuis, G., Wong, J.J.L., Bailey, C.G., Schmitz, U., and Rasko, J.E.J. (2019). The changing paradigm of intron retention: Regulation, ramifications and recipes. Nucleic Acids Res. *47*, 1149711513.

Moon, B.S., Bai, J., Cai, M., Liu, C., Shi, J., and Lu, W. (2018). Kruppel-like factor 4-dependent Staufen1-mediated mRNA decay regulates cortical neurogenesis. Nat. Commun. *9*.

Nakakura, E.K., Watkins, D.N., Schuebel, K.E., Sriuranpong, V., Borges, M.W., Nelkin, B.D., and Ball, D.W. (2001a). Mammalian scratch: A neural-specific Snail family transcriptional repressor. Proc. Natl. Acad. Sci. U. S. A. *98*, 4010–4015.

Nakakura, E.K., Watkins, D.N., Sriuranpong, V., Borges, M.W., Nelkin, B.D., and Ball, D.W. (2001b). Mammalian Scratch participates in neuronal differentiation in P19 embryonal carcinoma cells. Mol. Brain Res. *95*, 162–166.

Naro, C., Jolly, A., Di Persio, S., Bielli, P., Setterblad, N., Alberdi, A.J., Vicini, E., Geremia, R., De la Grange, P., and Sette, C. (2017). An Orchestrated Intron Retention Program in Meiosis Controls Timely Usage of Transcripts during Germ Cell Differentiation. Dev. Cell *41*, 82-93.e4.

Ni, T., Yang, W., Han, M., Zhang, Y., Shen, T., Nie, H., Zhou, Z., Dai, Y., Yang, Y., Liu, P., et al. (2016). Global intron retention mediated gene regulation during CD4+ T cell activation. Nucleic Acids Res. *44*, 6817–6829.

Nieto, M.A. (2002). The snail superfamily of zinc-finger transcription factors. Nat. Rev. Mol. Cell Biol. *3*, 155–166.

Ninomiya, K., Kataoka, N., and Hagiwara, M. (2011). Stress-responsive maturation of Clk1/4 pre-mRNAs promotes phosphorylation of SR splicing factor. J. Cell Biol. *195*, 27–40.

Noack, F., and Calegari, F. (2018). Epitranscriptomics: A new regulatory mechanism of brain development and function. Front. Neurosci. *12*, 1–9.

Obernier, K., and Alvarez-Buylla, A. (2019). Neural stem cells: Origin, heterogeneity and regulation in the adult mammalian brain. Dev. *146*.

Obernier, K., Cebrian-Silla, A., Thomson, M., Parraguez, J.I., Anderson, R., Guinto, C., Rodas Rodriguez, J., Garcia-Verdugo, J.M., and Alvarez-Buylla, A. (2018). Adult Neurogenesis Is Sustained by Symmetric Self-Renewal and Differentiation. Cell Stem Cell *22*, 221-234.e8.

Orford, K.W., and Scadden, D.T. (2008). Deconstructing stem cell self-renewal: Genetic insights into cell-cycle regulation. Nat. Rev. Genet. *9*, 115–128.

Paul, V., Tonchev, A.B., Henningfeld, K.A., Pavlakis, E., Rust, B., Pieler, T., and Stoykova, A. (2014). Scratch2 modulates neurogenesis and cell migration through antagonism of bHLH proteins in the developing neocortex. Cereb. Cortex *24*, 754–772.

Peinado, H., Ballestar, E., Esteller, M., and Cano, A. (2004). Peinado 2004 Snail Mediates E-Cadherin Repression by the Recruitment of the.pdf. *24*, 306–319.

Peinado, H., Iglesias-de La Cruz, M.D.C., Olmeda, D., Csiszar, K., Fong, K.S.K., Vega, S., Nieto, M.A., Cano, A., and Portillo, F. (2005). A molecular role for lysyl oxidase-like 2 enzyme in Snail regulation and tumor progression. EMBO J. *24*, 3446–3458.

Pera, M.F., and Tam, P.P.L. (2010). Extrinsic regulation of pluripotent stem cells. *465*, 713–720.

Perry, R.P., and Kelley, D.E. (1974). Existence of methylated messenger RNA in mouse L

cells. Cell *1*, 37–42.

Petreanu, L., and Alvarez-buylla, A. (2002). Maturation and Death of Adult-Born Olfactory Bulb Granule Neurons: Role of Olfaction. J. Neurosci. *22*, 6106–6113.

Pimentel, H., Parra, M., Gee, S.L., Mohandas, N., Pachter, L., and Conboy, J.G. (2016). A dynamic intron retention program enriched in RNA processing genes regulates gene expression during terminal erythropoiesis. Nucleic Acids Res. *44*, 838–851.

Ponti, G., Obernier, K., Guinto, C., Jose, L., Bonfanti, L., and Alvarez-Buylla, A. (2013a). Cell cycle and lineage progression of neural progenitors in the ventricular-subventricular zones of adult mice. Proc. Natl. Acad. Sci. U. S. A. *110*.

Ponti, G.P., Obernier, K., and Alvarez-Buylla, A. (2013b). Lineage progression from stem cells to new neurons in the adult brain ventricularsubventricular zone. Cell Cycle *12*, 1649–1650.

Porlan, E., Morante-redolat, J.M., Marqués-torrejón, M.Á., Andreu-agulló, C., Carneiro, C., Gómez-ibarlucea, E., Soto, A., Vidal, A., Ferrón, S.R., and Fariñas, I. (2013). Transcriptional repression of Bmp2 by p21(Waf1/Cip1) links quiescence to neural stem cell maintenance. Nat. Neurosci. *16*, 1567–1575.

Potts, R.C., Zhang, P., Wurster, A.L., Precht, P., Mughal, M.R., Wood, W.H., Zhang, Y., Becker, K.G., Mattson, M.P., and Pazin, M.J. (2011). CHD5, a brain-specific paralog of Mi2 chromatin remodeling enzymes, regulates expression of neuronal genes. PLoS One *6*.

Raj, B., and Blencowe, B.J. (2015). Alternative Splicing in the Mammalian Nervous System: Recent Insights into Mechanisms and Functional Roles. Neuron *87*, 14–27.

Ramat, A., Audibert, A., Louvet-Vallée, S., Simon, F., Fichelson, P., and Gho, M. (2016). Escargot and Scratch regulate neural commitment by antagonizing Notch activity in Drosophila sensory organs. Dev. *143*, 3024–3034.

Reece-Hoyes, J.S., Deplancke, B., Barrasa, M.I., Hatzold, J., Smit, R.B., Arda, H.E., Pope, P.A., Gaudet, J., Conradt, B., and Walhout, A.J.M. (2009). The C. elegans Snail homolog CES-1 can activate gene expression in vivo and share targets with bHLH transcription factors. Nucleic Acids Res. *37*, 3689–3698.

Ren, X., Zhang, K., Deng, R., and Li, J. (2019). RNA Splicing Analysis: From In Vitro Testing to Single-Cell Imaging. Chem *5*, 2571–2592.

Reynolds, B.A., and Weiss, S. (1992). Generation of neurons and astrocytes from isolated cells of the adult mammalian central nervous system. Science (80-.). *255*, 1707–1710.

Roark, M., Sturtevant, M.A., Emery, J., Vaessin, H., Grell, E., and Bier, E. (1995). Scratch, a Pan-Neural Gene Encoding a Zinc Finger Protein Related To Snail, Promotes Neuronal Development. Genes Dev. *9*, 2384–2398.

Rodríguez-Aznar, E., and Nieto, M.A. (2011). Repression of Puma by Scratch2 is required for neuronal survival during embryonic development. Cell Death Differ. *18*, 1196–1207.

Rodríguez-Aznar, E., Barrallo-Gimeno, A., and Nieto, M.A. (2013). Scratch2 prevents cell cycle re-entry by repressing miR-25 in postmitotic primary neurons. Ann. Intern. Med. *158*, 5095–5105.

Roost, C., Lynch, S.R., Batista, P.J., Qu, K., Chang, H.Y., and Kool, E.T. (2015). Structure

and thermodynamics of N6-methyladenosine in RNA: A spring-loaded base modification. J. Am. Chem. Soc. *137*, 2107–2115.

Roundtree, I.A., Evans, M.E., Pan, T., and He, C. (2017a). Dynamic RNA Modifications in Gene Expression Regulation. Cell *169*, 1187–1200.

Roundtree, I.A., Luo, G.Z., Zhang, Z., Wang, X., Zhou, T., Cui, Y., Sha, J., Huang, X., Guerrero, L., Xie, P., et al. (2017b). YTHDC1 mediates nuclear export of N6-methyladenosine methylated mRNAs. Elife *6*, 1–28.

Rowe, R.G., and Daley, G.Q. (2019). Induced pluripotent stem cells in disease modelling and drug discovery. Nat. Rev. Genet. *20*, 377–388.

Sawicka, K., Bushell, M., Spriggs, K.A., and Willis, A.E. (2008). Polypyrimidine-tract-binding protein: A multifunctional RNA-binding protein. Biochem. Soc. Trans. *36*, 641–647.

Schwertz, H., Tolley, N.D., Foulks, J.M., Denis, M.M., Risenmay, B.W., Buerke, M., Tilley, R.E., Rondina, M.T., Harris, E.M., Kraiss, L.W., et al. (2006). Signal-dependent splicing of tissue factor pre-mRNA modulates the thrombogenecity of human platelets. J. Exp. Med. *203*, 2433–2440.

Seo, K.W., and Kleiner, R.E. (2020). Mechanisms of epitranscriptomic gene regulation. Biopolymers.

Shalgi, R., Hurt, J.A., Lindquist, S., and Burge, C.B. (2014). Widespread inhibition of posttranscriptional splicing shapes the cellular transcriptome following heat shock. Cell Rep. *7*, 1362–1370.

Shashkin, P., Brown, G., Ghosh, A., Mathe, G., and McIntyre, M. (2008). Lipopolysaccharide is a Direct Agonist for Platelet RNA Splicing. J Immunol *181*, 3495–3502.

Shi, Y. (2017). Mechanistic insights into precursor messenger RNA splicing by the spliceosome. Nat. Rev. Mol. Cell Biol. *18*, 655–670.

Sibley, C.R., Blazquez, L., and Ule, J. (2016). Lessons from non-canonical splicing. Nat. Rev. Genet. *17*, 407–421.

Sohn, J., Orosco, L., Guo, F., Chung, S.H., Bannerman, P., Ko, E.M., Zarbalis, K., Deng, W., and Pleasure, D. (2015). The subventricular zone continues to generate corpus callosum and rostral migratory stream astroglia in normal adult mice. J. Neurosci. *35*, 3756–3763.

Spitale, R.C., Flynn, R.A., Zhang, Q.C., Crisalli, P., Lee, B., Jung, J.W., Kuchelmeister, H.Y., Batista, P.J., Torre, E.A., Kool, E.T., et al. (2015). Erratum: Structural imprints in vivo decode RNA regulatory mechanisms. Nature *527*, 264.

Stewart, M. (2019). Polyadenylation and nuclear export of mRNAs. J. Biol. Chem. *294*, 2977–2987.

Sulston, J.E., Schierenberg, E., White, J.G., and Thomson, J.N. (1983). The embryonic cell lineage of the nematode Caenorhabditis elegans. Dev. Biol. *100*, 64–119.

Takahashi, K., and Yamanaka, S. (2006). Induction of Pluripotent Stem Cells from Mouse Embryonic and Adult Fibroblast Cultures by Defined Factors. *2*, 663–676.

Takahashi, K., and Yamanaka, S. (2015). A developmental framework for induced pluripotency. 3274–3285.

Tewary, M., Shakiba, N., and Zandstra, P.W. (2018). Stem cell bioengineering: building from stem cell biology. Nat. Rev. Genet. *19*, 595–614.

Than-Trong, E., and Bally-Cuif, L. (2015). Radial glia and neural progenitors in the adult zebrafish central nervous system. Glia *63*, 1406–1428.

Thellmann, M., Hatzold, J., and Conradt, B. (2003). The Snail-like CES-1 protein of C. elegans can block the expression of the BH3-only-cell-death activator gene egl-1 by antagonizing the function of bHLH proteins. Development *130*, 4057–4071.

Thomson, J.A., Itskovitz-eldor, J., Shapiro, S.S., Waknitz, M.A., Swiergiel, J.J., Marshall, V.S., and Jones, J.M. (1998). Embryonic Stem Cell Lines Derived from Human Blastocysts. *282*, 1145–1148.

Till, J.E., and McCulloch, E.A. (1961). A direct measurement of the radiation sensitivity of normal mouse bone marrow cells. Radiat. Res. *14*, 213–222.

Trounson, A., and DeWitt, N.D. (2016). Pluripotent stem cells progressing to the clinic. Nat. Rev. Mol. Cell Biol. *17*, 194–200.

Tullai, J.W., Schaffer, M.E., Mullenbrock, S., Sholder, G., Kasif, S., and Cooper, G.M. (2007). Immediate-early and delayed primary response genes are distinct in function and genomic architecture. J. Biol. Chem. *282*, 23981–23995.

Vargas, D.Y., Shah, K., Batish, M., Levandoski, M., Sinha, S., Marras, S.A.E., Schedl, P., and Tyagi, S. (2011). Single-molecule imaging of transcriptionally coupled and uncoupled splicing. Cell *147*, 1054–1065.

Vestin, A., and Mills, A.A. (2013). The tumor suppressor Chd5 is induced during neuronal differentiation in the developing mouse brain. Gene Expr Patterns *13*.

Vieceli, F.M., Simões-Costa, M., Turri, J.A., Kanno, T., Bronner, M., and Yan, C.Y.I. (2013). The transcription factor chicken Scratch2 is expressed in a subset of early postmitotic neural progenitors. Gene Expr. Patterns *13*, 189–196.

Vu, L.P., Pickering, B.F., Cheng, Y., Zaccara, S., Nguyen, D., Minuesa, G., Chou, T., Chow, A., Saletore, Y., Mackay, M., et al. (2017). The N 6 -methyladenosine (m 6 A)-forming enzyme METTL3 controls myeloid differentiation of normal hematopoietic and leukemia cells. Nat. Med. *23*, 1369–1376.

Wagers, A.J., and Weissman, I.L. (2004). Plasticity of adult stem cells. Cell *116*, 639–648.

Wang, X., Feng, J., Xue, Y., Guan, Z., Zhang, D., Liu, Z., Gong, Z., Wang, Q., Huang, J., Tang, C., et al. (2016). Structural basis of N6-adenosine methylation by the METTL3-METTL14 complex. Nature *534*, 575–578.

Wang, Y., Li, Y., Yue, M., Wang, J., Kumar, S., Wechsler-Reya, R.J., Zhang, Z., Ogawa, Y., Kellis, M., Duester, G., et al. (2018). N 6-methyladenosine RNA modification regulates embryonic neural stem cell self-renewal through histone modifications. Nat. Neurosci. *21*, 195–206.

Wei, H., Yan, B., Gagneur, J., and Conradt, B. (2017). Caenorhabditis elegans CES-1 snail represses Pig-1 MELK expression to control asymmetric cell division. Genetics *206*, 2069–2084.

Weissman, I.L. (2000). Stem cells: Units of development, units of regeneration, and units in

evolution. Cell *100*, 157–168.

Weng, H., Huang, H., Wu, H., Qin, X., Zhao, B.S., Dong, L., Shi, H., Skibbe, J., Shen, C., Hu, C., et al. (2018). METTL14 Inhibits Hematopoietic Stem/Progenitor Differentiation and Promotes Leukemogenesis via mRNA m6A Modification. Cell Stem Cell *22*, 191-205.e9.

Wickramasinghe, V.O., and Laskey, R.A. (2015). Control of mammalian gene expression by selective mRNA export. Nat. Rev. Mol. Cell Biol. *16*, 431–442.

Winchester, C.L., Ferrier, R.K., Sermoni, A., Clark, B.J., and Johnson, K.J. (1999). Characterization of the expression of DMPK and SIX5 in the human eye and implications for pathogenesis in myotonic dystrophy. Hum. Mol. Genet. *8*, 481–492.

Wojtas, M.N., Pandey, R.R., Mendel, M., Homolka, D., Sachidanandam, R., and Pillai, R.S. (2017). Regulation of m6A Transcripts by the 3'→5' RNA Helicase YTHDC2 Is Essential for a Successful Meiotic Program in the Mammalian Germline. Mol. Cell *68*, 374-387.e12.

Wong, J.J.L., Ritchie, W., Ebner, O.A., Selbach, M., Wong, J.W.H., Huang, Y., Gao, D., Pinello, N., Gonzalez, M., Baidya, K., et al. (2013). Orchestrated intron retention regulates normal granulocyte differentiation. Cell *154*, 583–595.

Wu, C.L., Zukerberg, L.R., Ngwu, C., Harlow, E., and Lees, J.A. (1995). In vivo association of E2F and DP family proteins. Mol. Cell. Biol. *15*, 2536–2546.

Wu, R., Li, A., Sun, B., Sun, J.G., Zhang, J., Zhang, T., Chen, Y., Xiao, Y., Gao, Y., Zhang, Q., et al. (2019). A novel m6A reader Prrc2a controls oligodendroglial specification and myelination. Cell Res. *29*, 23–41.

Xiao, W., Adhikari, S., Dahal, U., Chen, Y.S., Hao, Y.J., Sun, B.F., Sun, H.Y., Li, A., Ping, X.L., Lai, W.Y., et al. (2016). Nuclear m6A Reader YTHDC1 Regulates mRNA Splicing. Mol. Cell *61*, 507–519.

Xu, K., Yang, Y., Feng, G.H., Sun, B.F., Chen, J.Q., Li, Y.F., Chen, Y.S., Zhang, X.X., Wang, C.X., Jiang, L.Y., et al. (2017). Mettl3-mediated m 6 A regulates spermatogonial differentiation and meiosis initiation. Cell Res. *27*, 1100–1114.

Yan, B., Memar, N., Gallinger, J., and Conradt, B. (2013). Coordination of Cell Proliferation and Cell Fate Determination by CES-1 Snail. PLoS Genet. *9*.

Yang, Y., Hsu, P.J., Chen, Y.S., and Yang, Y.G. (2018). Dynamic transcriptomic m6A decoration: Writers, erasers, readers and functions in RNA metabolism. Cell Res. *28*, 616–624.

Yoon, K.J., Ringeling, F.R., Vissers, C., Jacob, F., Pokrass, M., Jimenez-Cyrus, D., Su, Y., Kim, N.S., Zhu, Y., Zheng, L., et al. (2017). Temporal Control of Mammalian Cortical Neurogenesis by m6A Methylation. Cell *171*, 877-889.e17.

Yuzwa, S.A., Borrett, M.J., Innes, B.T., Voronova, A., Ketela, T., Kaplan, D.R., Bader, G.D., and Miller, F.D. (2017). Developmental Emergence of Adult Neural Stem Cells as Revealed by Single-Cell Transcriptional Profiling. Cell Rep. *21*, 3970–3986.

Zeng, Y., Wang, S., Gao, S., Soares, F., Ahmed, M., Guo, H., Wang, M., Hua, J.T., Guan, J., Moran, M.F., et al. (2018). Refined RIP-seq protocol for epitranscriptome analysis with low input materials. PLoS Biol. *16*, 1–20.

Zhang, C., Chen, Y., Sun, B., Wang, L., Yang, Y., Ma, D., Lv, J., Heng, J., Ding, Y., Xue, Y.,

et al. (2017). M6A modulates haematopoietic stem and progenitor cell specification. Nature *549*, 273–276.

Zhang, M., Zhai, Y., Zhang, S., Dai, X., and Li, Z. (2020). Roles of N6-Methyladenosine (m6A) in Stem Cell Fate Decisions and Early Embryonic Development in Mammals. Front. Cell Dev. Biol. *8*, 1–15.

Zheng, G., Dahl, J.A., Niu, Y., Fedorcsak, P., Huang, C.M., Li, C.J., Vågbø, C.B., Shi, Y., Wang, W.L., Song, S.H., et al. (2013). ALKBH5 Is a Mammalian RNA Demethylase that Impacts RNA Metabolism and Mouse Fertility. Mol. Cell *49*, 18–29.

Zhou, J., Wan, J., Gao, X., Zhang, X., Jaffrey, S.R., and Qian, S.B. (2015). Dynamic m6 A mRNA methylation directs translational control of heat shock response. Nature *526*, 591–594.

Ziegler, A., Levison, S., and Wood, T. (2015). Insulin and IGF receptor signalling in neural-stem-cell homeostasis. Nat Rev Endocrinol *11*, 161–170.

Annex

11th Meeting of the Spanish Society for Developmental Biology (2016), Girona, Spain

Scratch factors in the neural stem cell niche

Ainara González-Iglesias, Ana Domingo-Muelas, Isabel Fariñas, M. Angela Nieto

Abstract

In mammals, adult neurogenesis is restricted to few niches in the central nervous system, being the subependymal zone (SEZ) the largest germinal region of the adult mammalian brain. In rodents, the neural stem cells (NSCs) that reside in this region give rise to neuroblasts that migrate and integrate in the olfactory bulb (OB), where they contribute to neural plasticity of olfactory information processing. The balance between self-renewal and differentiation of adult NSCs in this niche is tightly controlled. A group of transcription factors that might regulate this process in mammals is Scratch family, which belongs to the Snail superfamily and has been shown to promote neuronal differentiation in different species. We show that *Scratch1* is expressed in the SEZ both in NSCs and in neuroblasts, although its expression level is higher in the latter cell type. In addition, *Scratch1* mRNA presents different subcellular distributions between these cell types, showing a canonical cytoplasmic distribution in neuroblasts, whereas its mRNA seems to accumulate in specific regions of the nucleus in NSCs. This differential subcellular distribution suggests that *Scratch1* mRNA export might be selectively regulated in this neurogenic niche. Considering the role of this gene in promoting neuronal differentiation, selective *Scratch1* mRNA export might constitute a mechanism involved in the generation of new neurons in the adult brain.

17th National Congress of the Spanish Society of Neuroscience (2017), Alicante, Spain

Scratch1 in the neural stem cell niche

Ainara González-Iglesias, Ana Domingo-Muelas, Isabel Fariñas, M. Angela Nieto

Abstract

In mammals, adult neurogenesis is restricted to few niches in the central nervous system, being the subependymal zone (SEZ) the largest germinal region of the adult mammalian brain. In rodents, the neural stem cells (NSCs) that reside in this region give rise to neuroblasts that migrate and integrate in the olfactory bulb (OB), where they contribute to neural plasticity of olfactory information processing. A group of transcription factors that might regulate this process in mammals is the Scratch family, which belongs to the Snail superfamily of transcription factors and has been shown to promote neuronal differentiation in different species. We show that *Scratch1* is expressed in the SEZ both in NSCs and in neuroblasts, although its transcripts present different subcellular localizations in these two cell types. In NSCs *Scratch1* mRNA accumulates in the nucleus, probably due to alterations in splicing, which in turn affects mRNA export to the cytoplasm. In addition, ESCs and iPSCs reprogrammed from adult NSCs do not express *Scratch1*. This indicates that *Scratch1* starts to be expressed when stem cell are committed to the neural lineage, although its mRNA is not available for translation until differentiation is induced. We propose that mRNA nuclear retention can operate as a mechanism to tightly control the timing on neural differentiation in the adult stem cell niche.

Symposium "Cell plasticity in development and disease" (2018), Sant Joan d'Alicant, Spain

Scratch1 in the adult neural stem cell niche

Ainara González-Iglesias, Ana Domingo-Muelas, Isabel Fariñas, M. Angela Nieto

Abstract

In mammals, adult neurogenesis is restricted to few niches in the central nervous system, being the subependymal zone (SEZ) the largest germinal region of the adult mammalian brain. In rodents, the neural stem cells (NSCs) that reside in this region give rise to neuroblasts that migrate and integrate in the olfactory bulb (OB), where they contribute to the neural plasticity of olfactory information processing. A group of transcription factors that might regulate this process is the Scratch family, which belongs to the Snail superfamily and has been shown to promote neuronal differentiation in different species. We show that Scratch1 is expressed in the SEZ both in NSCs and in neuroblasts, although its transcripts present different subcellular localizations in these two cell types. In NSCs, *Scratch1* mRNA accumulates in the nucleus, due to inefficient splicing, which in turn affect mRNA export to the cytoplasm. During differentiation, RNA methylation promotes the splicing and export of *Scratch1* mRNA, which is then available for translation. In addition, ESCs and iPSCs reprogrammed from adult NSCs do not express *Scratch1*. This indicates that *Scratch1* starts to be expressed when stem cell are committed to the neural lineage. Moreover, this regulatory mechanism is not implemented in zebrafish or in the subgranular zone (SGZ) of the mouse hippocampus. Therefore, we propose that *Scratch1* mRNA nuclear retention can operate as a mechanism to tightly control the timing on neural differentiation specifically in the adult SEZ.

4th Meeting of the Portuguese Society for Developmental Biology (2018), Porto, Portugal

Intron retention regulates Scratch1 expression during adult neurogenesis

Ainara González-Iglesias, Ana Domingo-Muelas, Aida Arcas, Estefania Mancini, Juan Valcárcel, Isabel Fariñas, M. Angela Nieto

Abstract

In mammals, adult neurogenesis is restricted to few niches in the central nervous system, being the subependymal zone (SEZ) the largest germinal region of the adult mammalian brain. In rodents, the neural stem cells (NSCs) that reside in this region give rise to neuroblasts that migrate and integrate in the olfactory bulb (OB), where they contribute to the neural plasticity of olfactory information processing. A group of transcription factors that might regulate this process is the Scratch family, which belongs to the Snail superfamily and has been shown to promote neuronal differentiation in different species. We show that *Scratch1* is expressed in the SEZ both in NSCs and in neuroblasts, although its transcripts present different subcellular localizations in these two cell types. In NSCs, *Scratch1* mRNA accumulates in the nucleus, due to intron retention, which in turn affects mRNA export to the cytoplasm. During differentiation, RNA methylation promotes the splicing and export of *Scratch1* mRNA. Moreover, this regulatory mechanism is not implemented in zebrafish or in the subgranular zone (SGZ) of the mouse hippocampus, but seems specific to the SEZ. In addition, we have found that the expression of other genes implicated in NSCs differentiation might be also regulated by mRNA nuclear retention. Therefore, we propose that intron retention can operate as a mechanism to tightly control the timing on neural differentiation specifically in the adult SEZ.

European Developmental Biology Congress (2019), Alicante, Spain

Intron retention as a mechanism to tightly control the timing of neuronal differentiation

Ainara González-Iglesias, Ana Domingo-Muelas, Aida Arcas, Estefania Mancini, Juan Valcárcel, Isabel Fariñas, M. Angela Nieto

Abstract

In mammals, adult neurogenesis is restricted to few niches in the central nervous system, being the subependymal zone (SEZ) the largest germinal region of the adult mammalian brain. In rodents, the neural stem cells (NSCs) that reside in this region give rise to neuroblasts that migrate and integrate in the olfactory bulb (OB), where they contribute to the neural plasticity of olfactory information processing. A group of transcription factors that might regulate this process is the Scratch family, which belongs to the Snail superfamily and has been shown to promote neuronal differentiation in different species. We show that *Scratch1* is expressed in the SEZ both in NSCs and in neuroblasts, although its transcripts present different subcellular localizations in these two cell types. In NSCs, *Scratch1* mRNA accumulates in the nucleus, due to intron retention, which in turn affects mRNA export to the cytoplasm. During differentiation, RNA methylation promotes the splicing and export of *Scratch1* mRNA. In addition, we have found that the expression of other genes implicated in NSCs differentiation might be also regulated by mRNA nuclear retention. Therefore, we propose that intron retention can operate as a mechanism to tightly control the timing on neural differentiation specifically in the adult SEZ.